Supplementary Material

1.0 Spatial resolution tests for our slip inversions

To test the spatial resolution enabled by our onshore and offshore instrument coverage, we undertake checkerboard tests using the TDEFNODE parameterization that inverts for slip at nodes, rather than slip sources defined by elliptical basis functions. We generate three checkerboard slip patterns (Figure S1a, 1f, 1k) with nodes of 250/150/50 mm alternating with nodes of 0 mm slip and forward model the theoretical displacements at instrument locations (both onshore and offshore). The three checkerboards alternate slip values every node along-strike and every second node in the down-dip direction (Figures S1), which is analogous to the size of slip patches we are interested in resolving at the Gisborne and Hawke's Bay SSE regions. We add Gaussian distributed random noise with uncertainties consistent with what is expected of the respective geodetic displacement components (horizontal, vertical, and LOS displacements) for each data type; this random noise is added to the forward model displacements prior to the inversions for the checkerboard test. We then invert the forward model surface displacement field (with random noise added) at each of the nodes to assess how much of the checkerboard can be recovered. For each checkerboard, we conduct tests for cases with only onshore geodetic data (continuous GNSS and InSAR displacements; Figures S1b, 1g, 1l), and cases with both onshore and offshore geodetic data (continuous GNSS, InSAR, and seafloor vertical displacements from pressure data; Figures S1c, 1h, 1m), to assess changes in spatial resolution provided by the seafloor geodetic data.

The apparent greater resolution offshore of Hawke Bay (compared to offshore Gisborne) is due to the larger spacing between fault nodes here (e.g., coarser checkers). We utilize the checkerboard tests to estimate the spatial resolution contours of the final model presented in Figure 2 (see red and blue dashed lines).

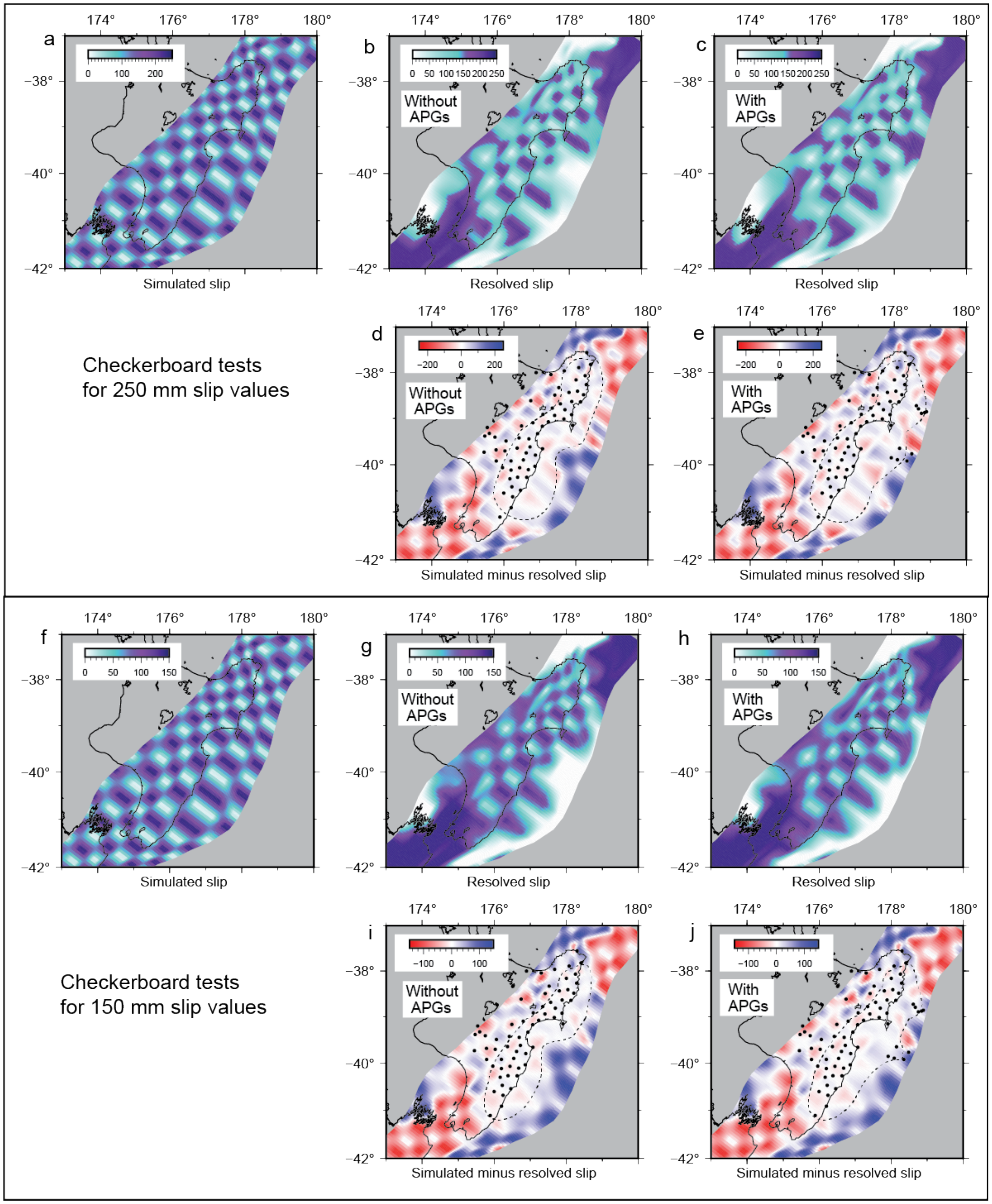
Checkerboard tests
for 250 mm slip values
Checkerboard tests
for 150 mm slip values
a
b
c
d
e
f
g
h
i
j
Without
APGs
With
APGs
Simulated slip
Resolved slip
Simulated minus resolved slip
174°
176°
178°
180°
−38°
−40°
−42°

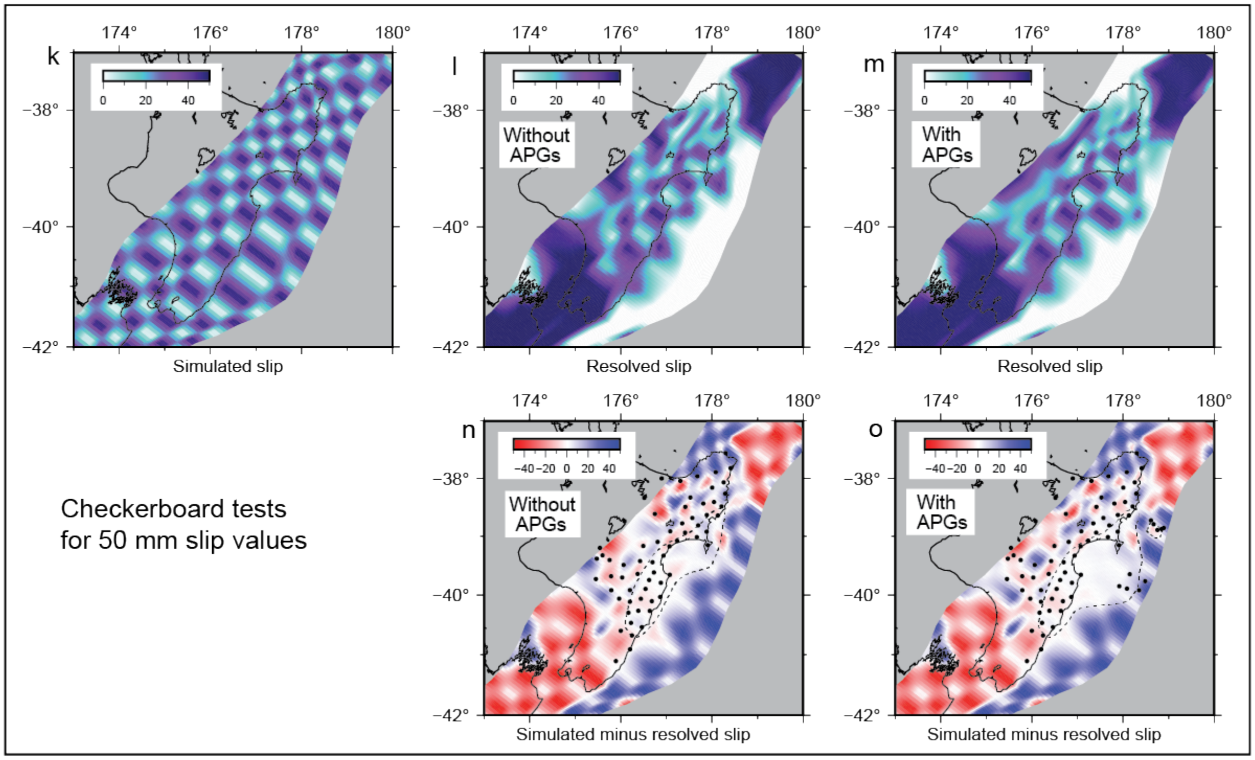

Figure S1: Checkerboard test results for 250 mm slip scenario (a-e), 150 mm (f-j), and 50 mm slip (k-o). Forward model slip distributions (with alternating nodes of slip and no slip) are shown in (a) 250 mm slip (f) 150 mm slip, and (k) 50 mm slip. Sites used in the test are shown as a block dot. Resolved slip using theoretical displacements (with noise added) from only onshore (continuous GNSS) instrumentation (b) 250 mm, (g) 150 mm, and (l) 50 mm. Resolved slip using both onshore and offshore instrumentation; (c) 250 mm, (h) 150 mm, (m) 50 mm. Panels (d), (i) and (n) show Forward model slip (a,f,k) minus resolved slip checkerboards (b,g,l) for inversions with only onshore data, with dashes indicating the estimated area of resolvable slip. Forward model slip (a,f,k) minus resolved slip checkerboards (c,h,m) for inversions using both onshore and offshore data.

2.0: Additional details of the Inversion set-up, data used, and results

We outline most of the details of the TDefnode model set-up and inversion in the main text, although we present some additional details here. Figure S2 shows the block boundary geometries, subduction interface nodes, and onshore and offshore geodetic stations used in this study, as well as data duration.

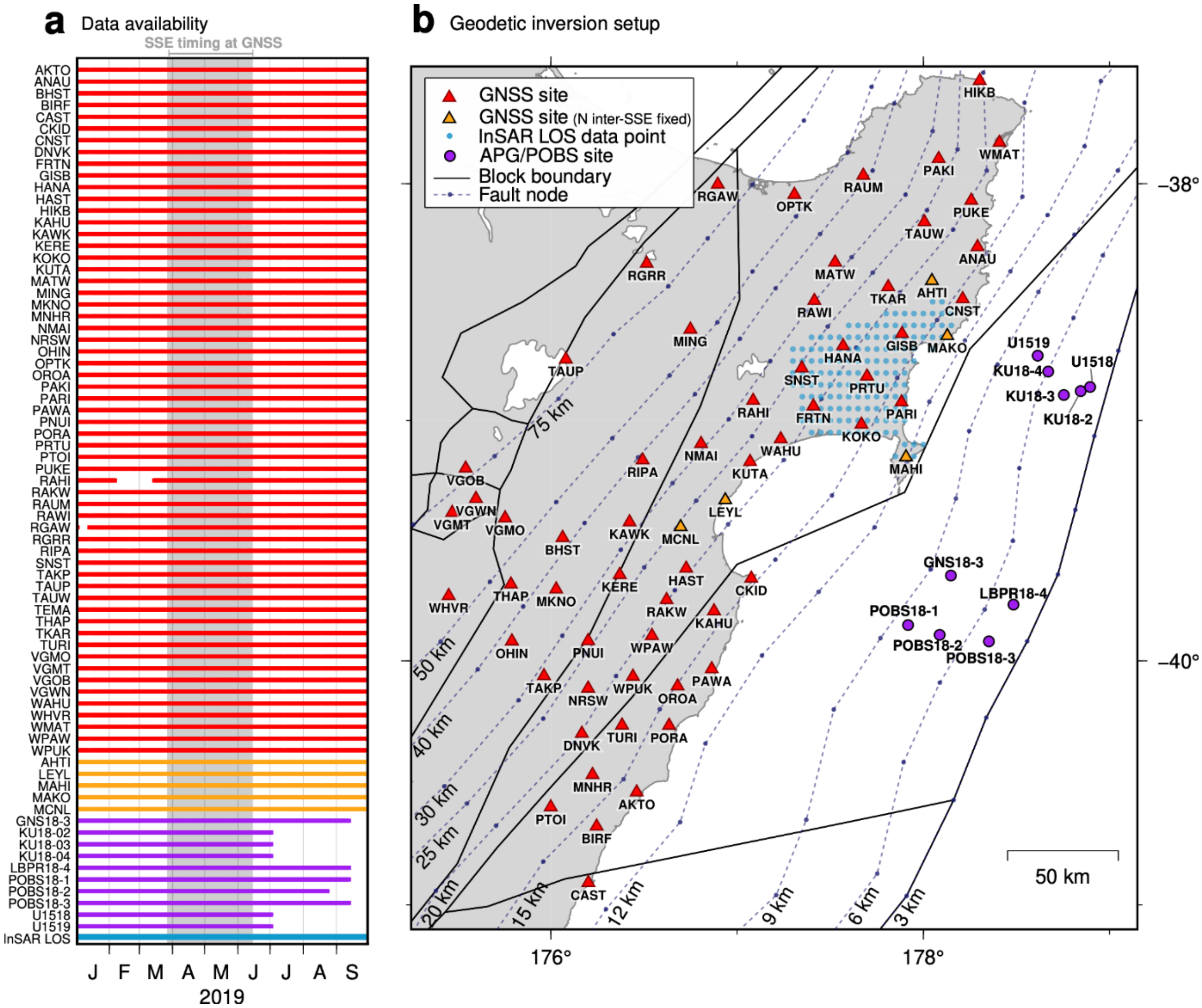

Figure S2: The TDEFNODE inversion framework for the inversion of geodetic data, and data timeframes used. a) Data timeframes used for the GNSS, seafloor pressure, and InSAR LOS data. Orange GNSS data have the north component inter-SSE rates fixed to the rates calculated by Wallace et al. (2012a), whereas these are resolved for the red GNSS data. b) Block model boundaries (Wallace et al., 2004, 2012a) are indicated by solid black lines, and the prescribed Hikurangi interface is shown by nodes (dark blue circles with dashed lines connecting nodes along the same depth contour, extracted from the geometry determined by Williams et al. (2013)). The locations of the GNSS, InSAR, and seafloor data points used in this study are overlain as red/orange triangles, light blue circles, and purple circles respectively.

To invert the seafloor vertical displacement time series with TDEFNODE, the data have to be treated like three component GNSS data, meaning an east and north component is required. To satisfy this, we set the east and north components of the seafloor time series to randomly generated data of uniformly distributed numbers in the interval from -500 mm to 500 mm. The east and north components are then given uncertainties of 499 mm. The large uncertainties means the inversion ignores the simulated data (no influence on the resolved model relative to the real data), and the wide range of east and north displacement values prevents the simulated data from acting as a restriction to the possible seafloor vertical displacement values.

In total the inversion contains 64,707 data points: 51,513 GNSS positions, 144 InSAR LOS points, and 13,050 seafloor vertical displacement points (8,700 simulated and 4,350 real). The data are weighted to account for the different number of data points, with the seafloor pressure time series and InSAR LOS displacements weighted four and 20 times more than the GNSS time series respectively. Due to the circular nature of the interferogram generation, (involving predicted SSE displacements), the InSAR data are not weighted high enough to be a controlling dataset for the resolved slip near Gisborne.

Source number	Parameter type	Minimum	Maximum
1	Longitude	177.9	178.7
1	Latitude	-39.1	-38.8
1	Down-dip width	3	55
1	Along-strike width	3	55
1	Origin Time	2019.18	2019.25
1	Time constant	0.5	3.2
2	Longitude	177.9	178.7
2	Latitude	-38.5	-38.1
2	Down-dip width	5	25
2	Along-strike width	5	25
2	Origin Time	2019.18	2019.25
2	Time constant	5	12
3	Longitude	177	178.4
3	Latitude	-39.5	-39
3	Down-dip width	3	20
3	Along-strike width	3	20
3	Origin Time	2019.31	2019.34
3	Time constant	0.9	2.5
4	Longitude	176.8	178.5
4	Latitude	-40.5	-39.7
4	Down-dip width	4	50
4	Along-strike width	4	50
4	Origin Time	2019.12	2019.18
4	Time constant	0.1	3
5	Longitude	177	178.2
5	Latitude	-39.7	-39
5	Down-dip width	3	55
5	Along-strike width	3	55
5	Origin Time	2019.18	2019.26
5	Time constant	7	18
6	Longitude	178	178.6
6	Latitude	-39.95	-39.25
6	Down-dip width	3	20

6	Along-strike width	3	20
6	Origin Time	2019.35	2019.45
6	Time constant	6	15
7	Longitude	178.2	178.8
7	Latitude	-39.1	-38.7
7	Down-dip width	3	30
7	Along-strike width	3	30
7	Origin Time	2019.1	2019.3
7	Time constant	12	20
8	Longitude	176.6	178.3
8	Latitude	-40.3	-39.6
8	Down-dip width	3	35
8	Along-strike width	3	35
8	Origin Time	2019.18	2019.28
8	Time constant	3	10

Table S1: Constraints applied to all parameter value bounds. We note that source amplitude and azimuth of the long-axis of the ellipse are not constrained.

Source	Duration (days)	Avg slip (cm)	Peak slip (cm)	Area (m^2)	Start	End	Longitude (center)	Latitude (center)	Site
1	11.5	2.7	7.5	1.45E+10	2019-03-25	2019-04-05	178.251	-38.906	MAKO
2	29.1	2.9	4.0	5.55E+09	2019-03-23	2019-04-21	178.118	-38.392	ANAU
3	6.7	2,5	8.8	6.35E+09	2019-04-29	2019-05-06	177.62	-39.201	MAHI
4	1.3	1.4	4.3	6.89E+09	2019-03-07	2019-03-08	177.459	-39.986	PAWA
5	72	3.5	10.3	1.67E+10	2019-03-14	2019-05-25	177.825	-39.608	CKID
6	42.8	4.8	12.5	5.93E+09	2019-05-18	2019-06-30	178.268	-39.626	POBS18-3
7	94.5	5.7	15.4	4.59E+09	2019-02-07	2019-05-12	178.491	-38.944	KU18-3
8	16.8	0.4	1.34	1.75E+10	2019-04-09	2019-04-26	176.905	-40.101	PAWA

Table S2: Source properties of each of the transient deformation sources in our time-dependent model (using TDefnode) of the for the 2019 SSE sequence, from our best-fitting model (reduced-Chi squared = 1.234). The last column lists an example of a GNSS or APG site that contains a notable signal due to the source. It is important to note that each transient (1-8) does not necessarily constitute a separate SSE, so this Table should <u>not</u> be used as an SSE catalog. In some cases, multiple transient sources are super-imposed to capture spatial migration of an individual event.

3.0 Additional InSAR figures and comparison to GNSS data

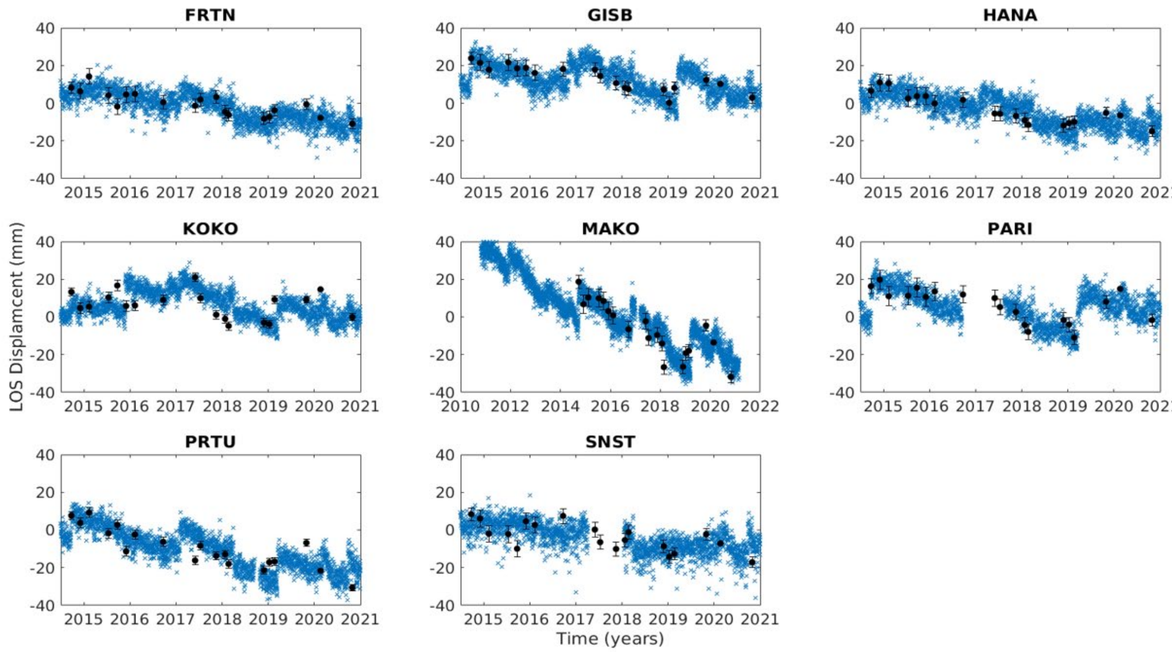

Figure S3: LOS displacement time series (in millimetres) from the August 2014 to November 2020 ALOS-2 InSAR data (black) for co-located pixels and GeoNet continuous GNSS (blue) at Gisborne for: Frasertown (FRTN), Gisborne (GISB), Hangaroa (HANA), Kokohu (KOKO), Makorori (MAKO), Paritu Road (PARI), Paparatu (PRTU), and Shannon Station (SNST). The GNSS data are the three-component GeoNet time series converted into the satellite LOS. Figure modified from Hamling and Wallace (2021).

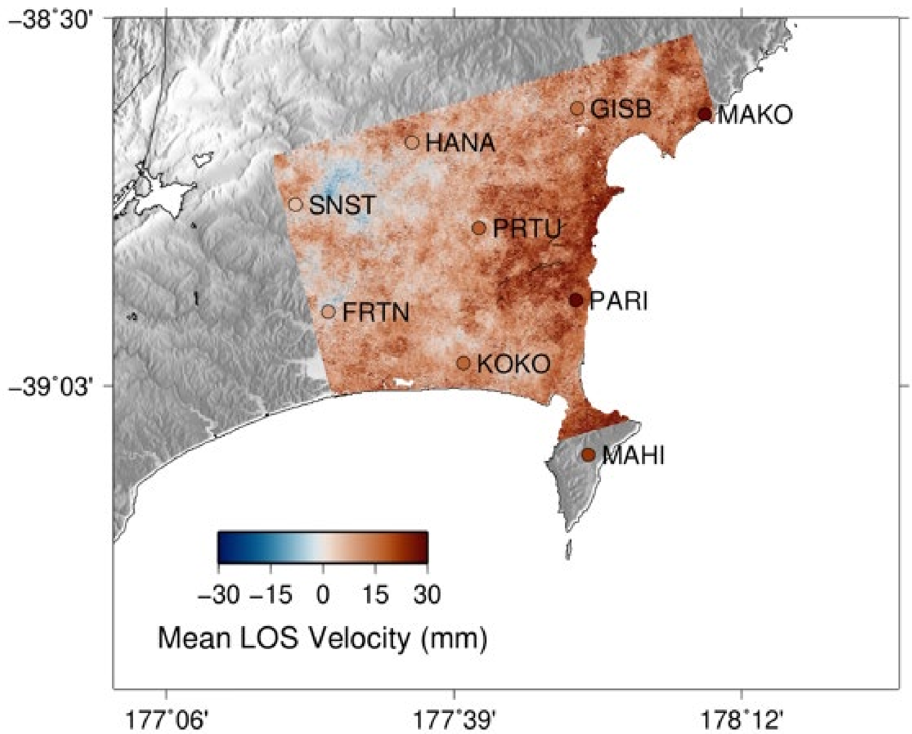

Figure S4: Resolved LOS displacement field at the Gisborne region for the 2019 SSE, extracted from the August 2014 to November 2020 InSAR time series. The coloured circles indicate the equivalent LOS displacement from GeoNet continuous GNSS sites. Positive LOS changes represent motion away from the satellite, which is equivalent to eastward, northward, and downward (subsidence) motion.

4.0 Fit to the observed GNSS and seafloor pressure timeseries

The following figures present the observed time series data with the displacement time series produced by our best-fitting model (presented in Figures 2 and 4). The plot for each site shows the east component observed displacements in red, the north component observed displacement in gold, the up component observed displacement in purple, the forward modelled displacement of our final solution as solid black lines, and the residual displacement for each component (observation minus modelled) as black circles.

AHTI

[178.046]   [-38.4115]

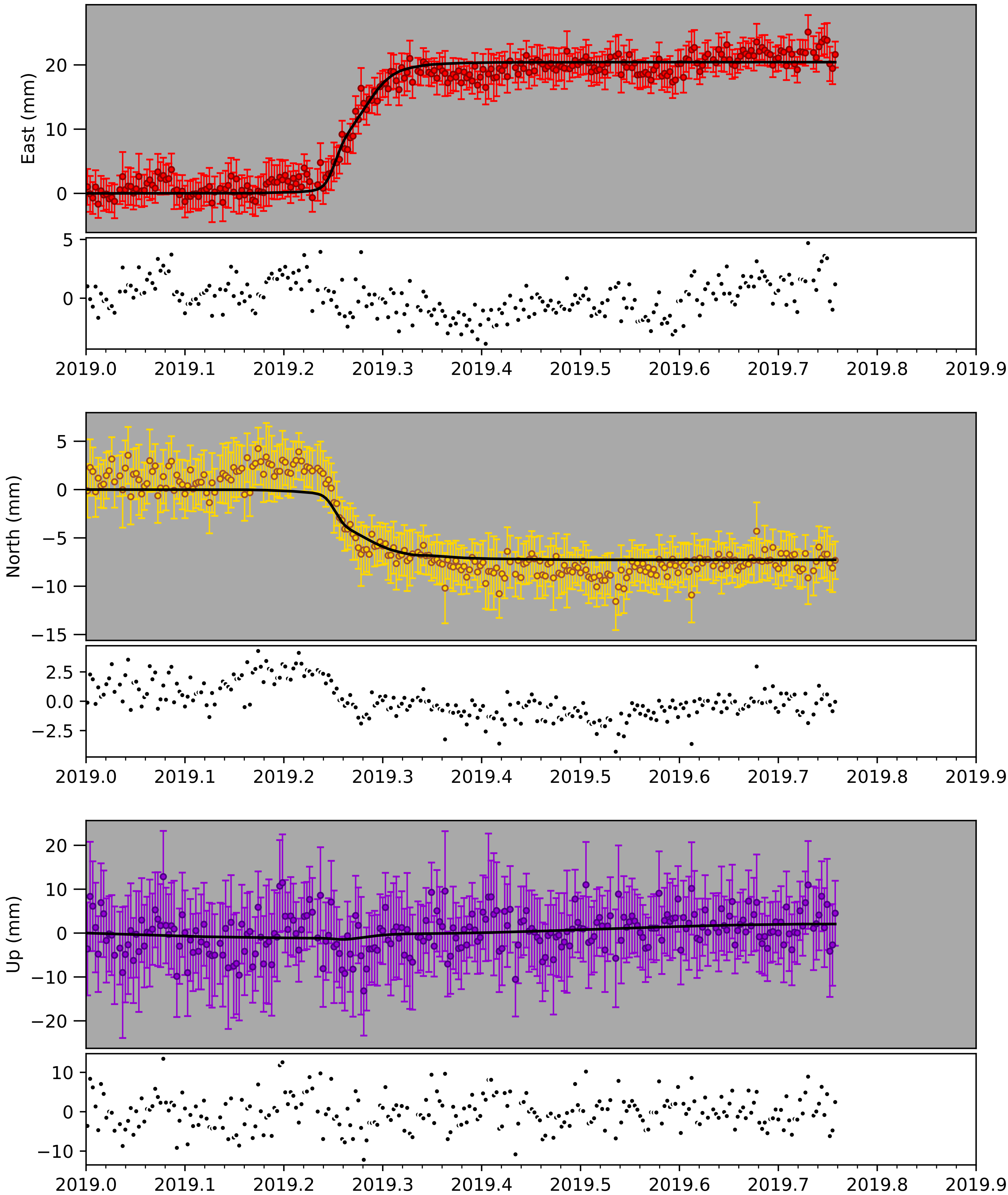

AKTO

[176.4612] [-40.5398]

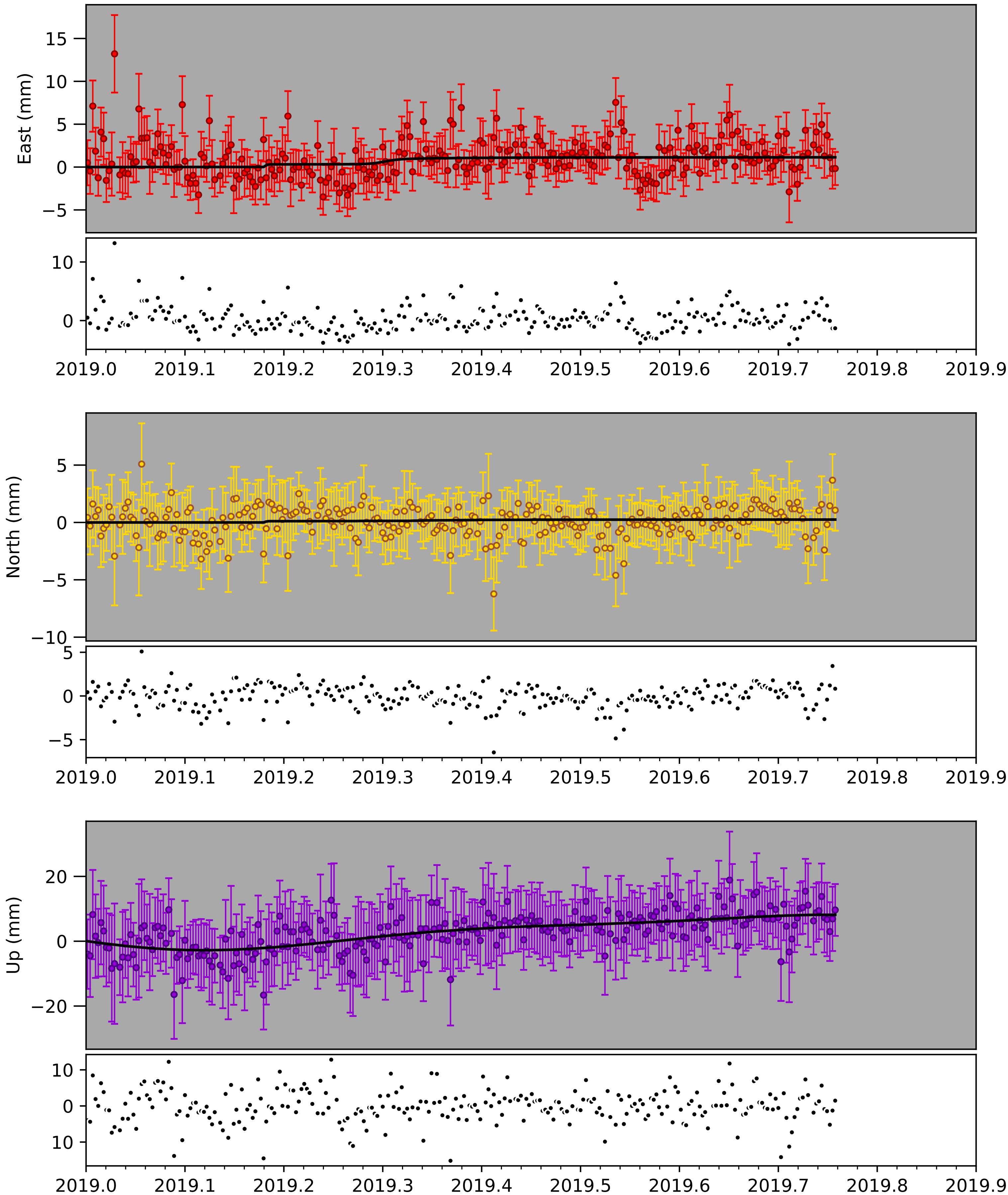

ANAU

[178.2912] [-38.2682]

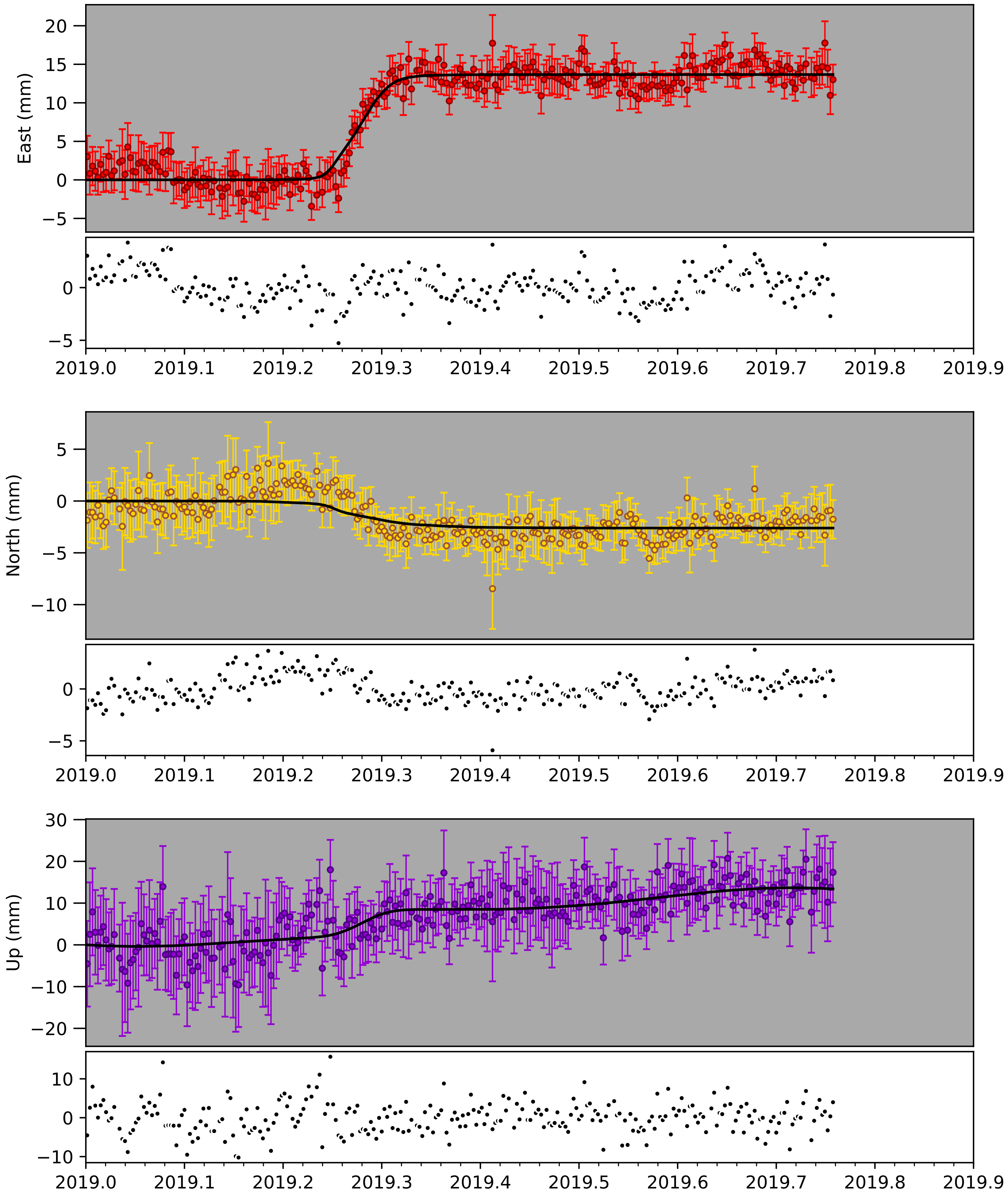

BHST

[176.0632] [-39.4892]

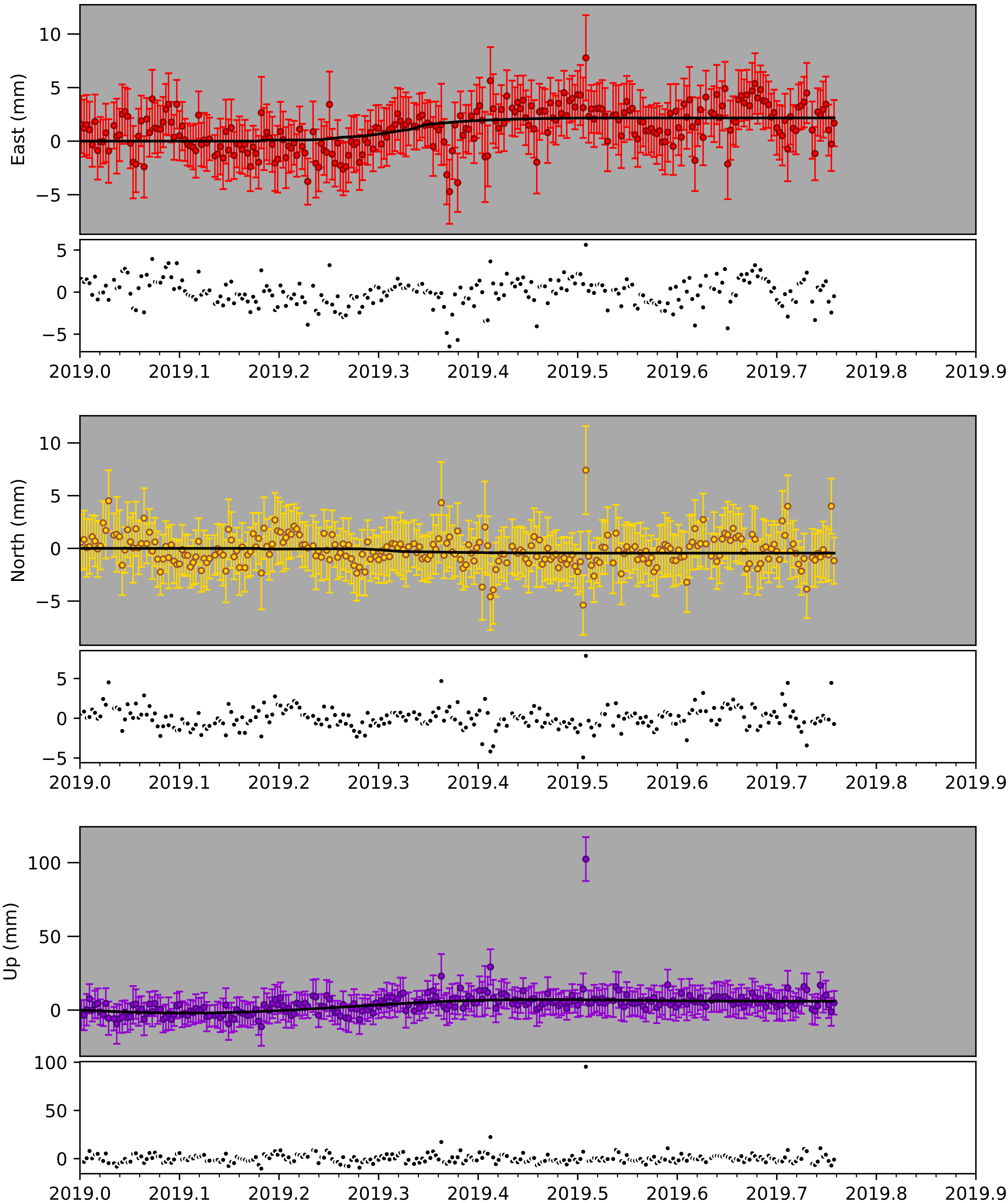

BIRF

[176.2461] [-40.6798]

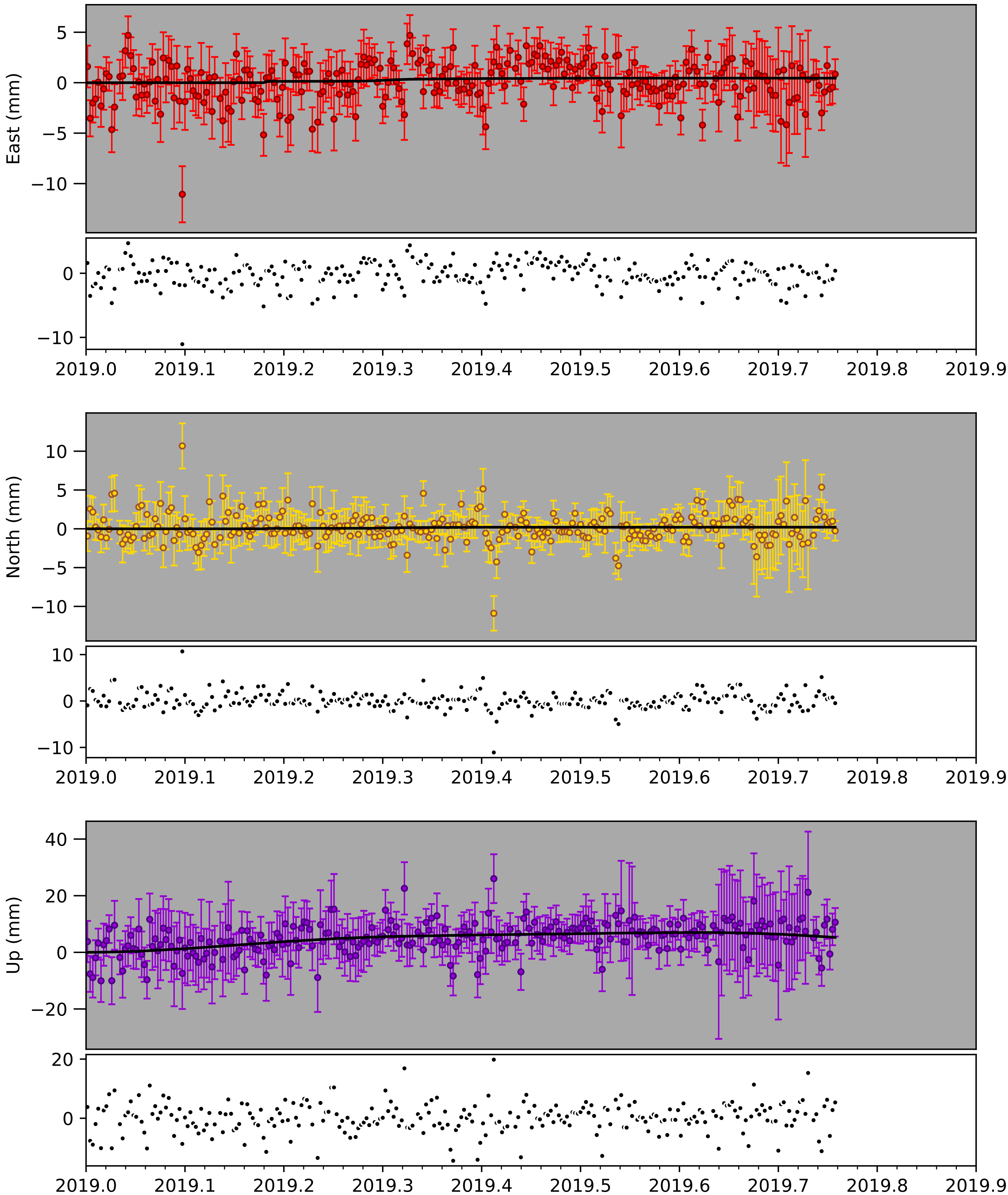

CAST

[176.2016] [-40.9098]

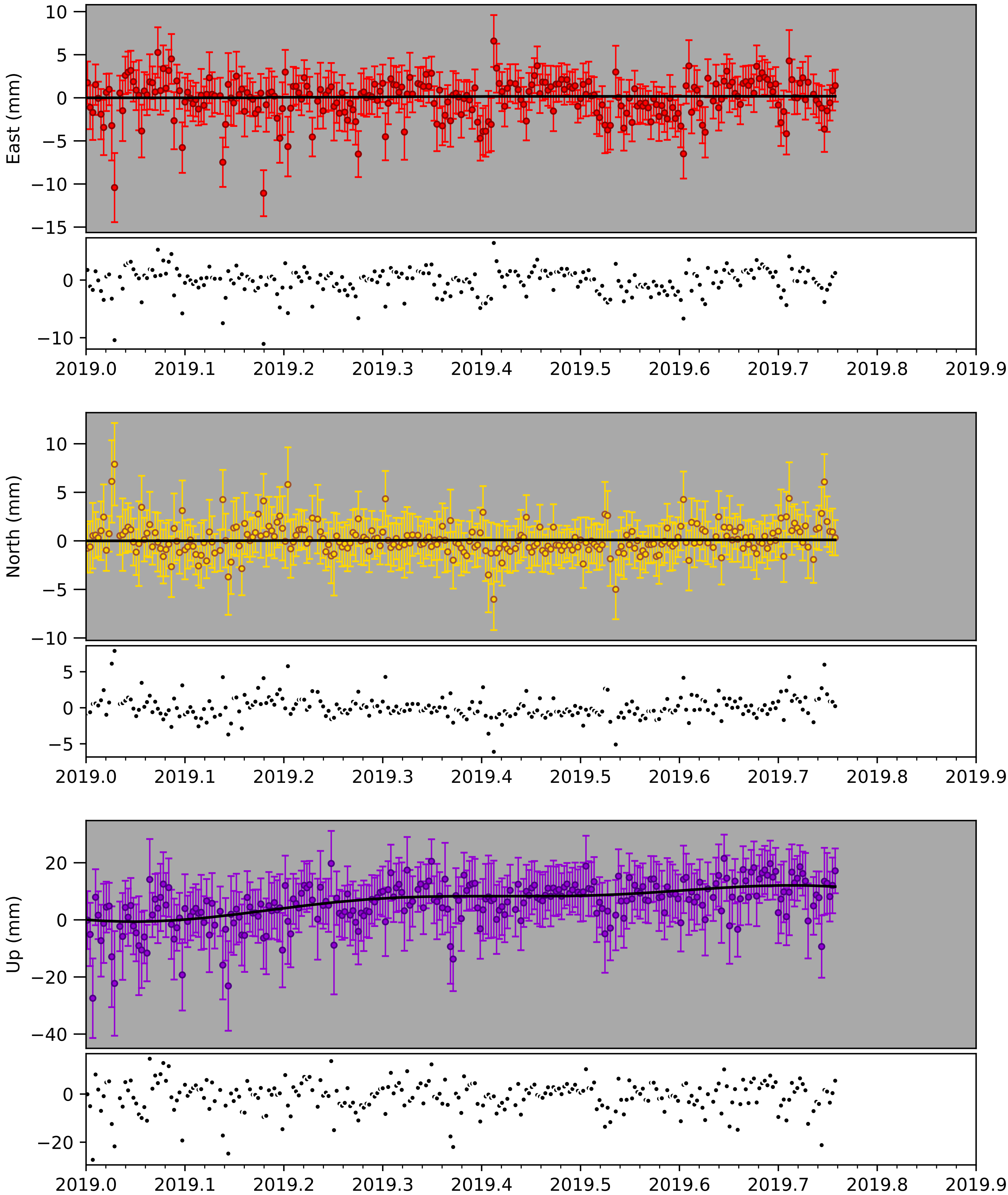

CKID

[177.0763] [-39.6579]

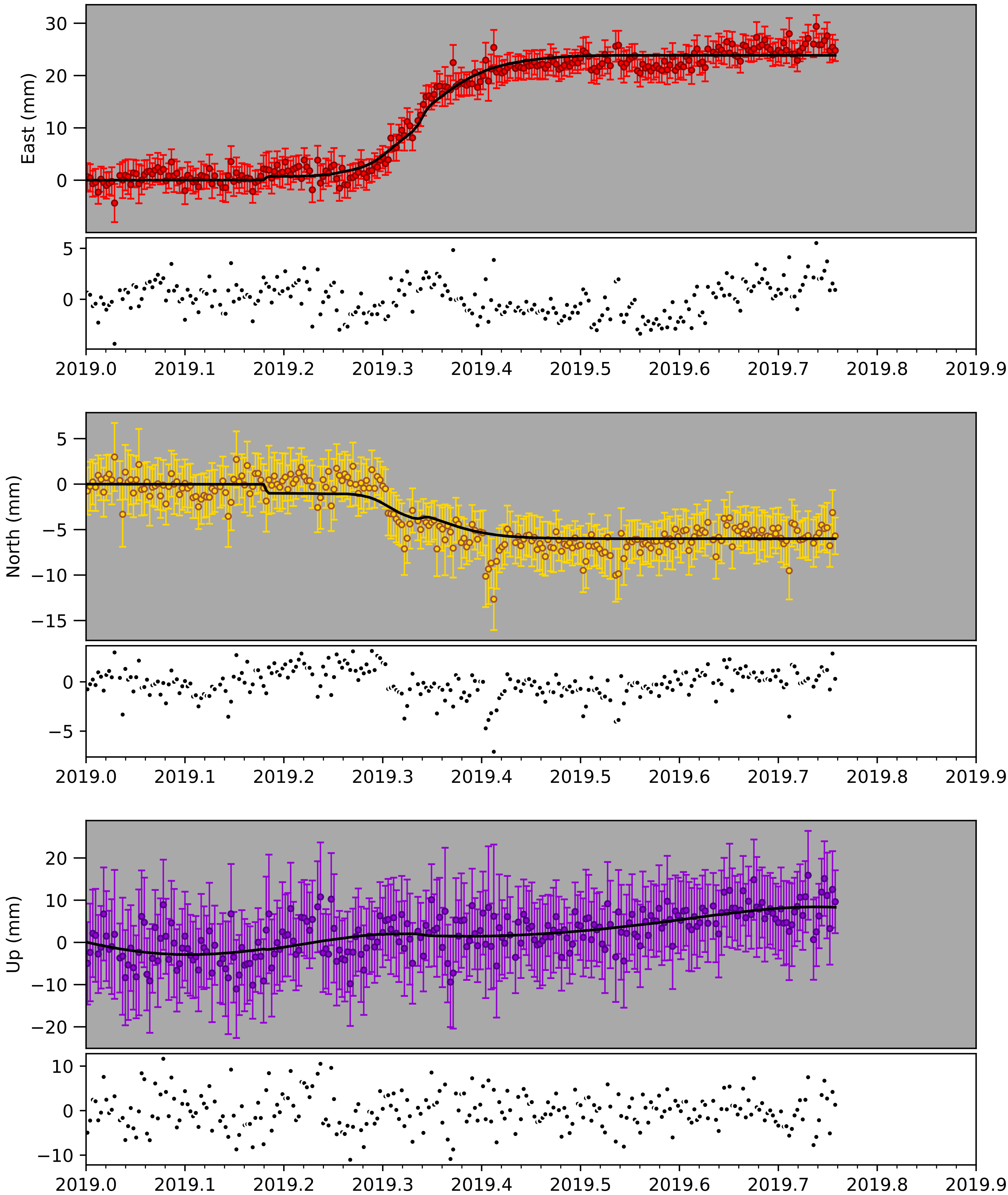

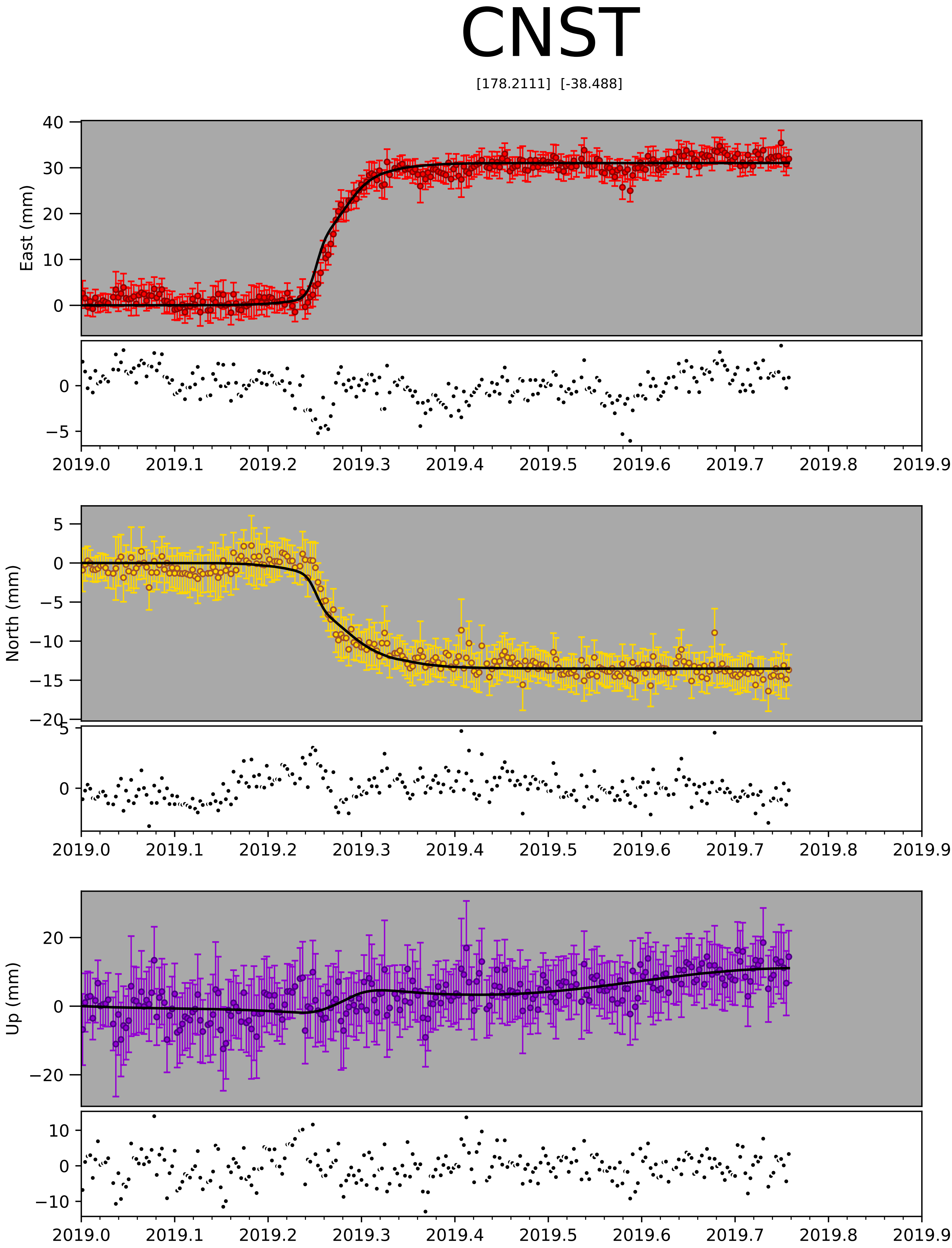
CNST
[178.2111] [-38.488]
East (mm)
North (mm)
Up (mm)
2019.0
2019.1
2019.2
2019.3
2019.4
2019.5
2019.6
2019.7
2019.8
2019.9

DNVK

[176.1667] [-40.2989]

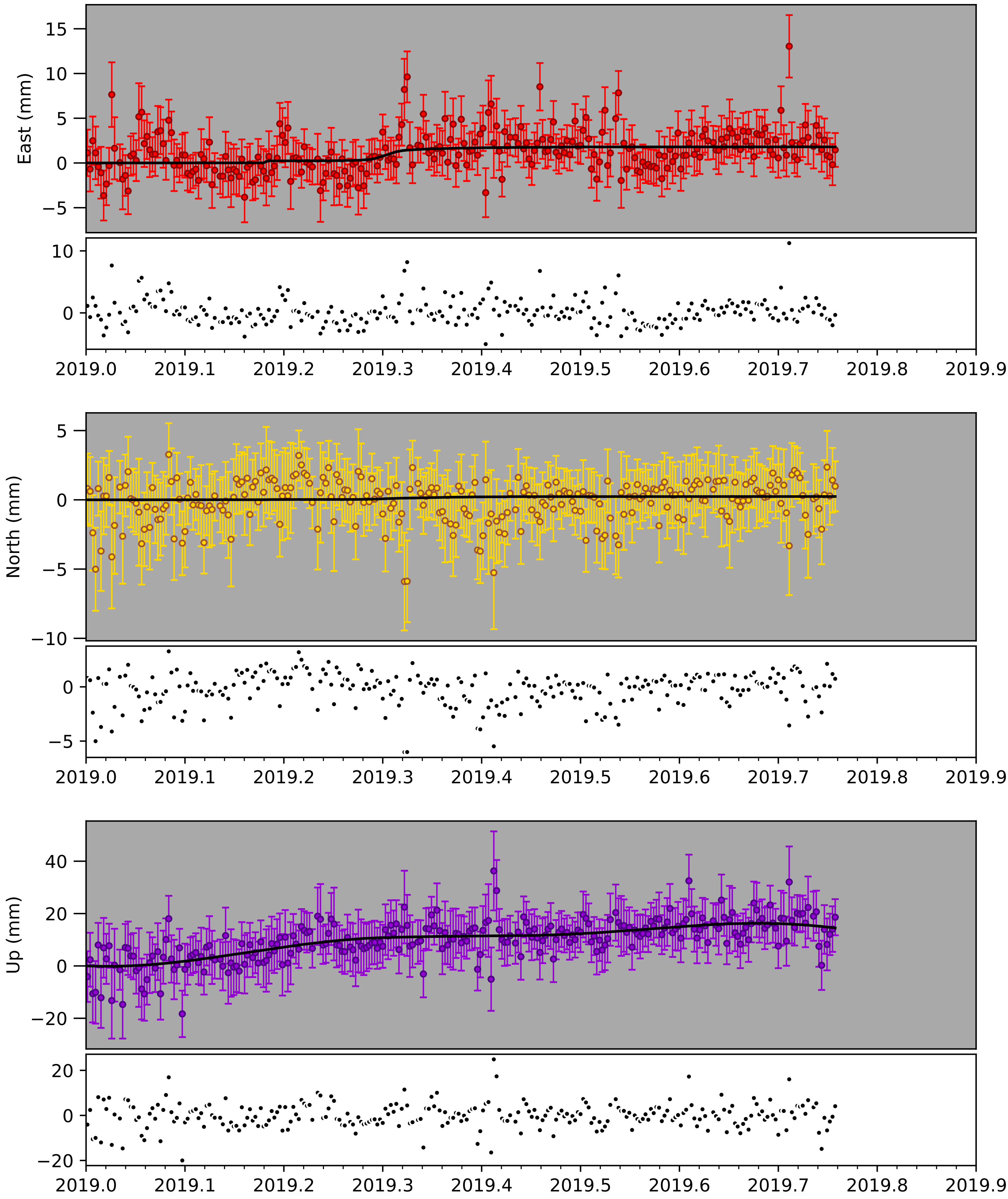

FRTN

[177.4099] [-38.9393]

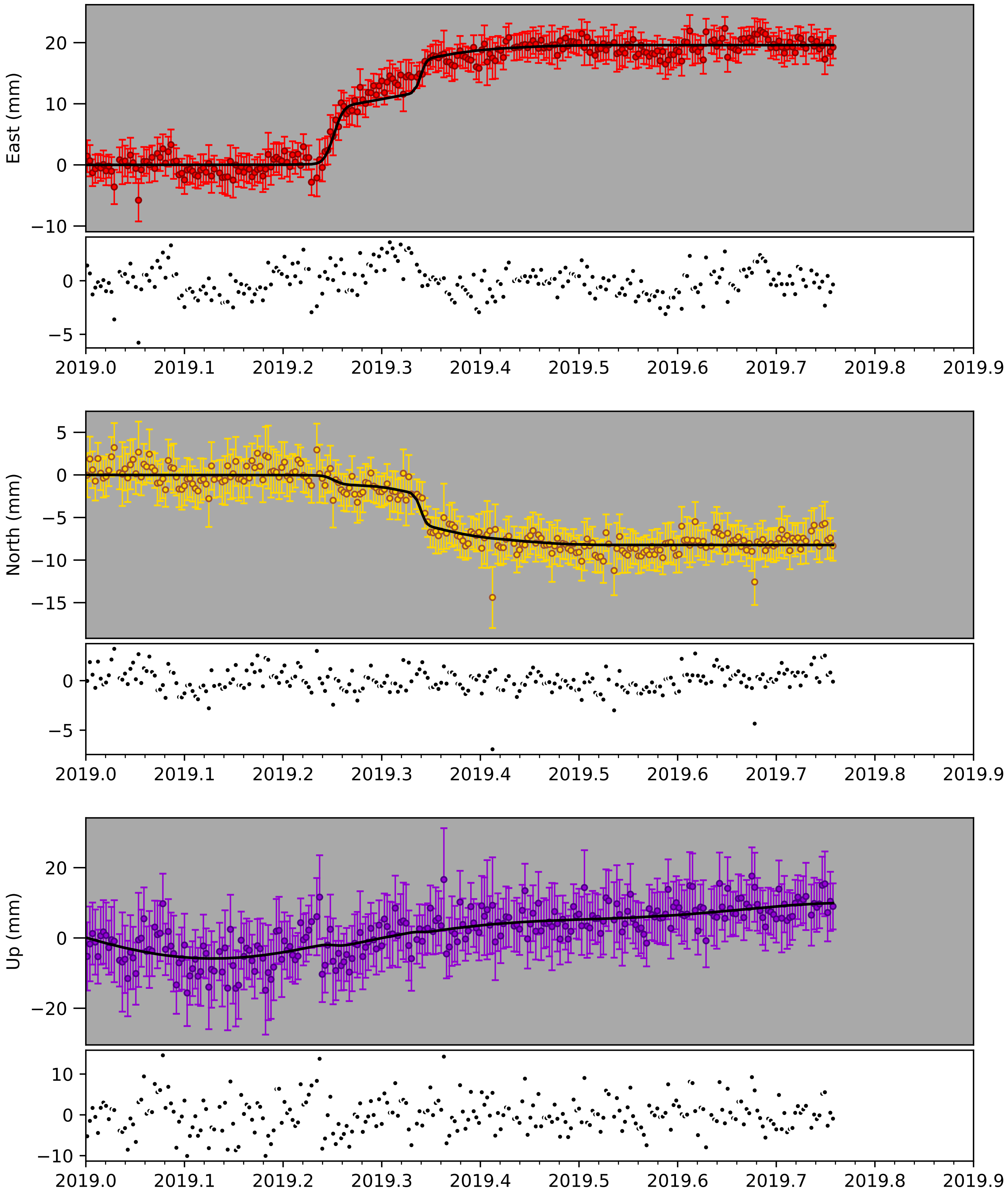

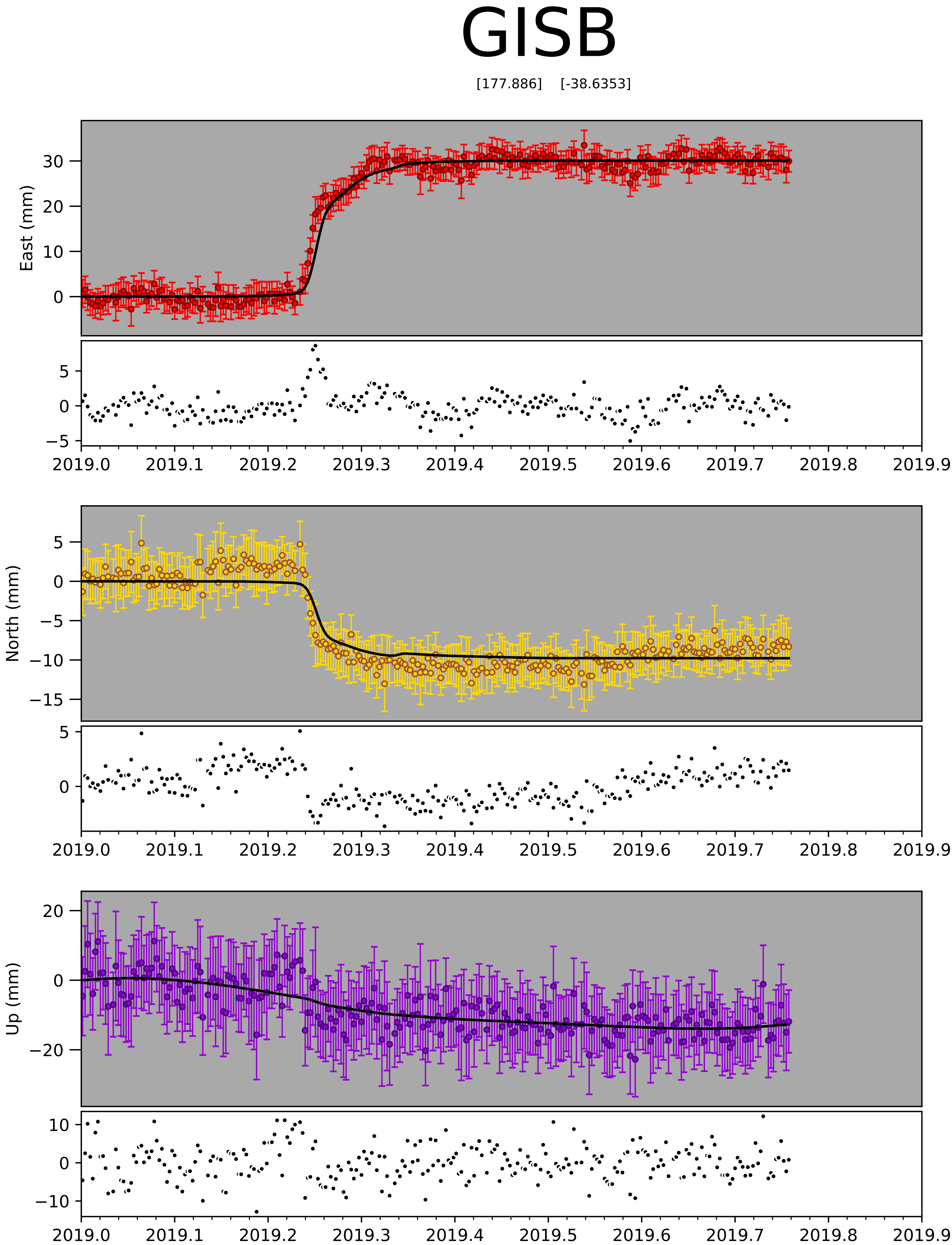
GISB
[177.886] [-38.6353]
East (mm)
North (mm)
Up (mm)
2019.0
2019.1
2019.2
2019.3
2019.4
2019.5
2019.6
2019.7
2019.8
2019.9

GNS3

[178.1485] [-39.6467]

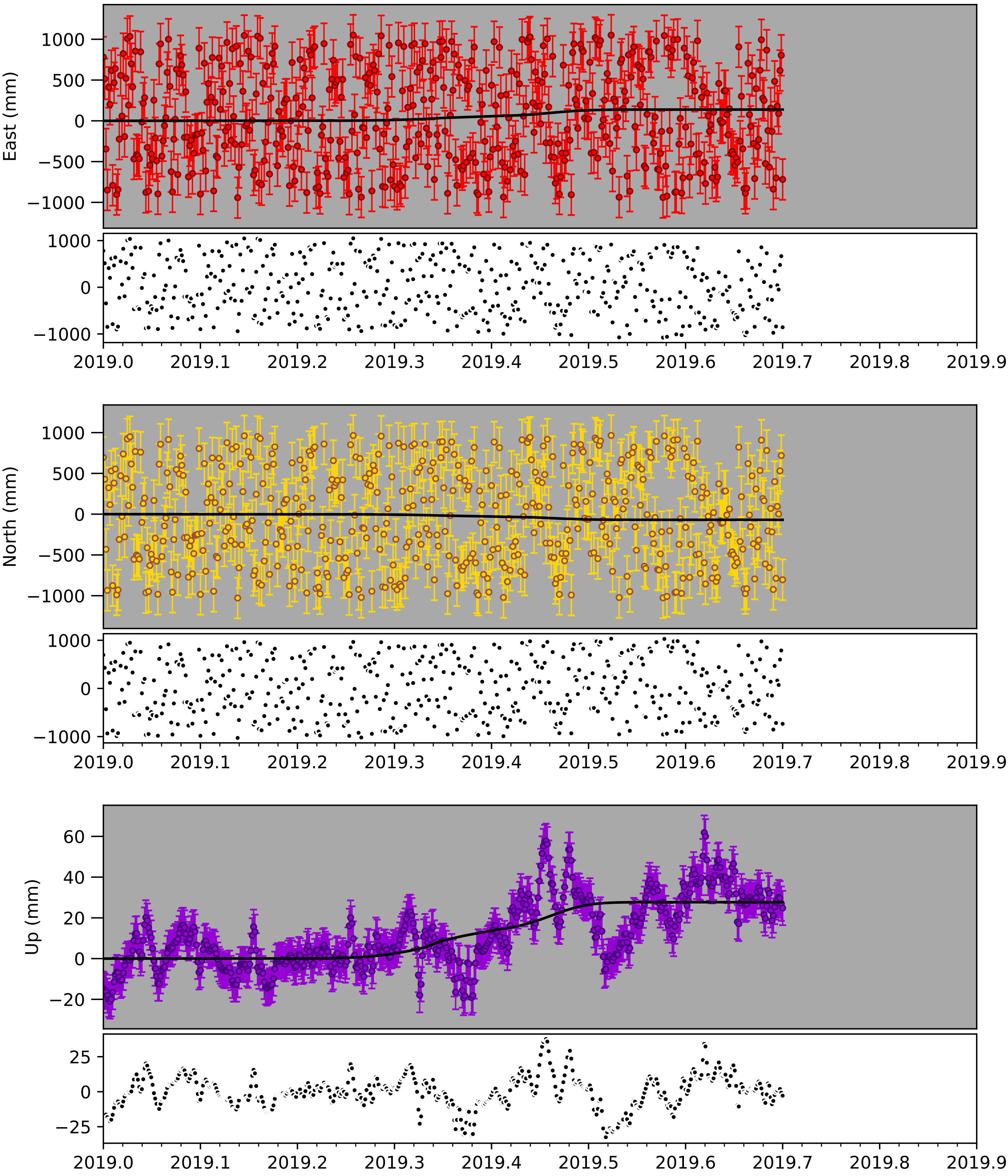

HANA

[177.5694] [-38.6868]

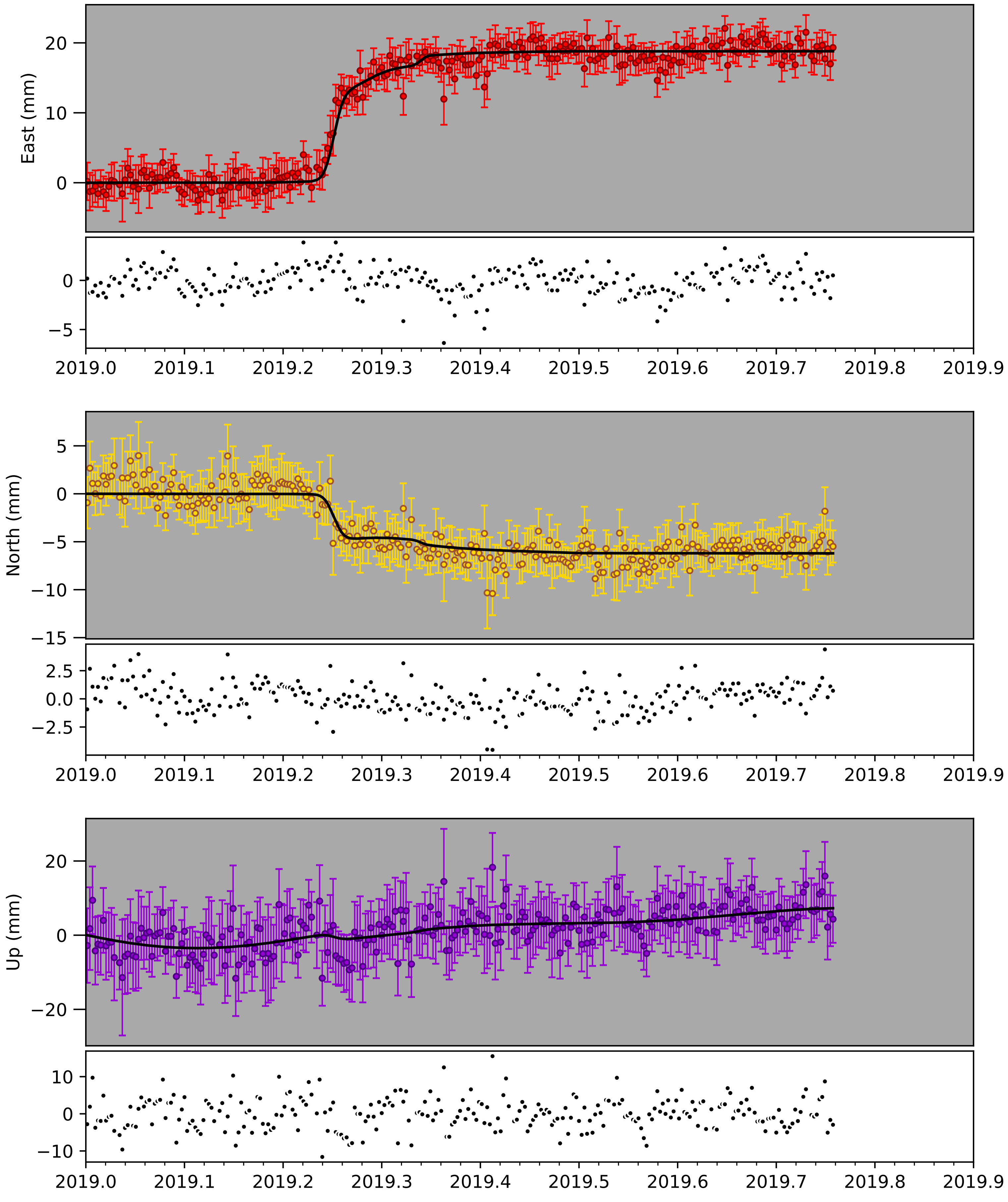

HAST

[176.7266] [-39.617]

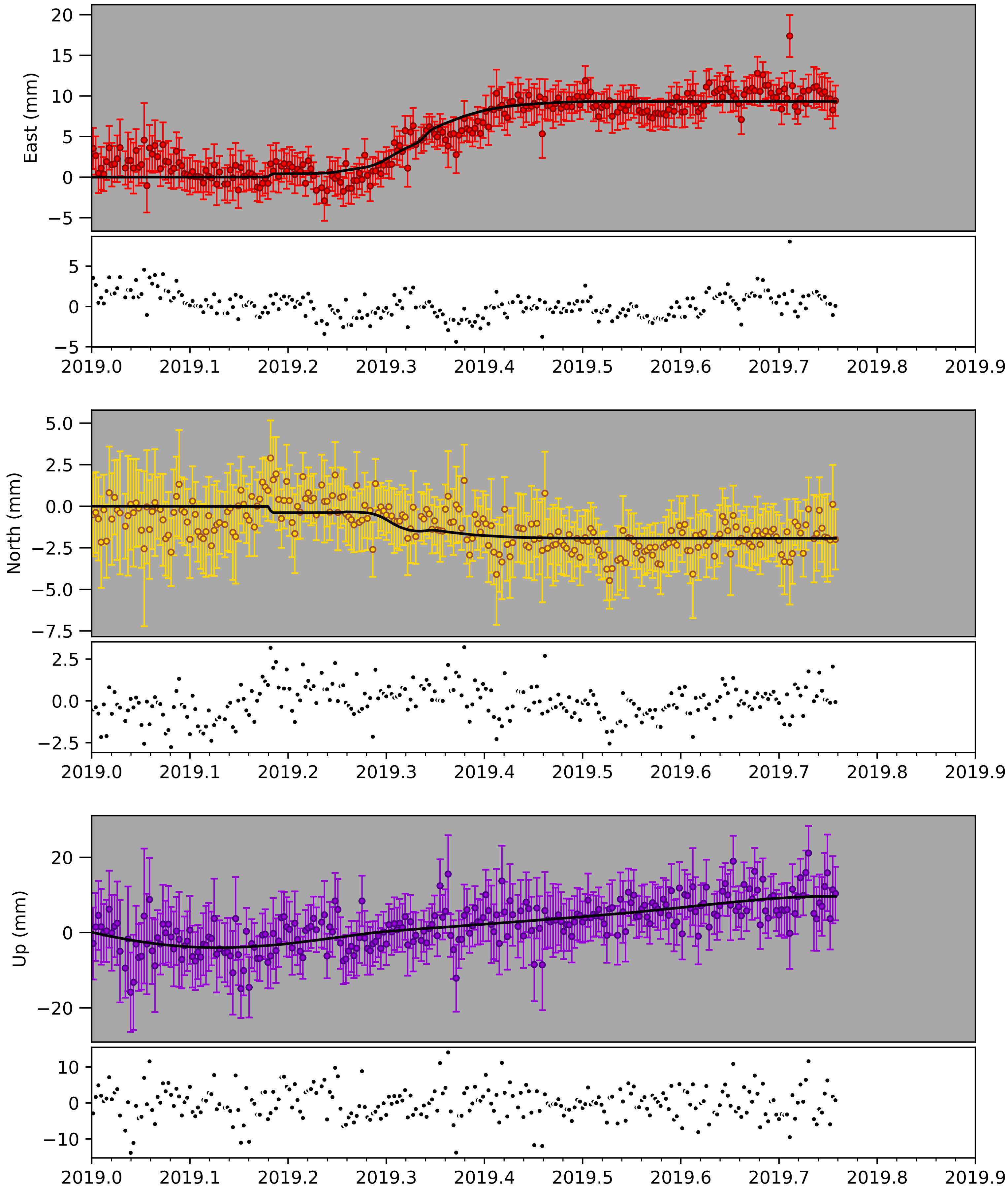

HIKB

[178.3033] [-37.561]

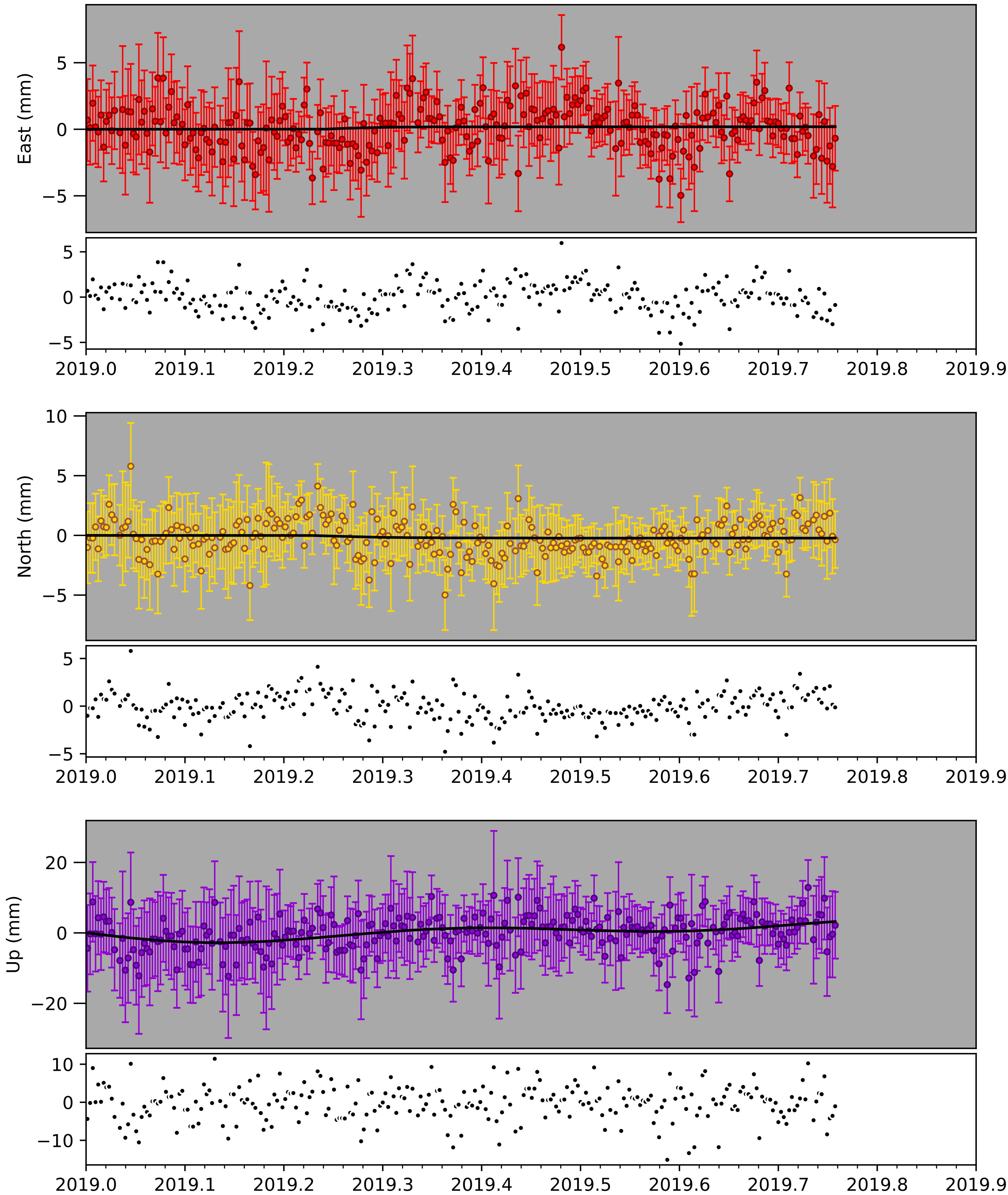

KAHU

[176.8763] [-39.7938]

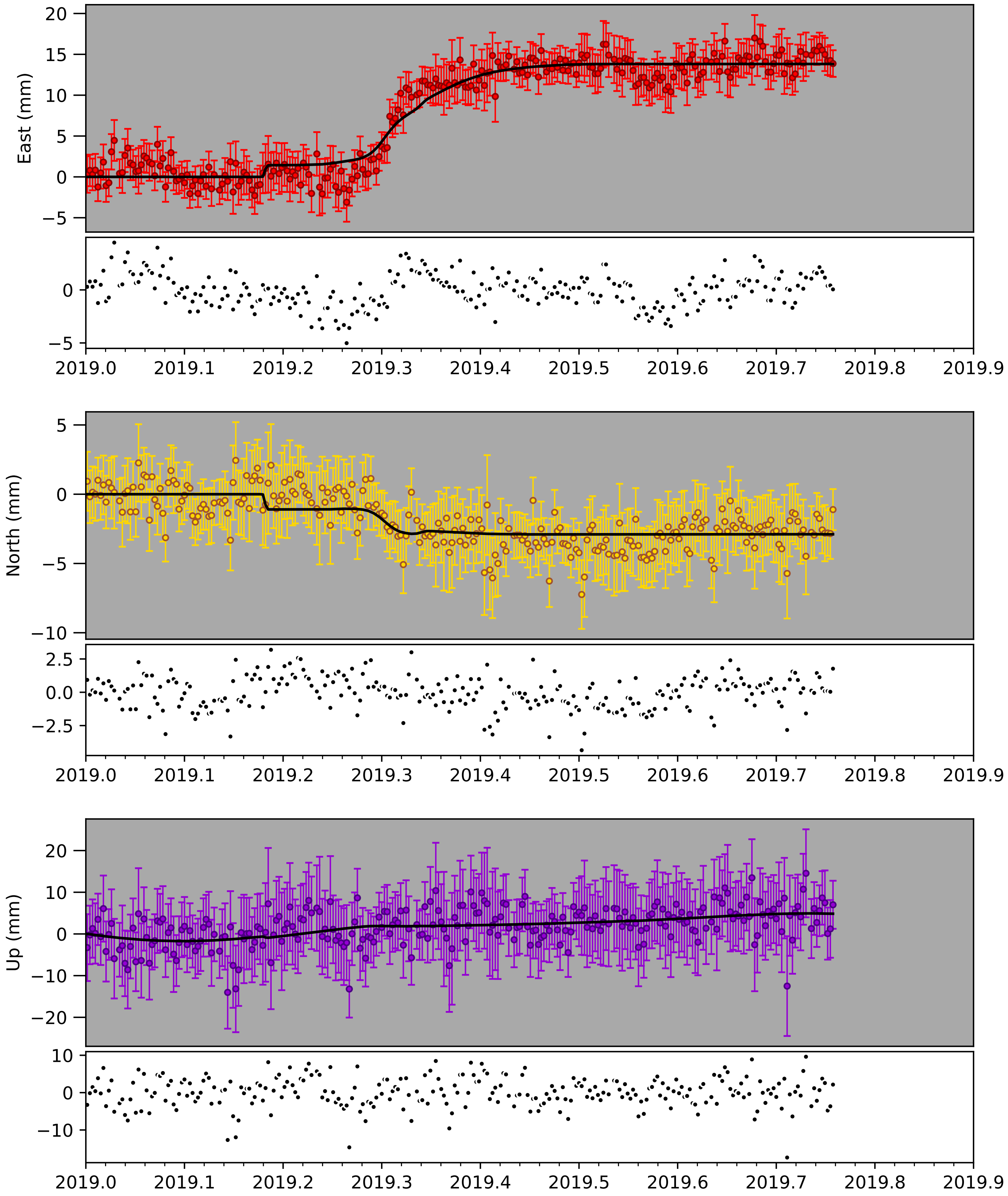

KAWK

[176.4228] [-39.424]

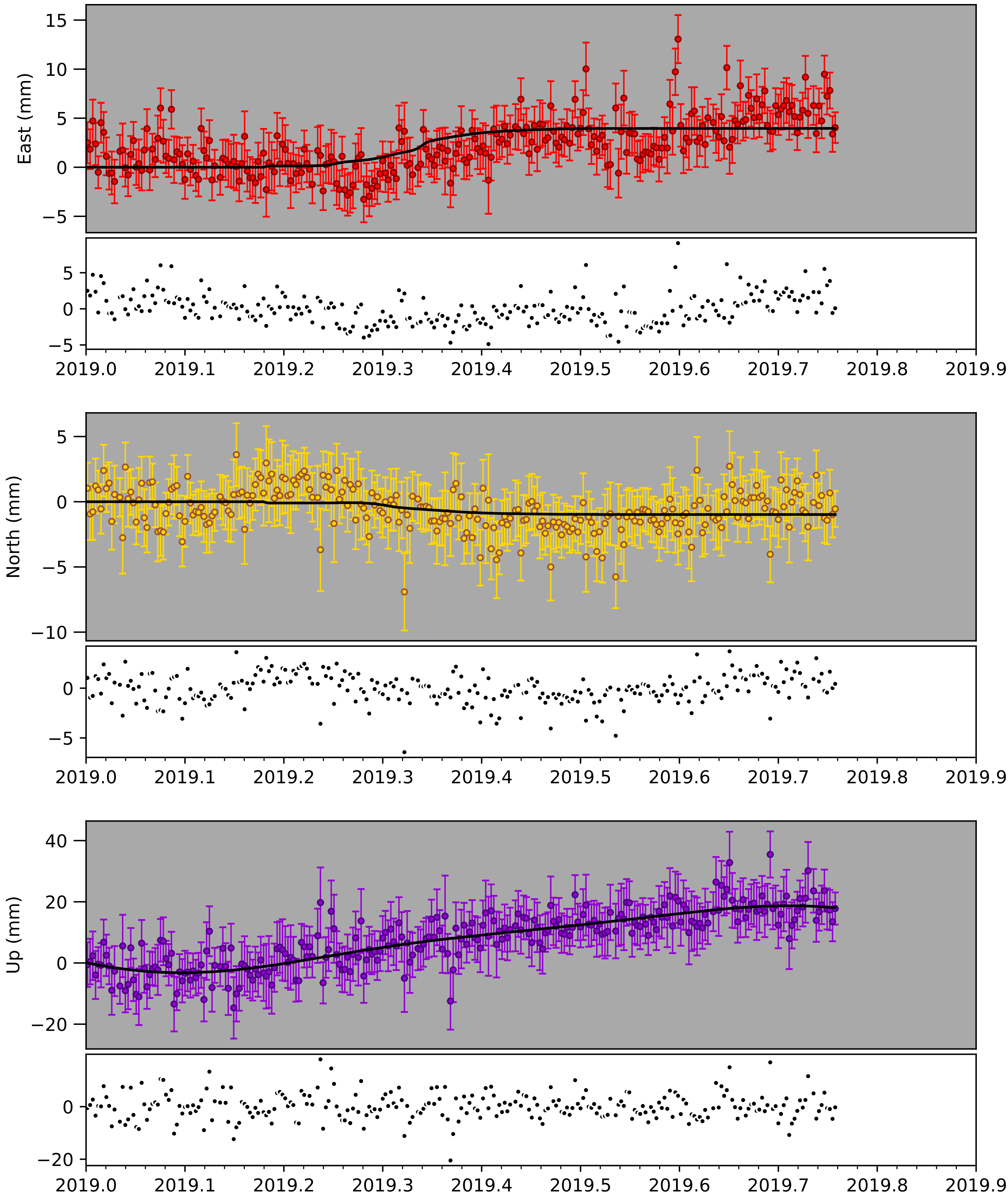

KERE

[176.3701] [-39.6432]

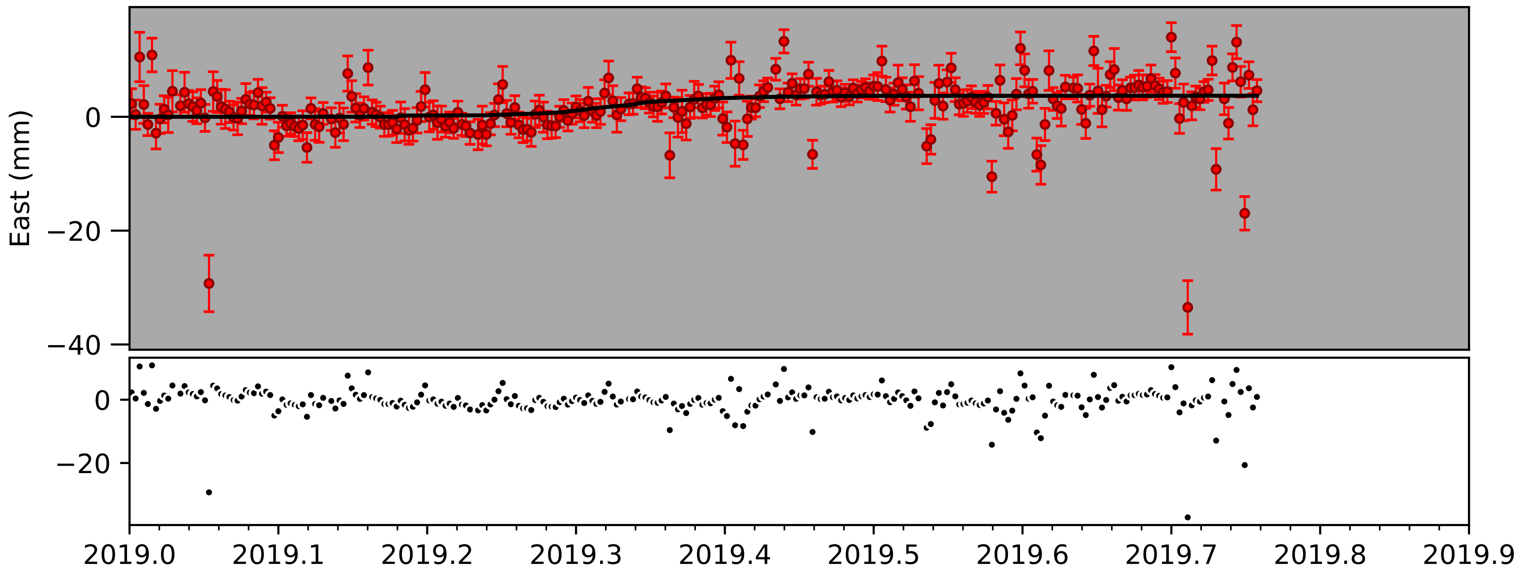

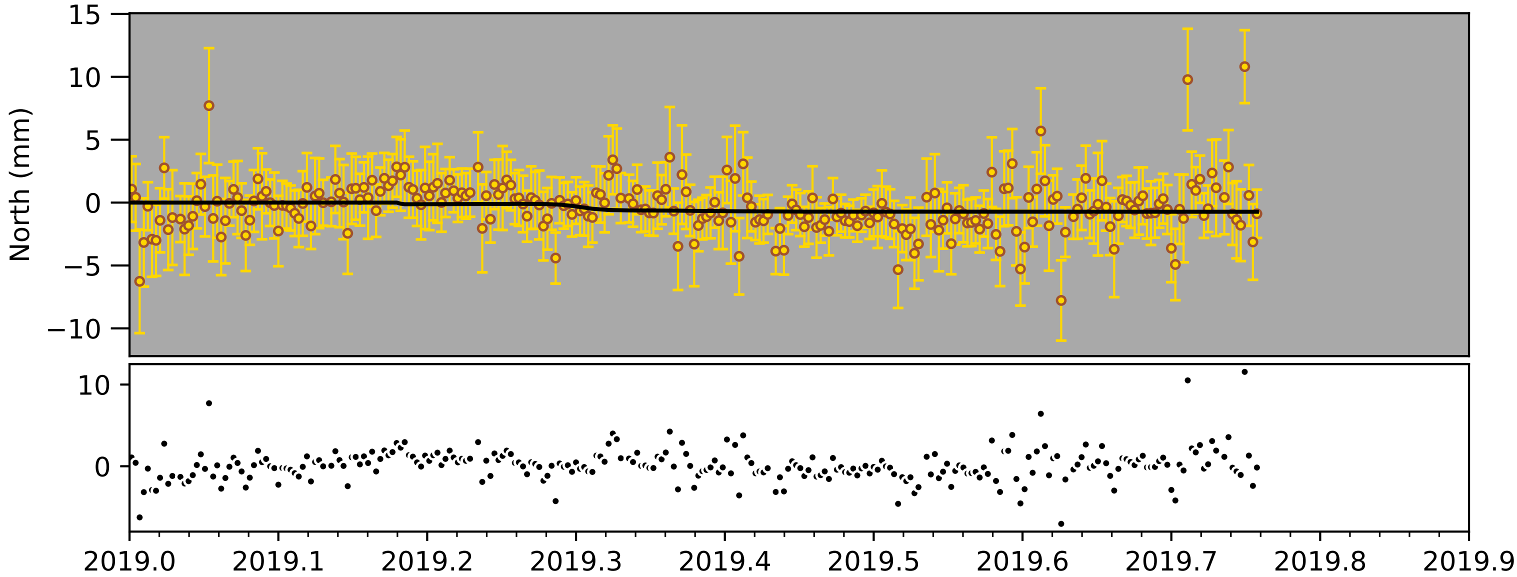

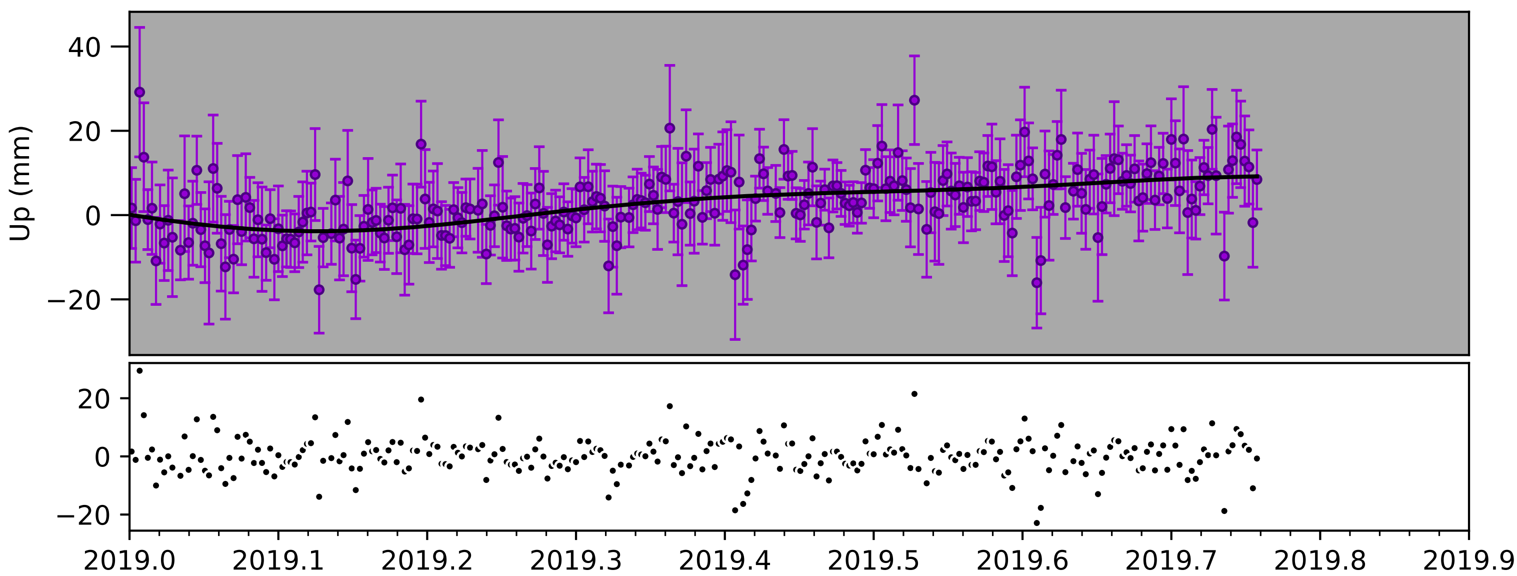

KOKO

[177.6678] [-39.0161]

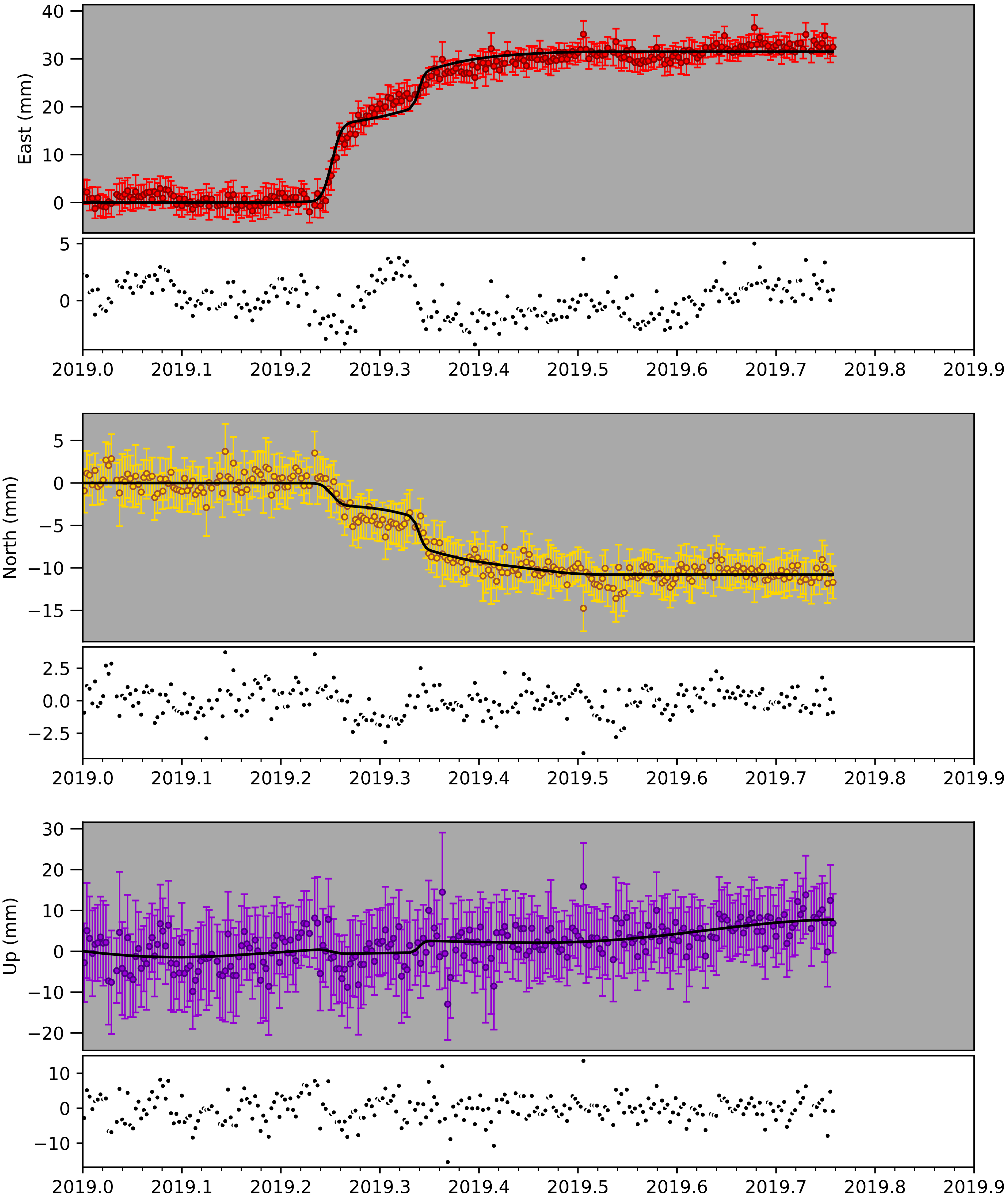

KU02

[178.8452] [-38.8762]

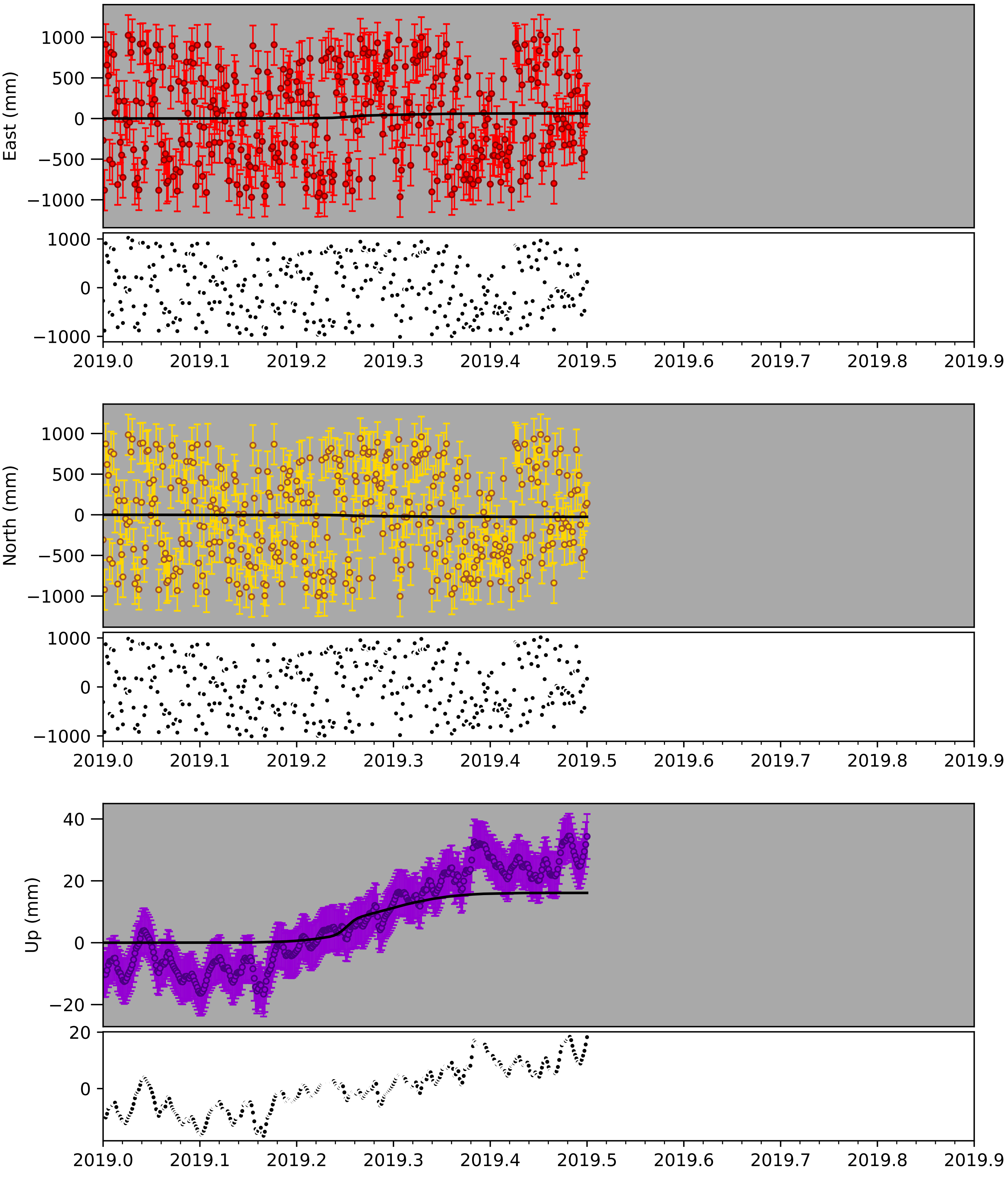

KU03

[178.7551] [-38.8926]

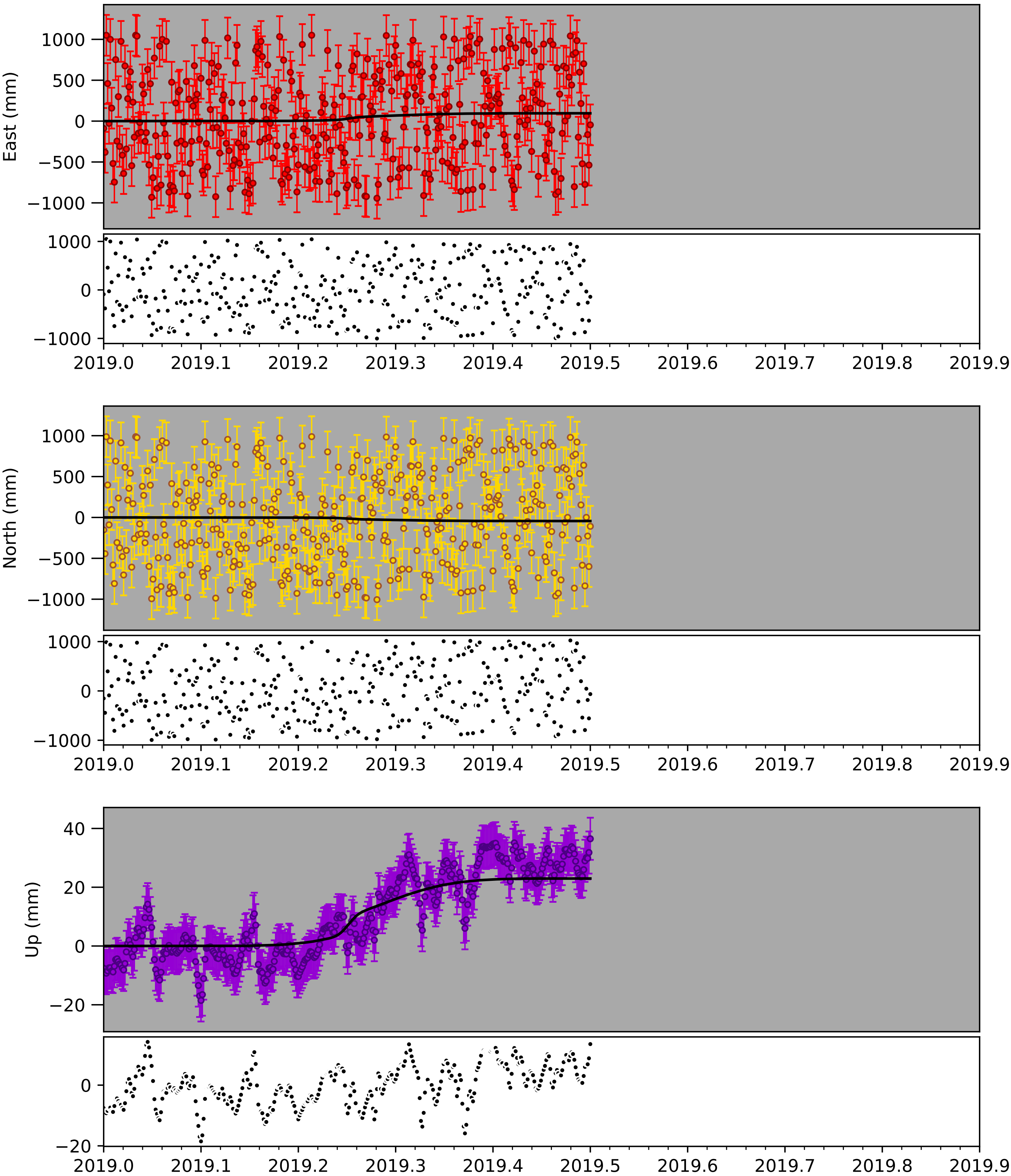

KU04

[178.671]   [-38.7939]

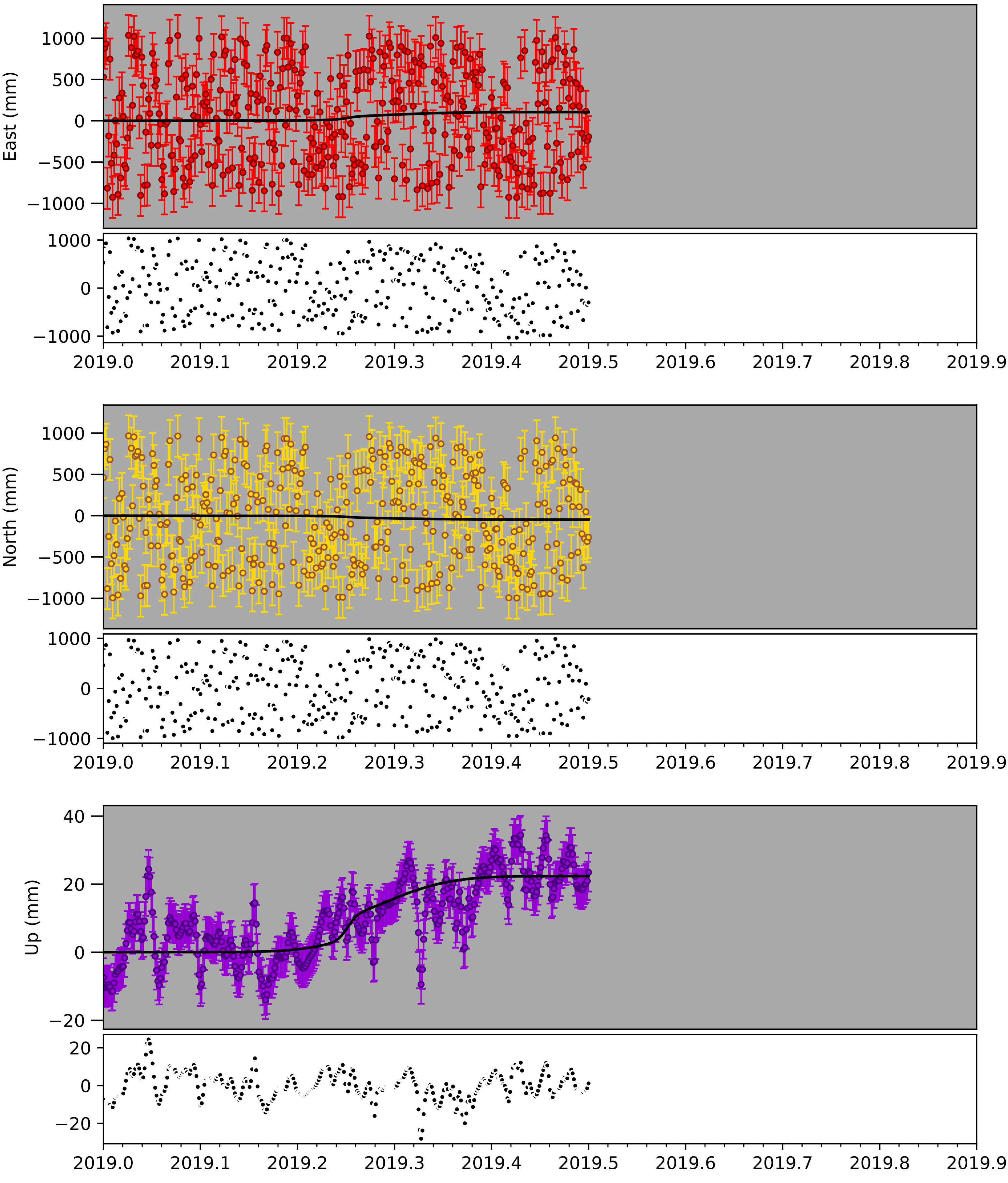

KUTA

[177.0698] [-39.1723]

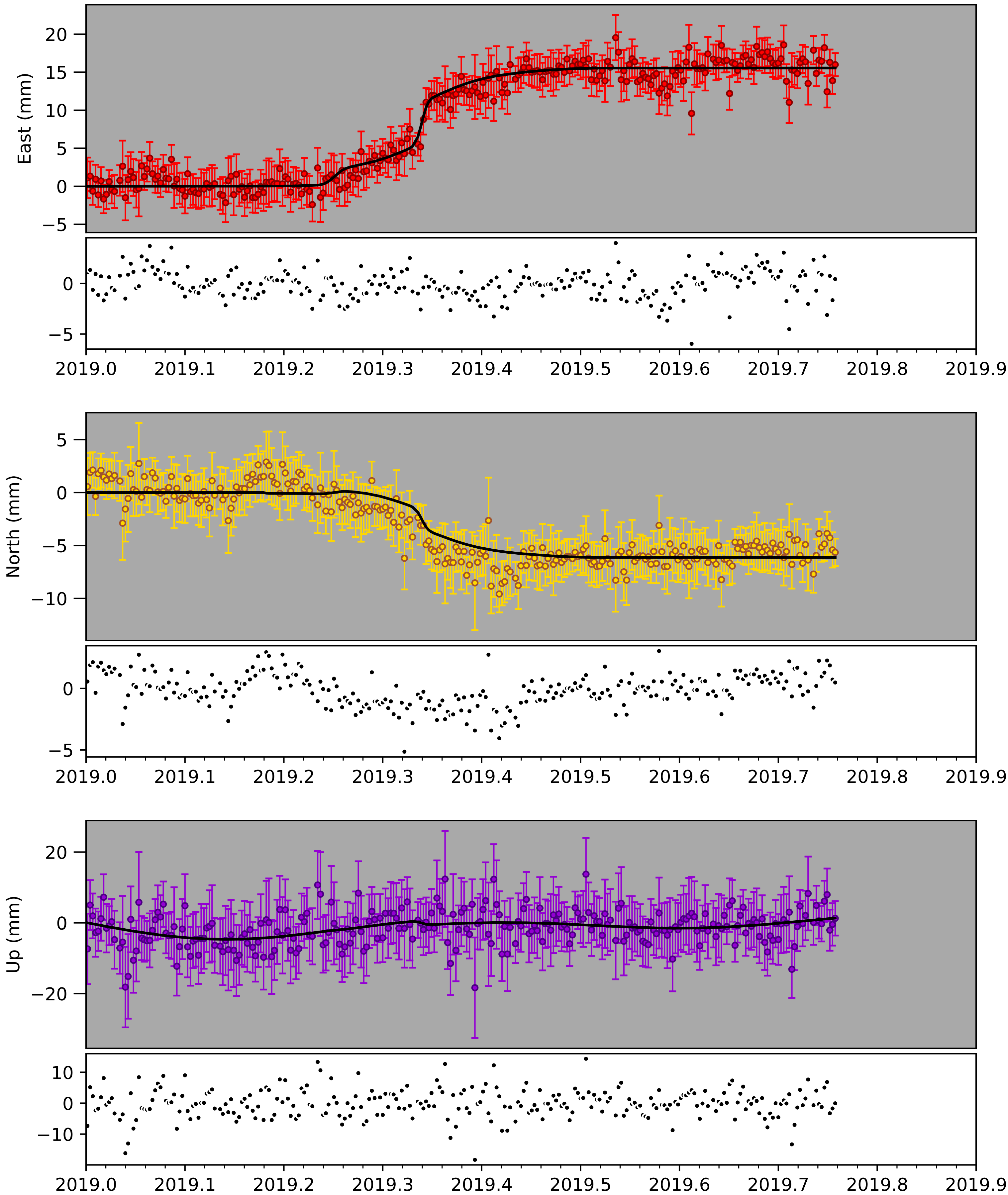

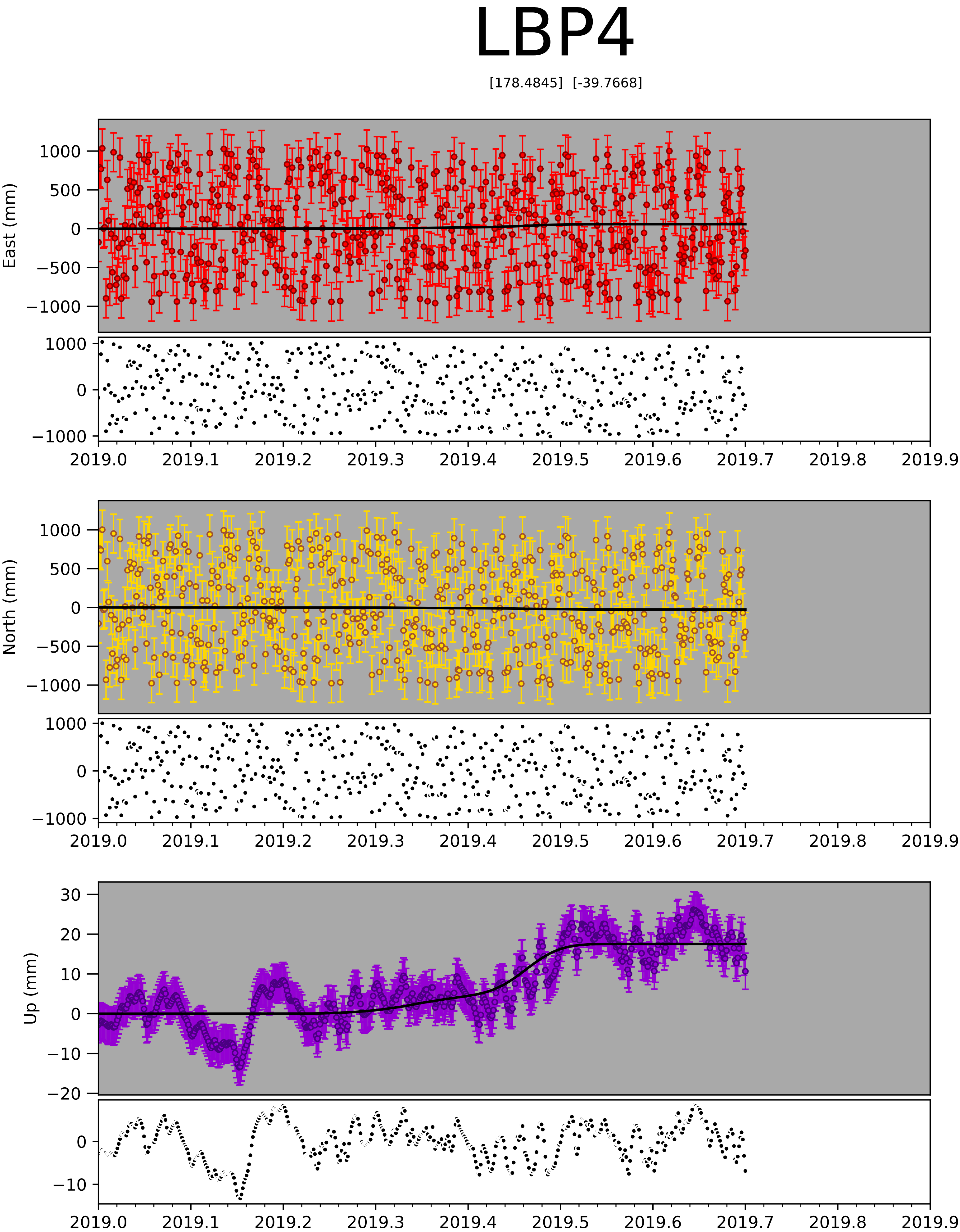

LBP4
[178.4845] [-39.7668]
East (mm)
1000
500
0
−500
−1000
1000
0
−1000
2019.0
2019.1
2019.2
2019.3
2019.4
2019.5
2019.6
2019.7
2019.8
2019.9
North (mm)
1000
500
0
−500
−1000
1000
0
−1000
2019.0
2019.1
2019.2
2019.3
2019.4
2019.5
2019.6
2019.7
2019.8
2019.9
Up (mm)
30
20
10
0
−10
−20
0
−10
2019.0
2019.1
2019.2
2019.3
2019.4
2019.5
2019.6
2019.7
2019.8
2019.9

LEYL

[176.9367] [-39.3323]

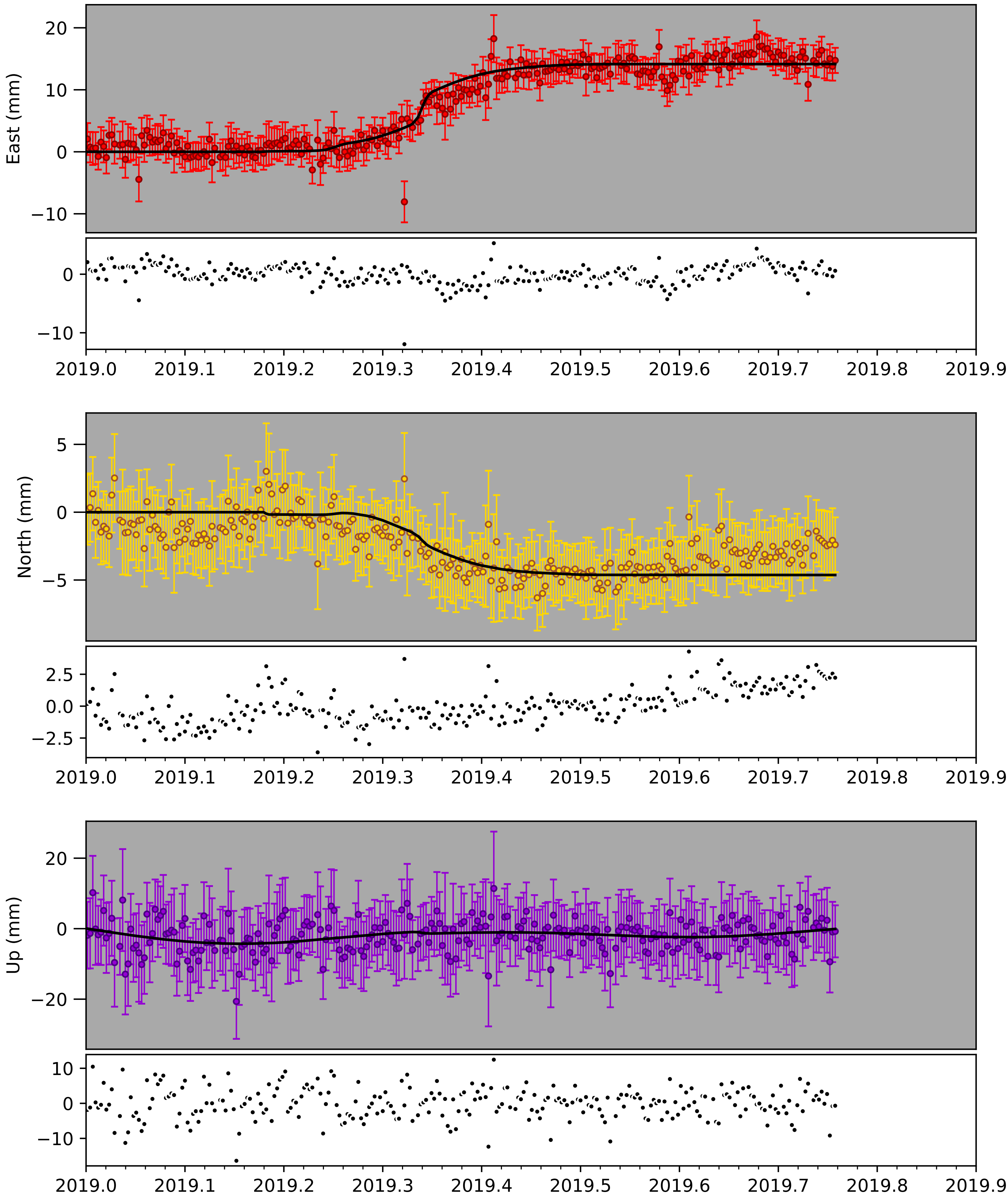

MAHI

[177.907] [-39.1526]

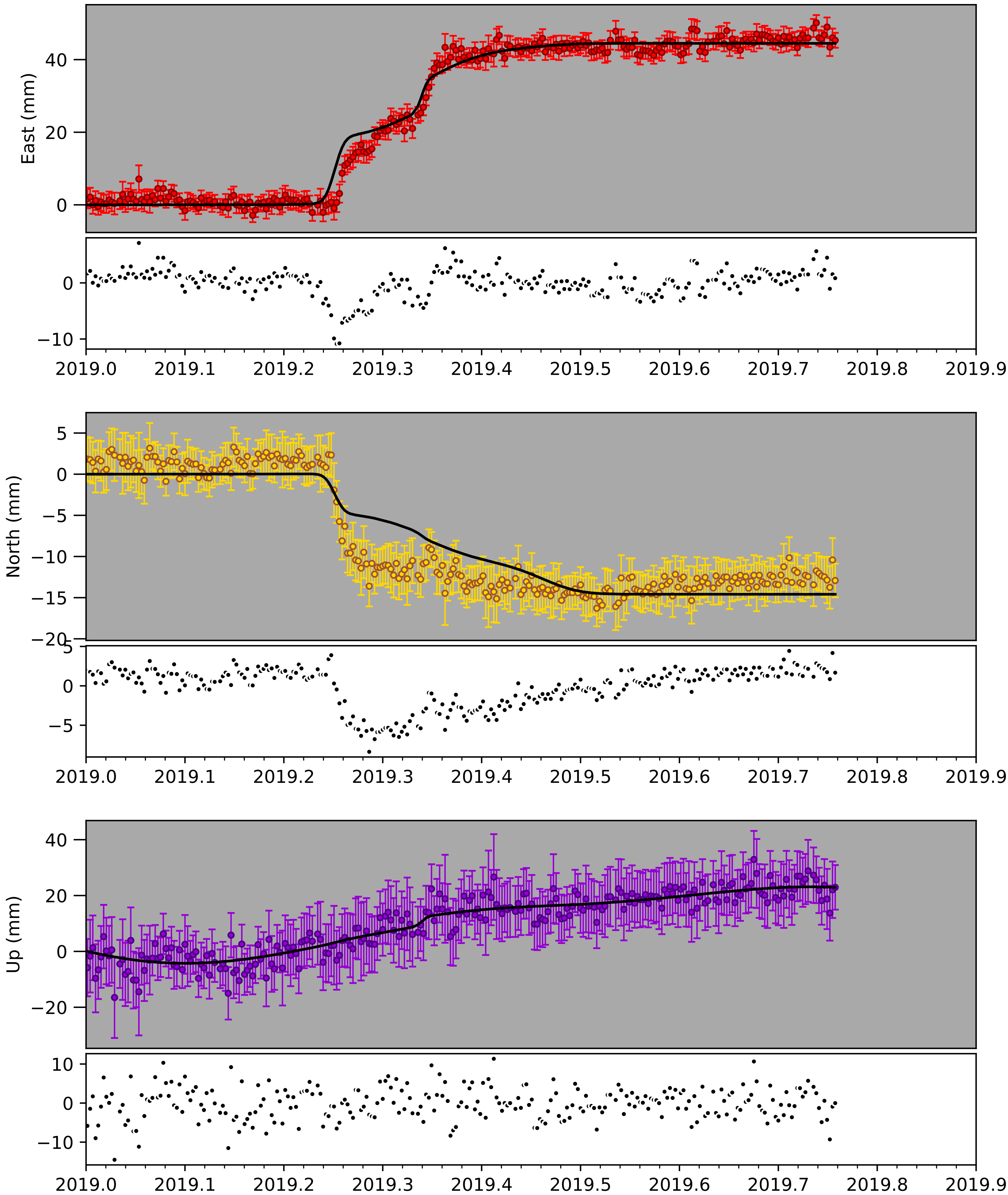

MAKO

[178.1291] [-38.6438]

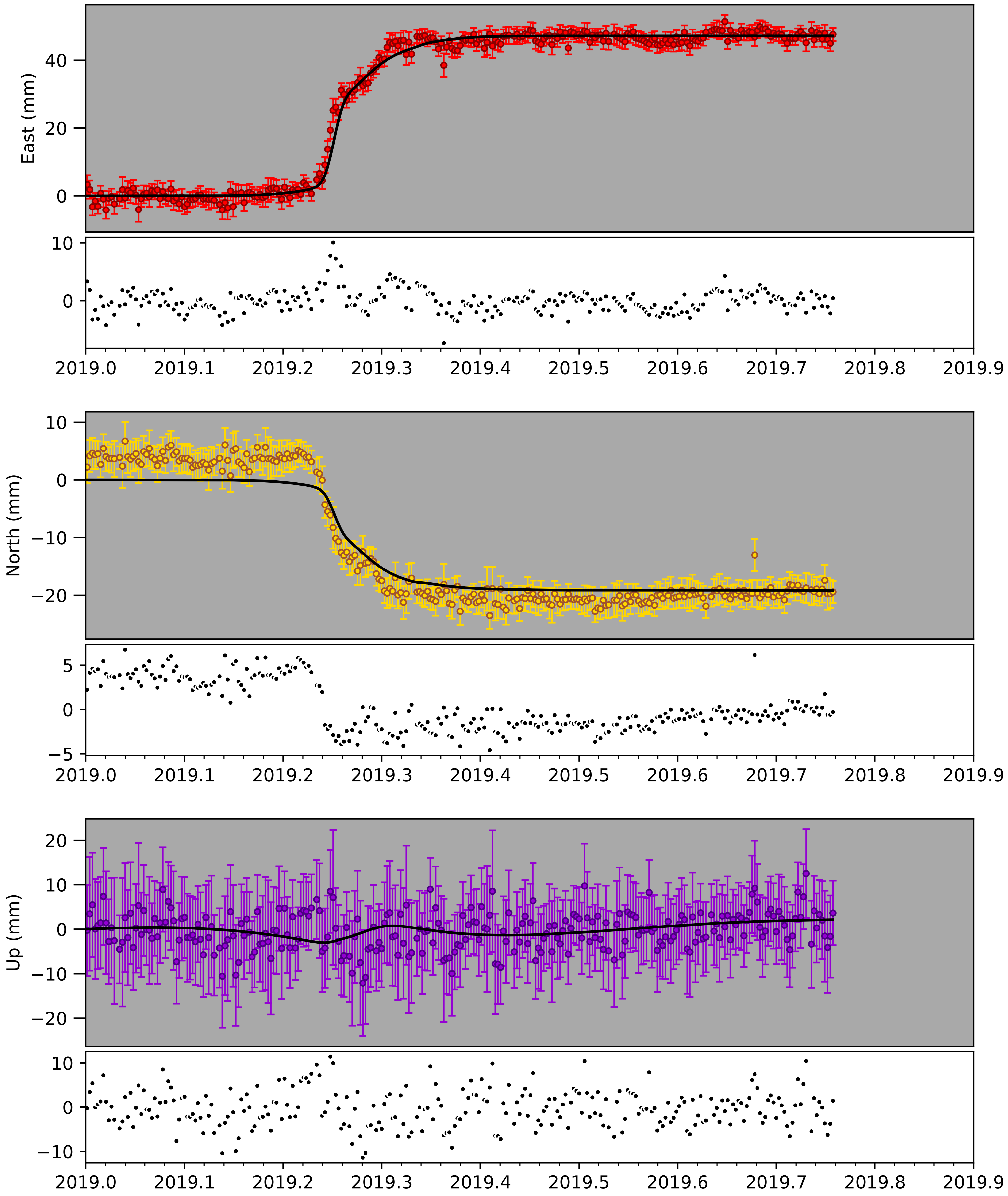

MATW

[177.5262] [-38.3338]

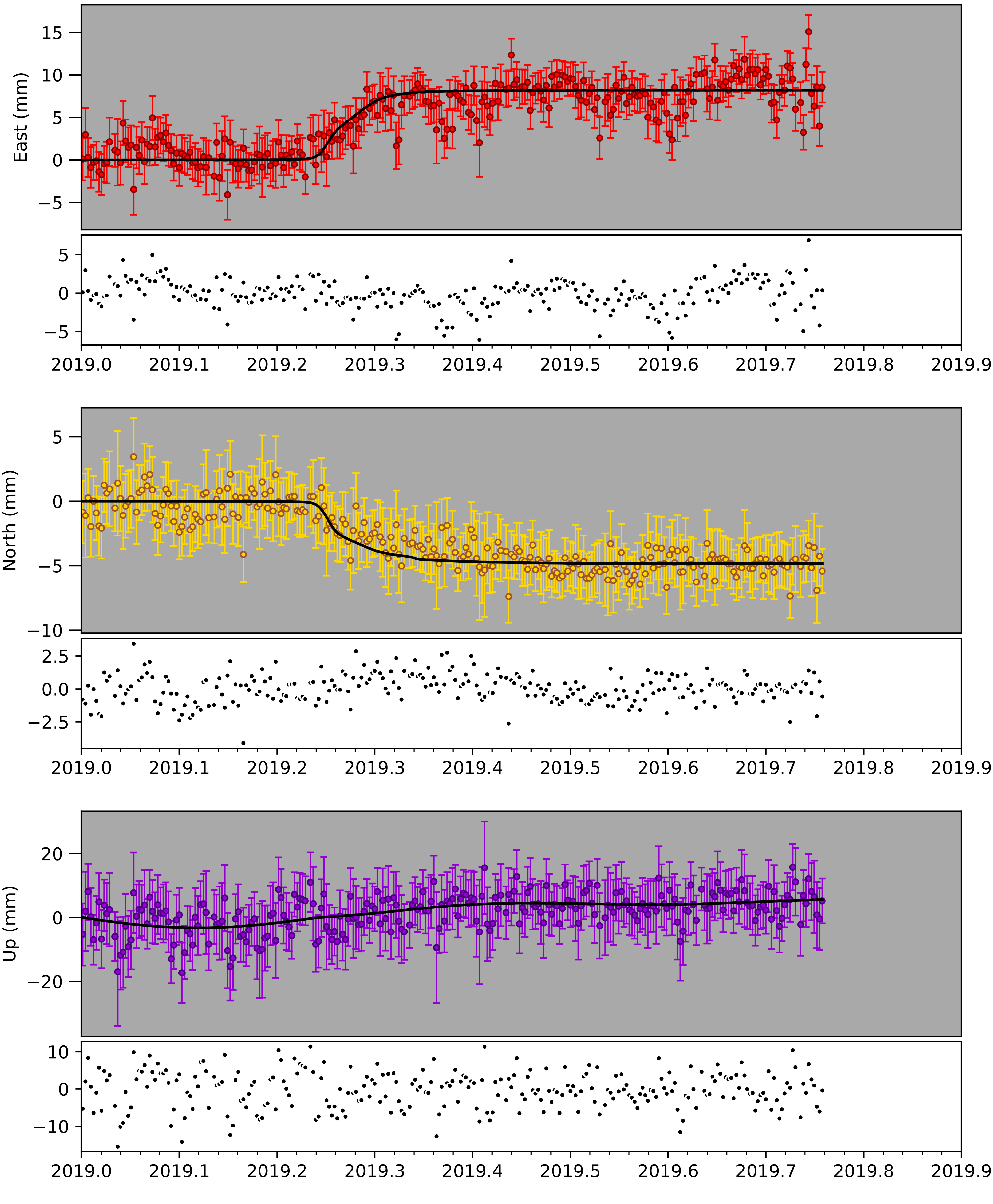

MCNL

[176.6966] [-39.4442]

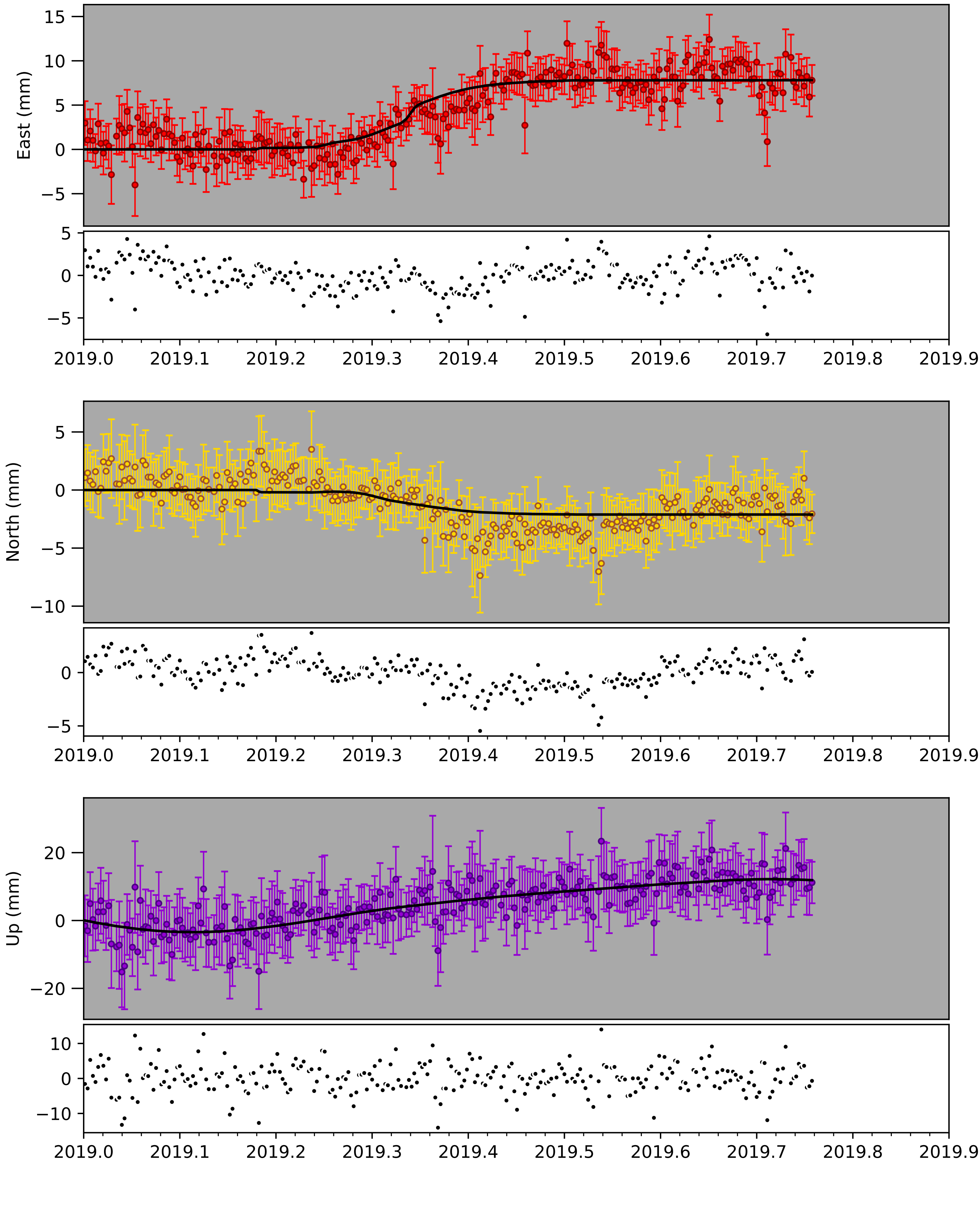

MING

[176.7497] [-38.6169]

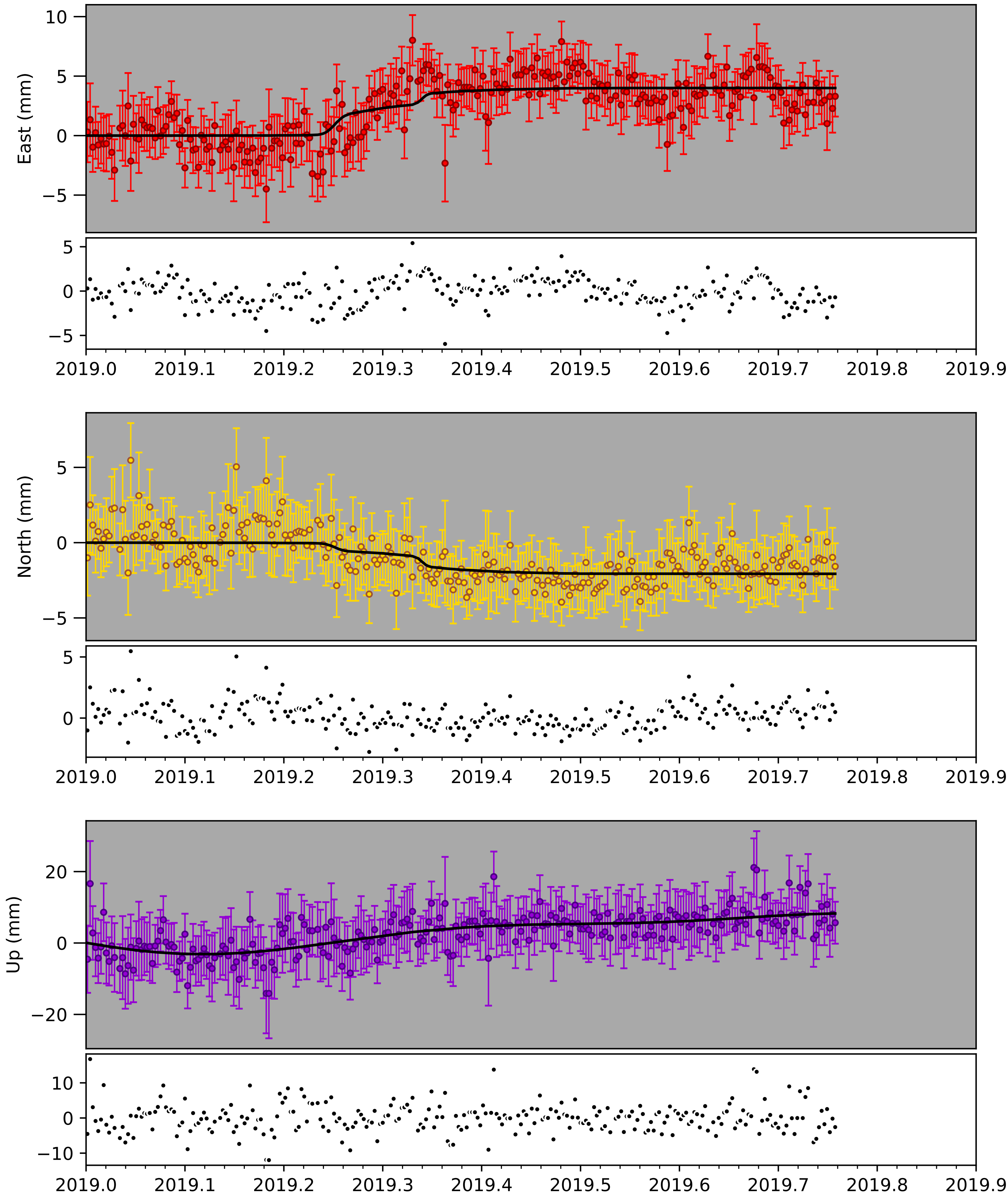

MKNO

[176.0288] [-39.7034]

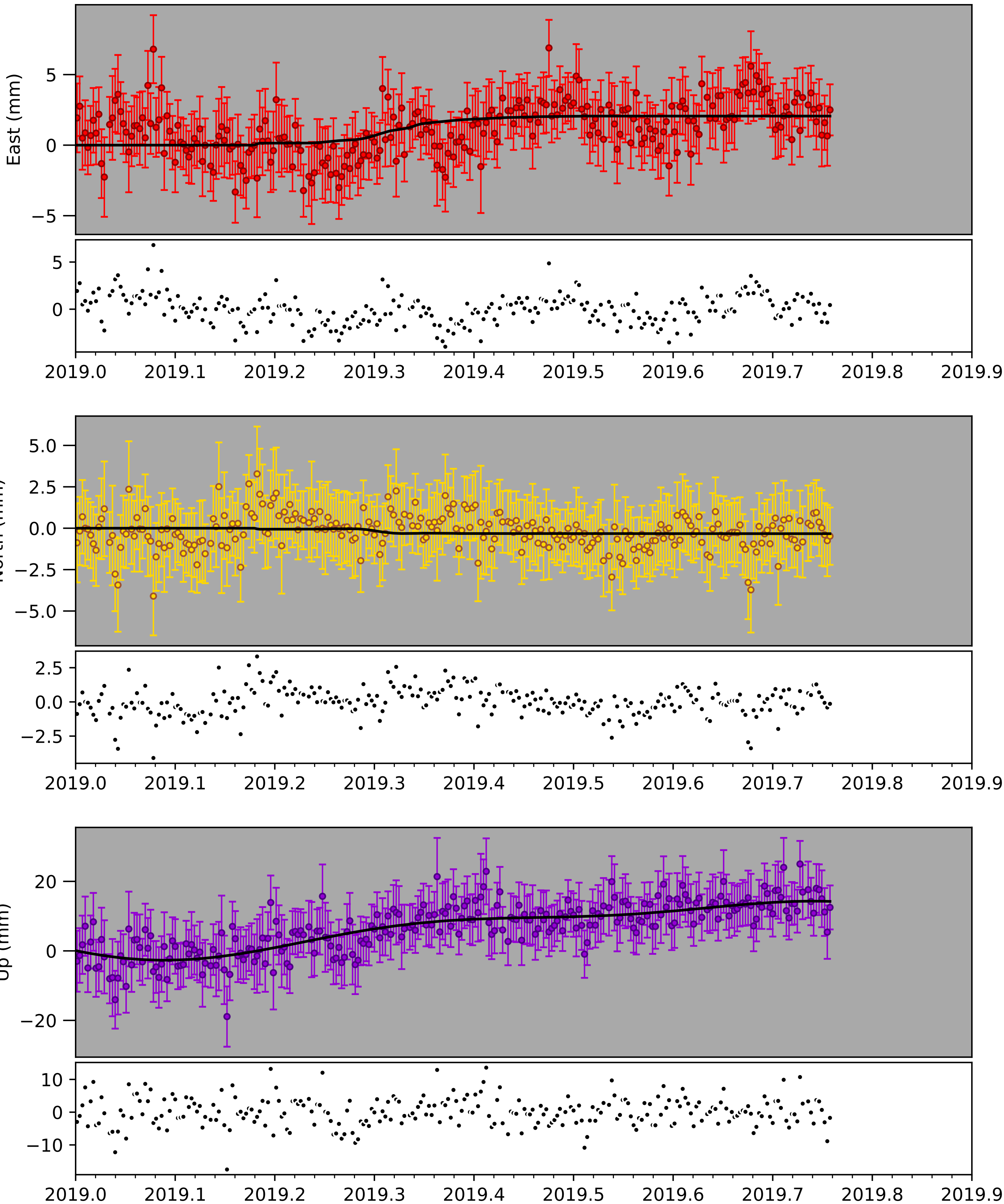

MNHR

[176.2234] [-40.4686]

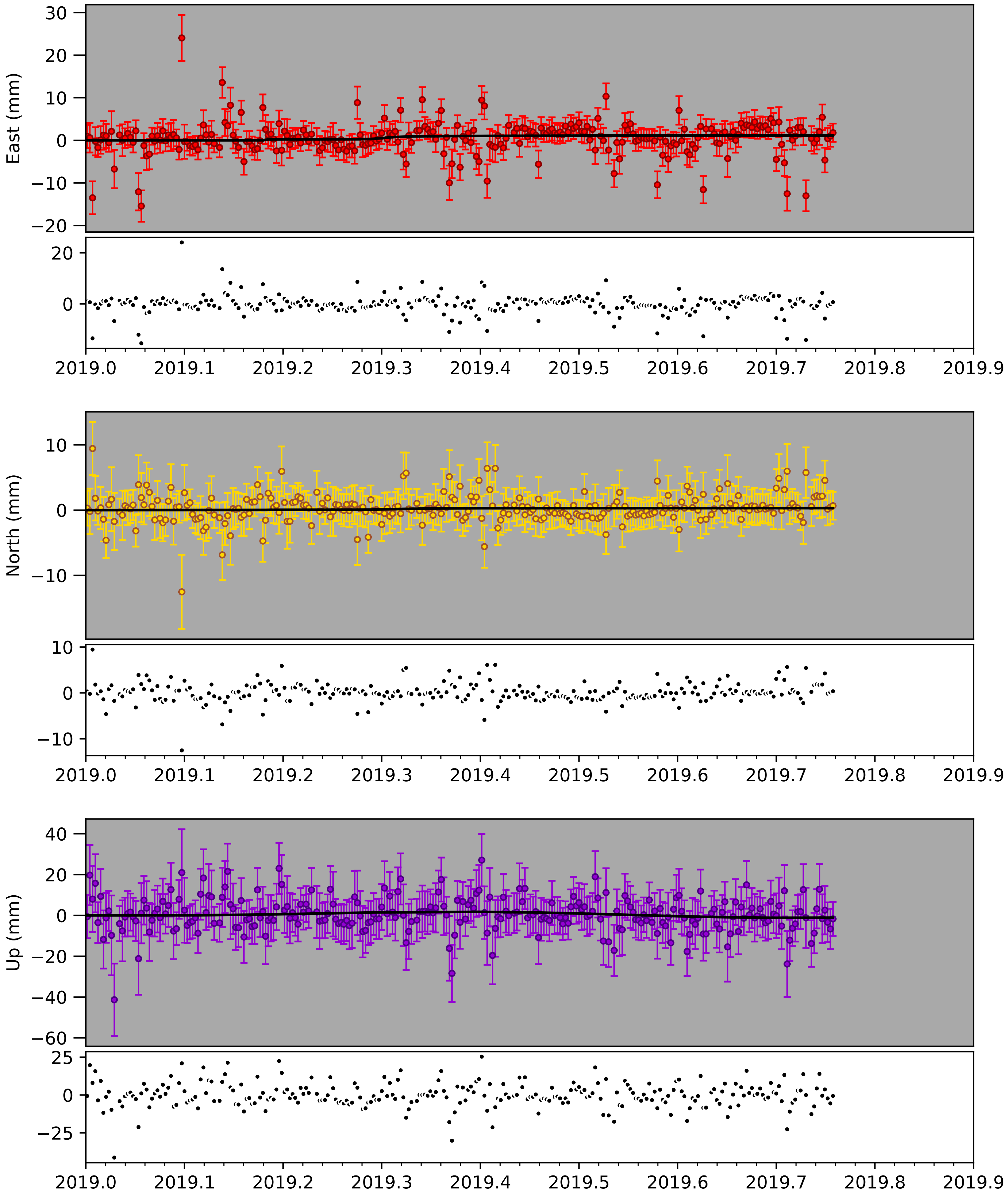

NMAI

[176.8066] [-39.097]

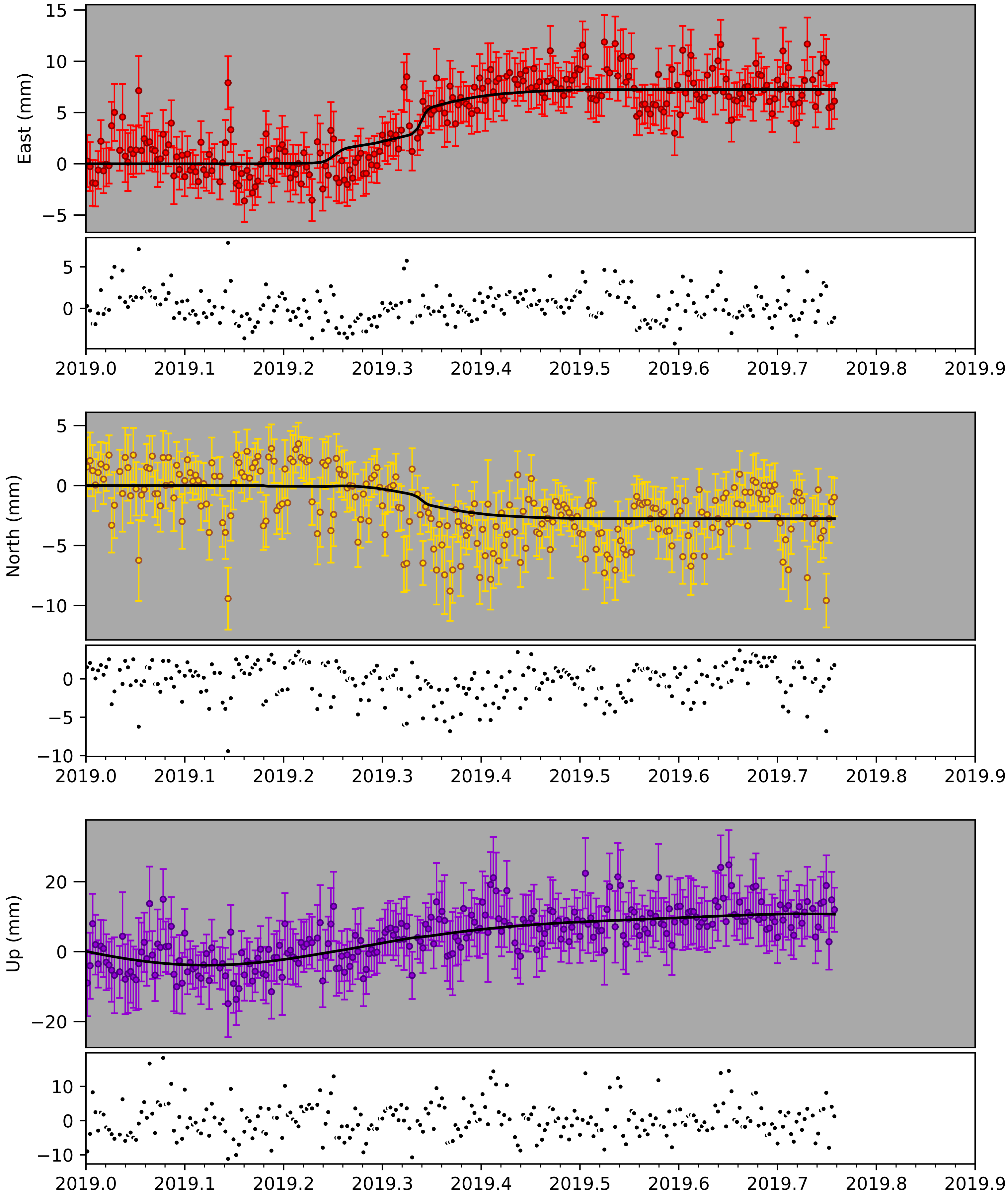

NRSW

[176.2] [-40.1133]

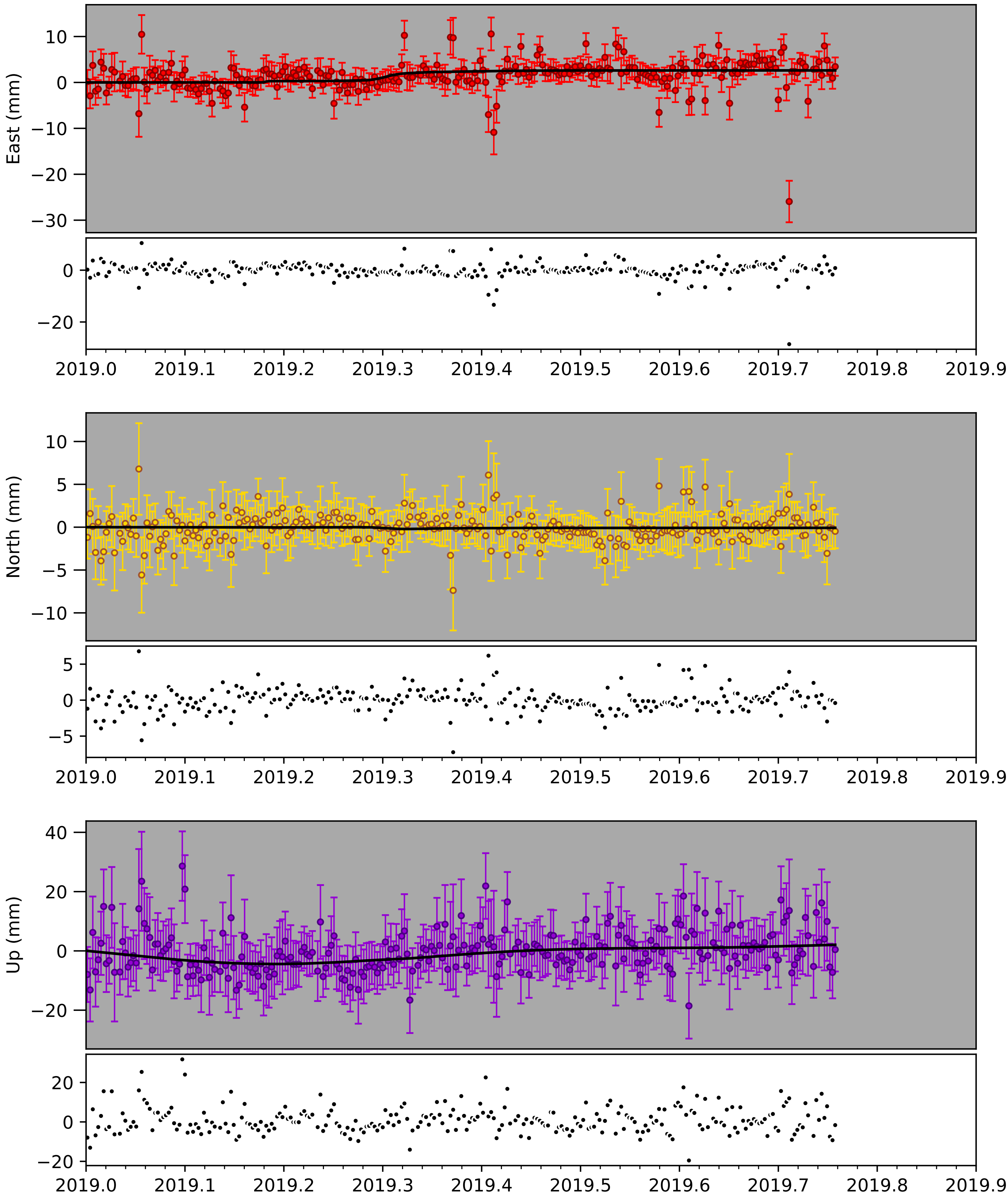

OHIN

[175.7907] [-39.9183]

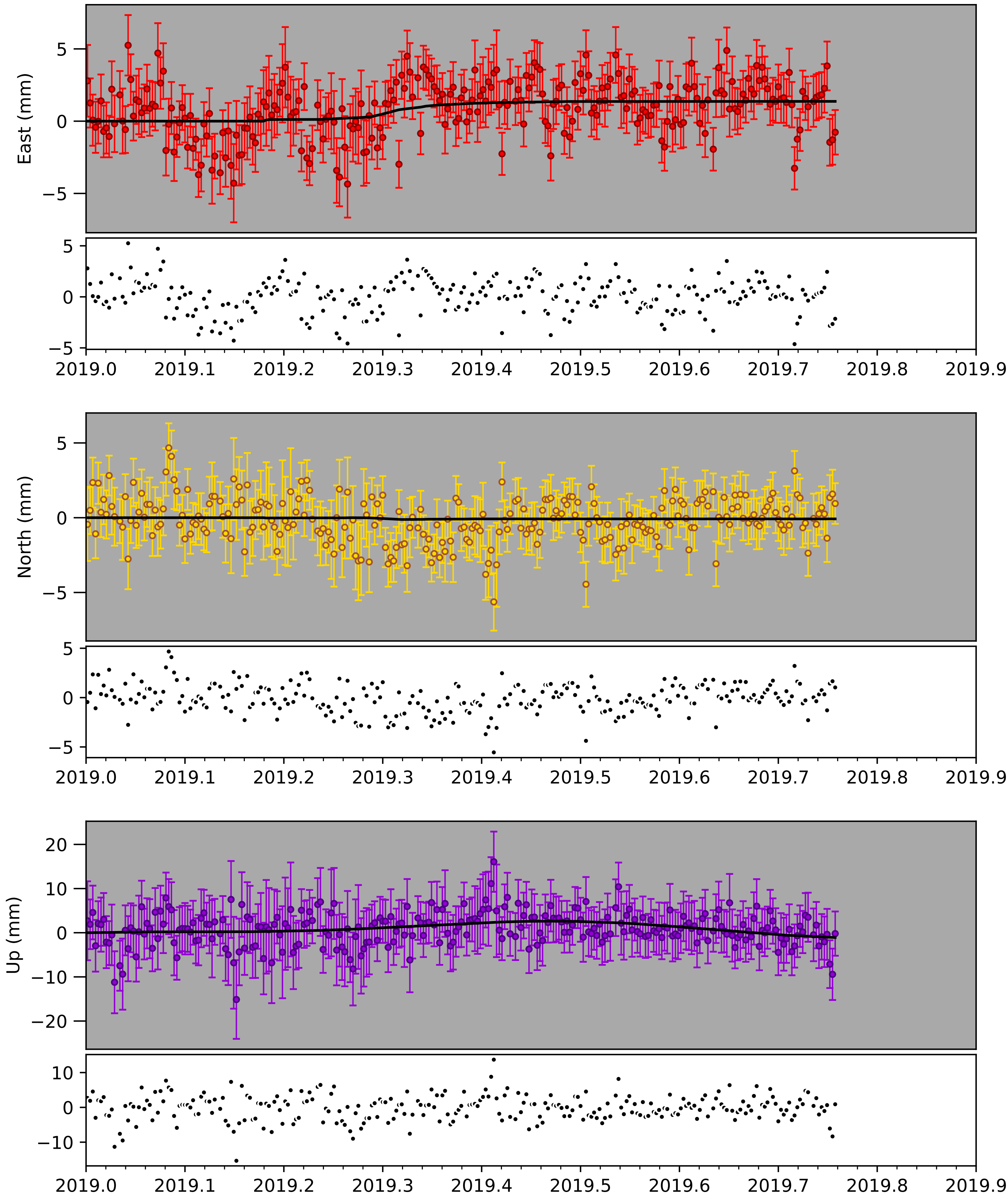

OPTK

[177.3076] [-38.0465]

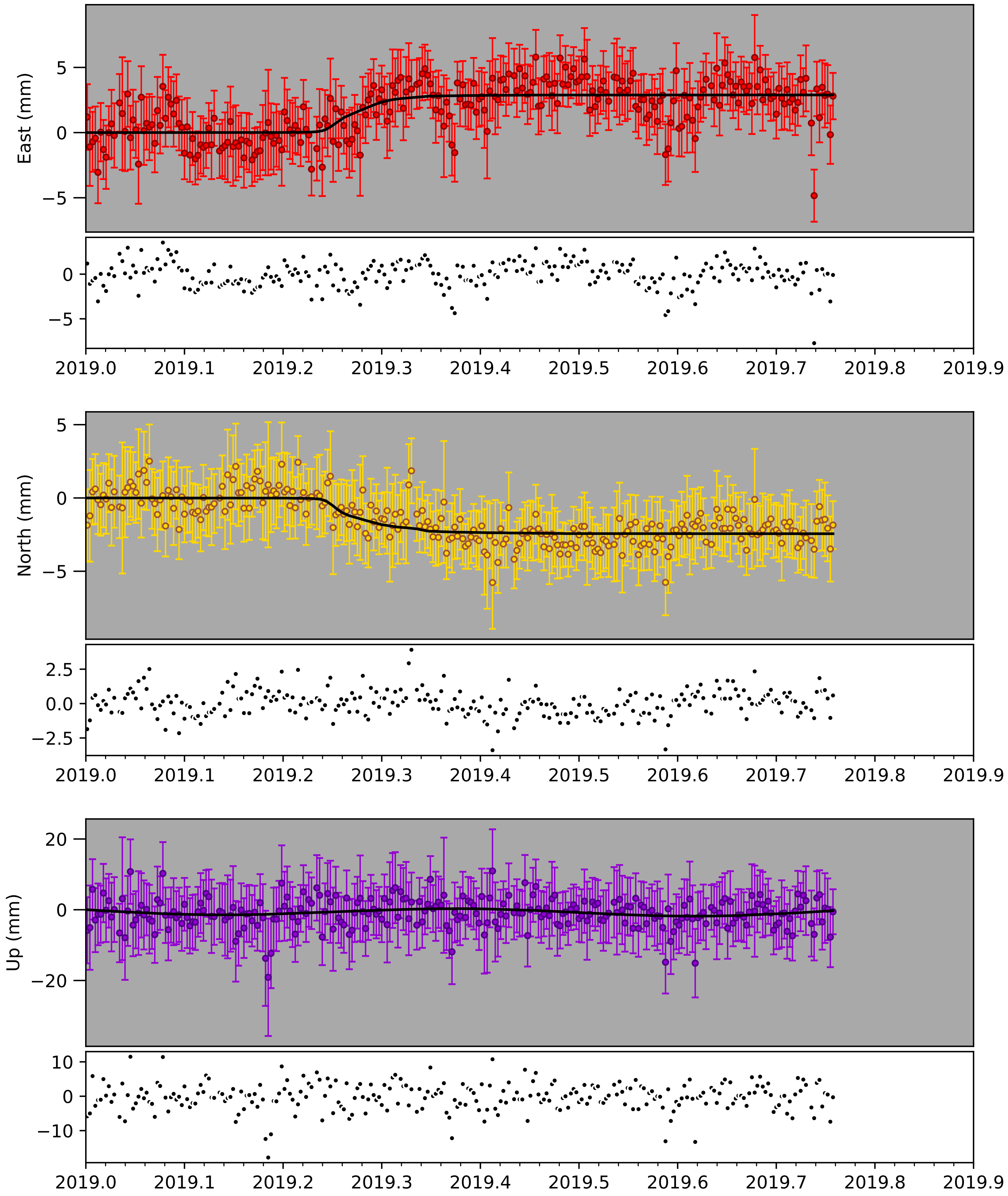

OROA

[176.6807] [-40.1044]

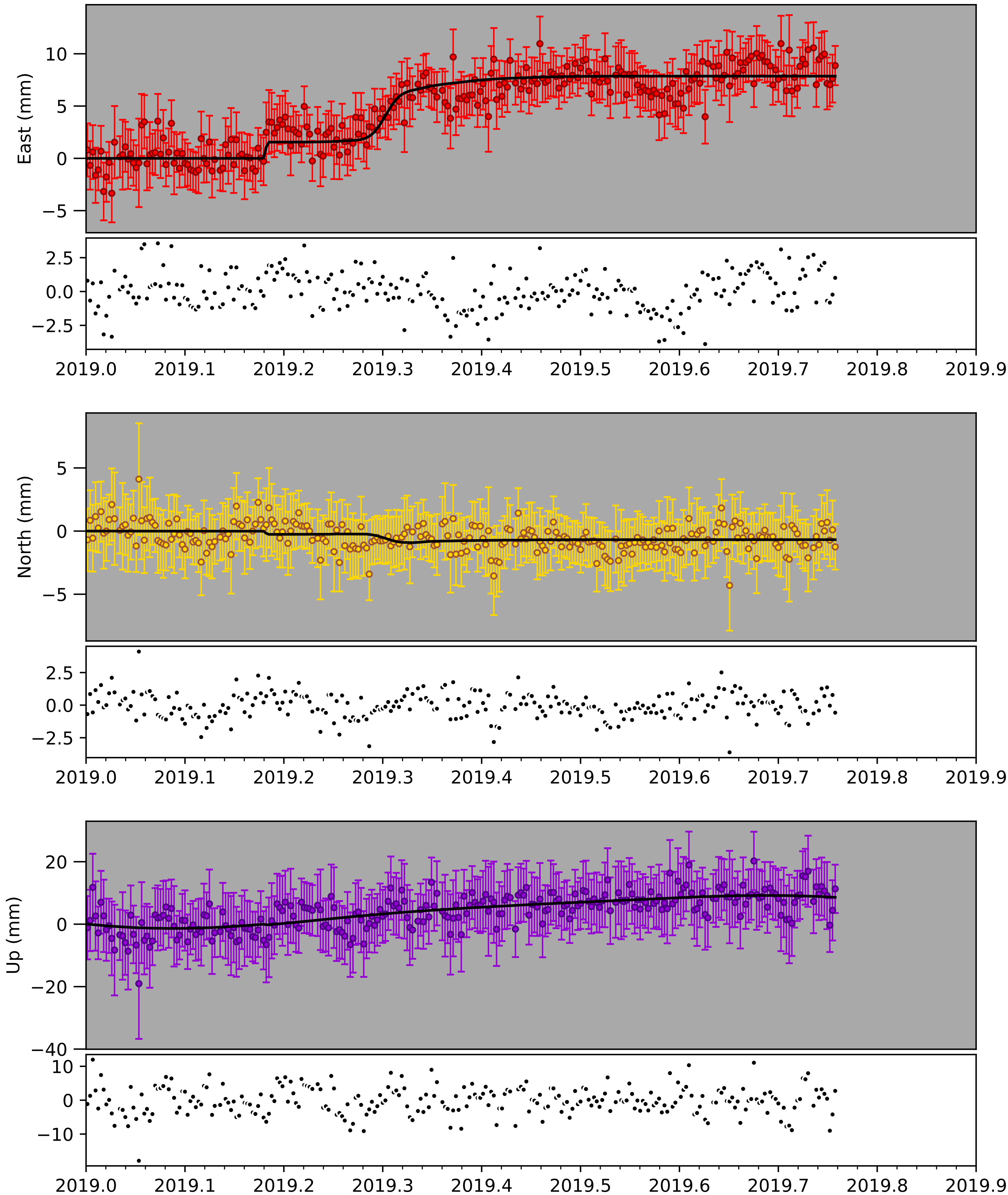

PAKI

[178.0826] [-37.894]

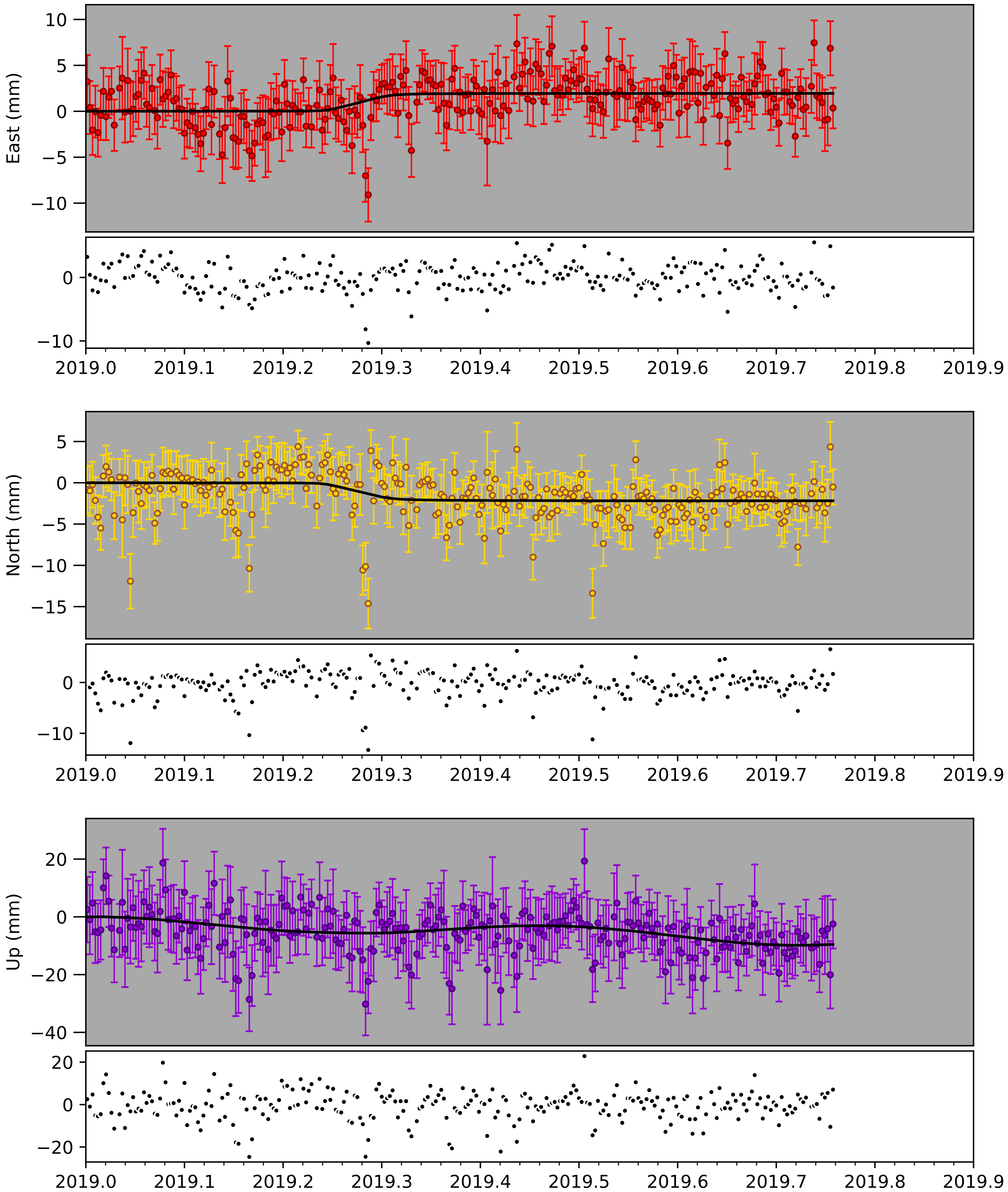

PARI

[177.8833] [-38.9226]

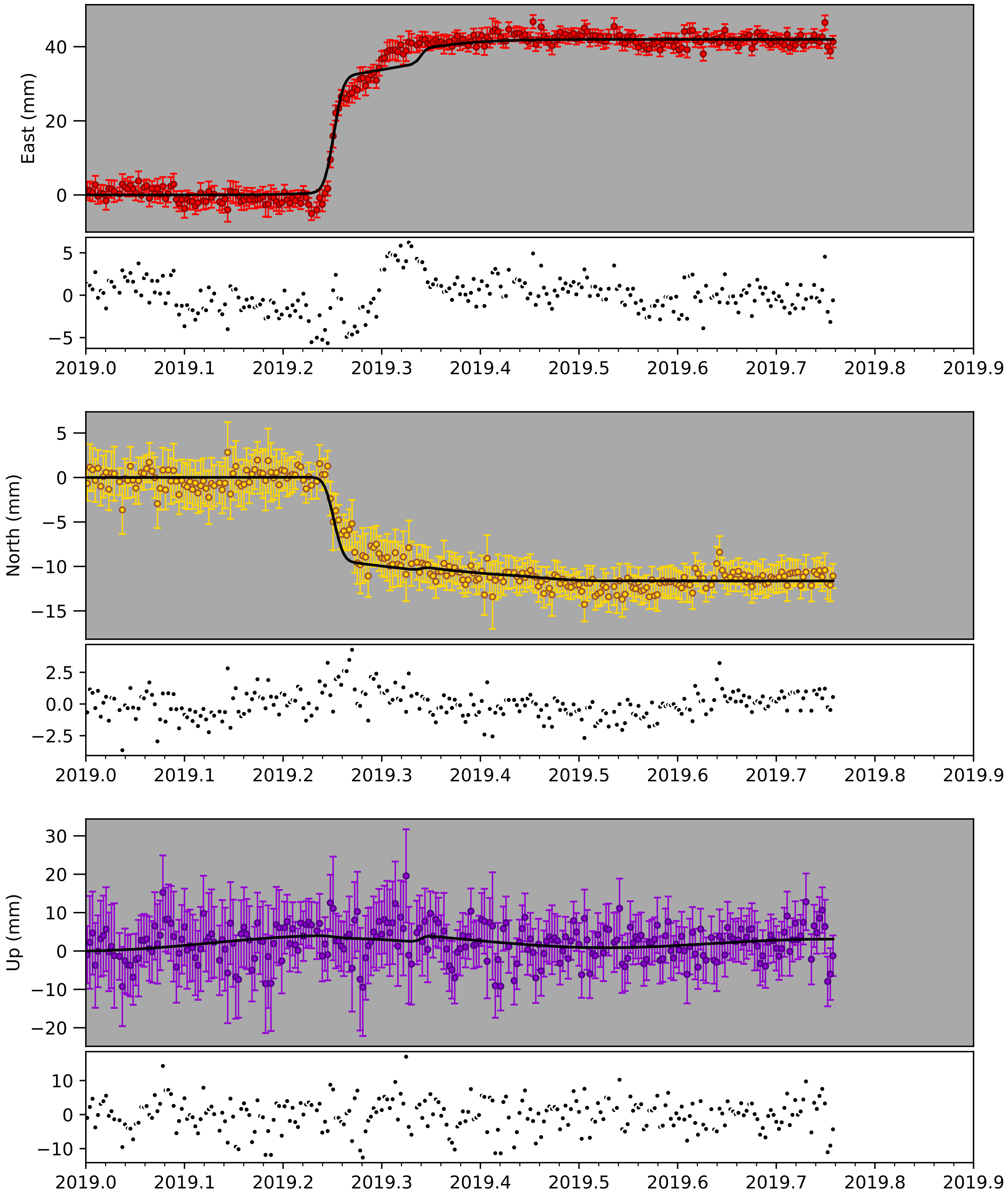

PAWA

[176.8639] [-40.0331]

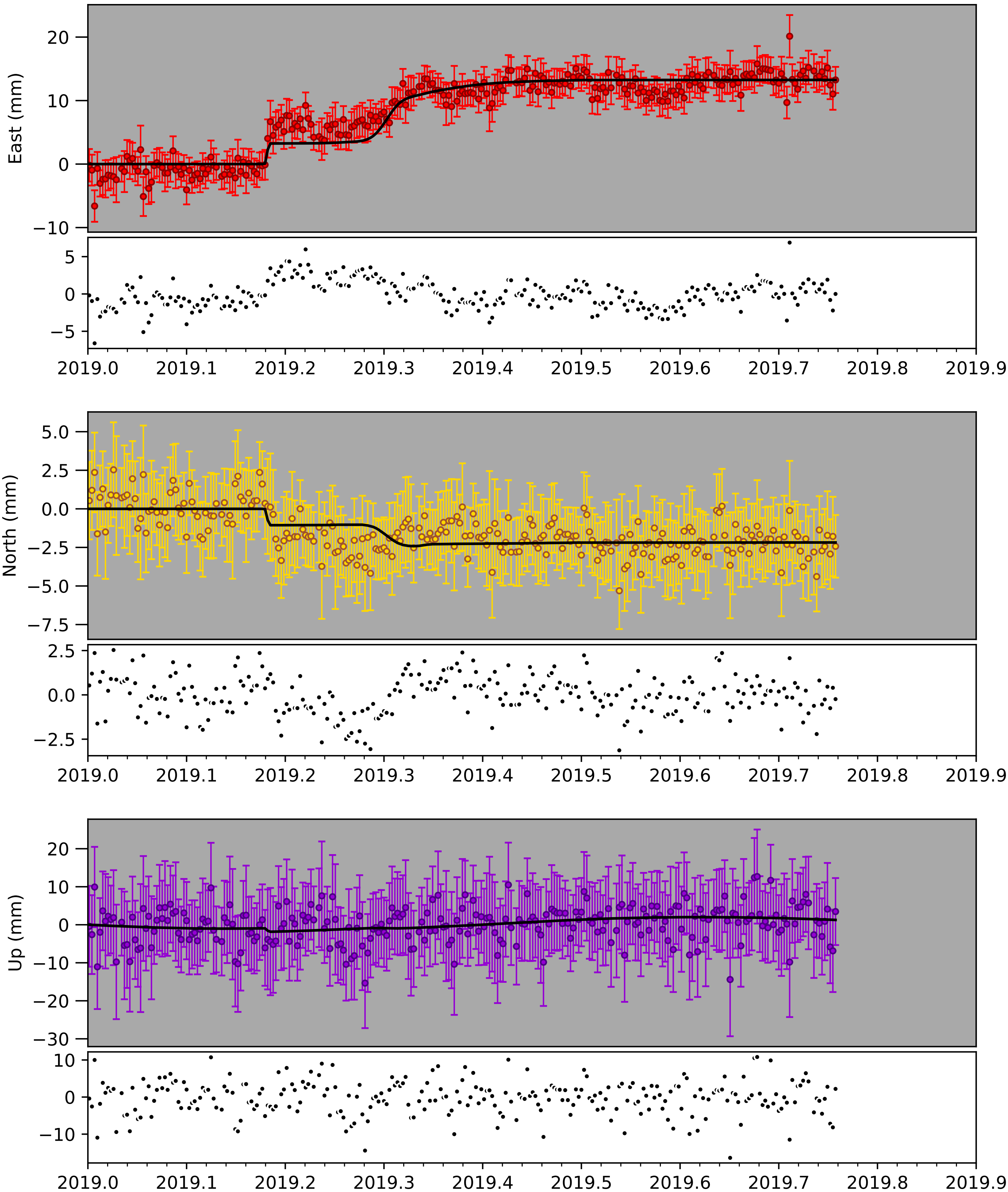

PBS1

[177.9184] [-39.8516]

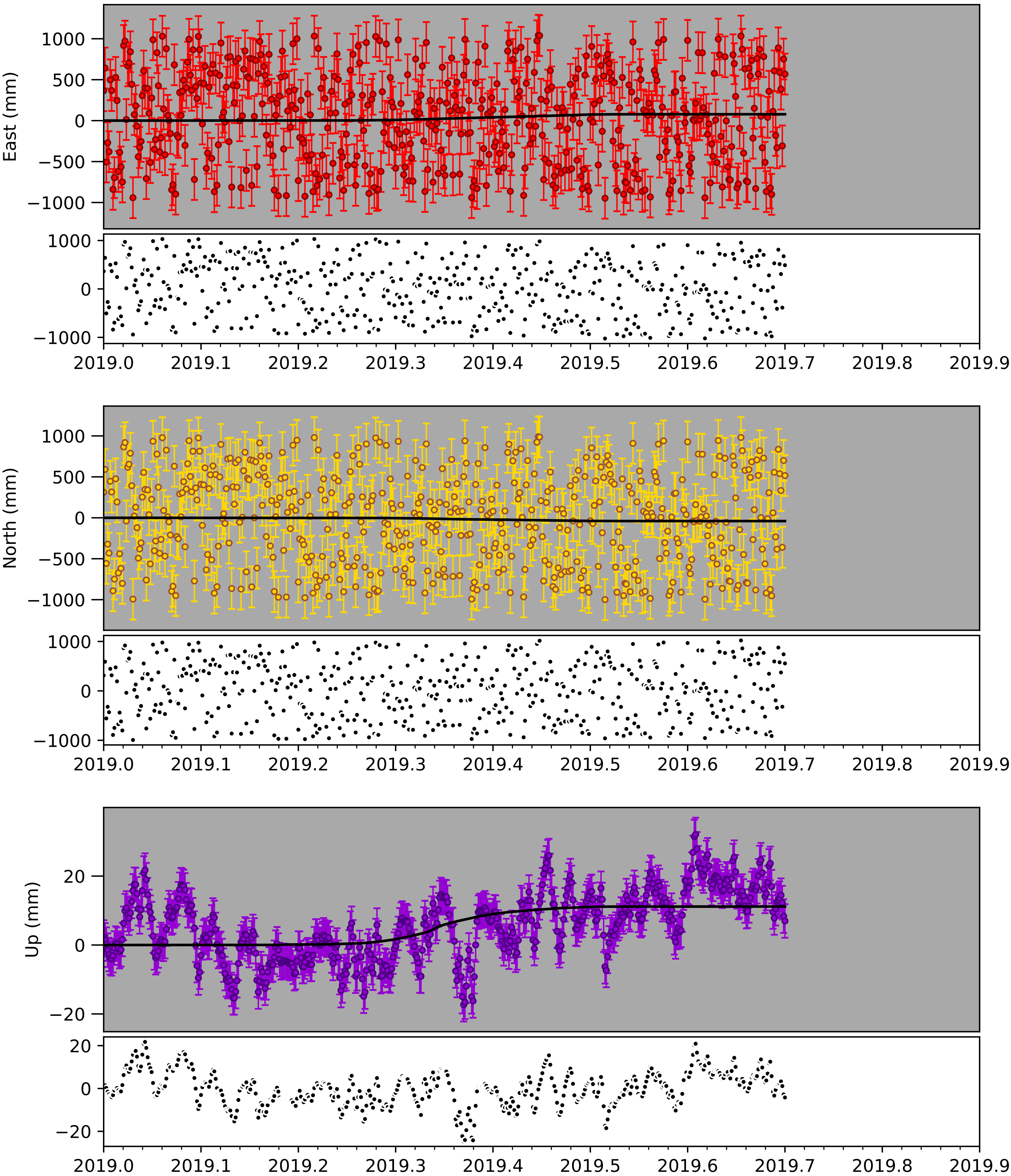

PBS2

[178.0876] [-39.8923]

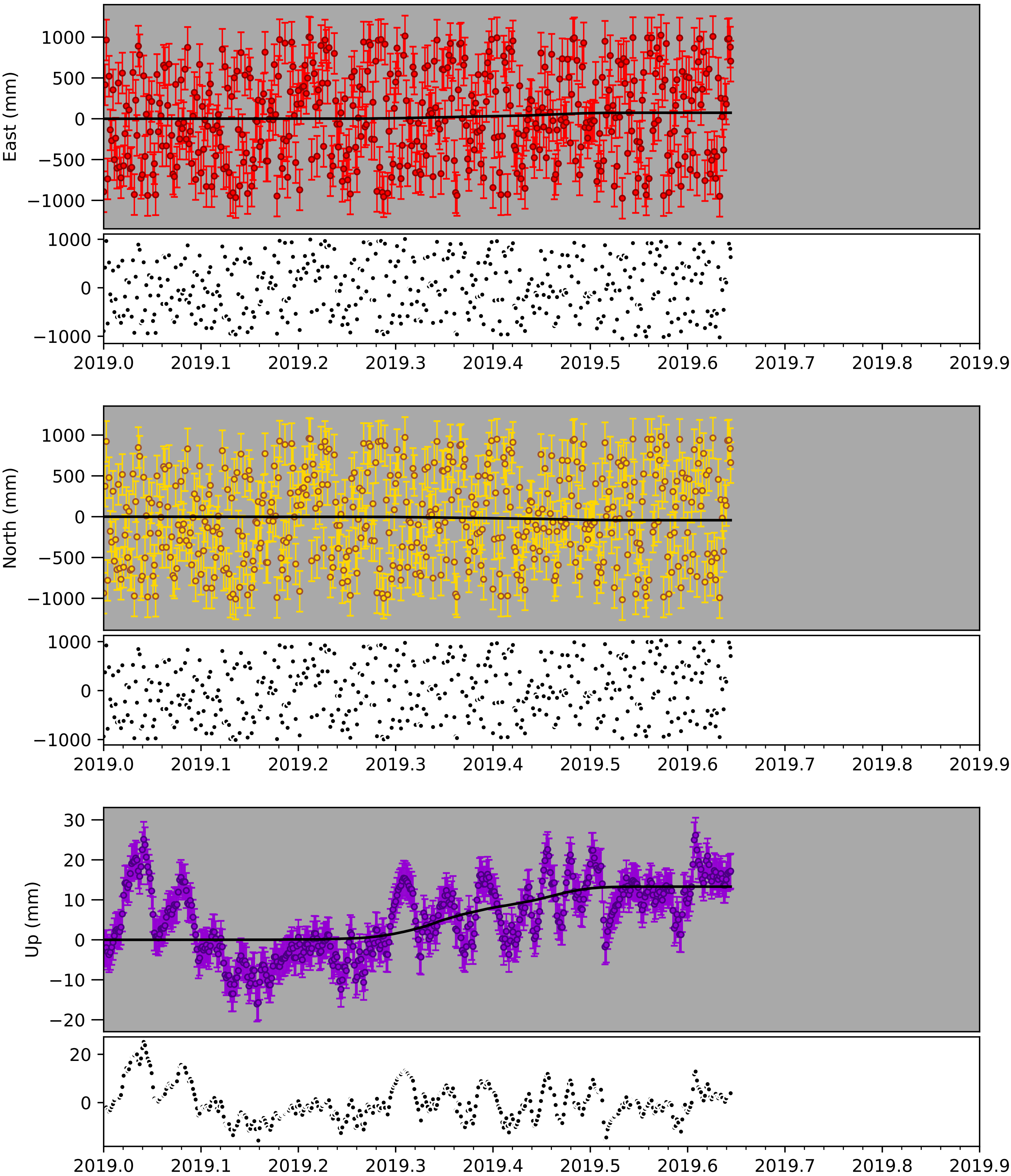

PBS3

[178.3524] [-39.9195]

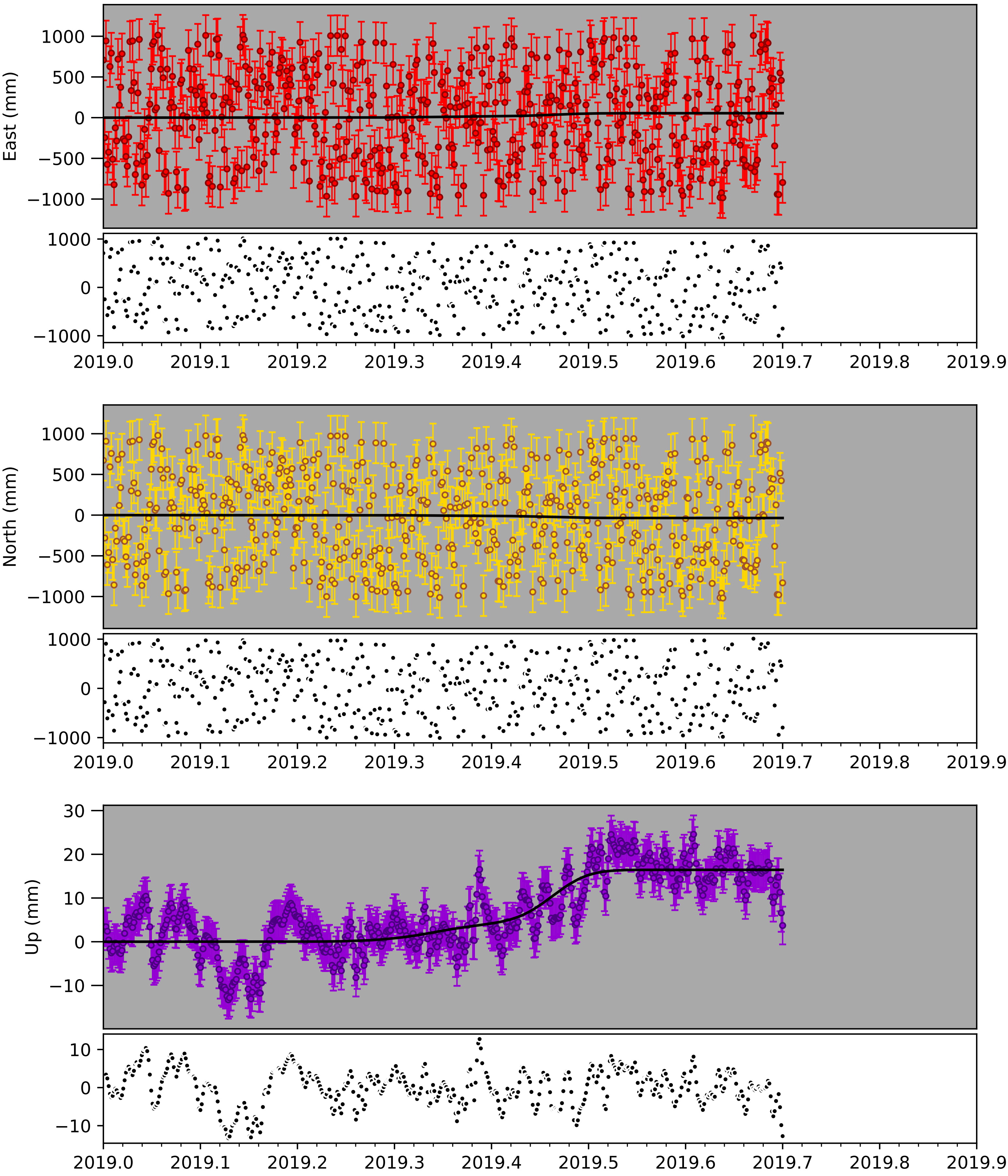

PNUI

[176.2005] [-39.9168]

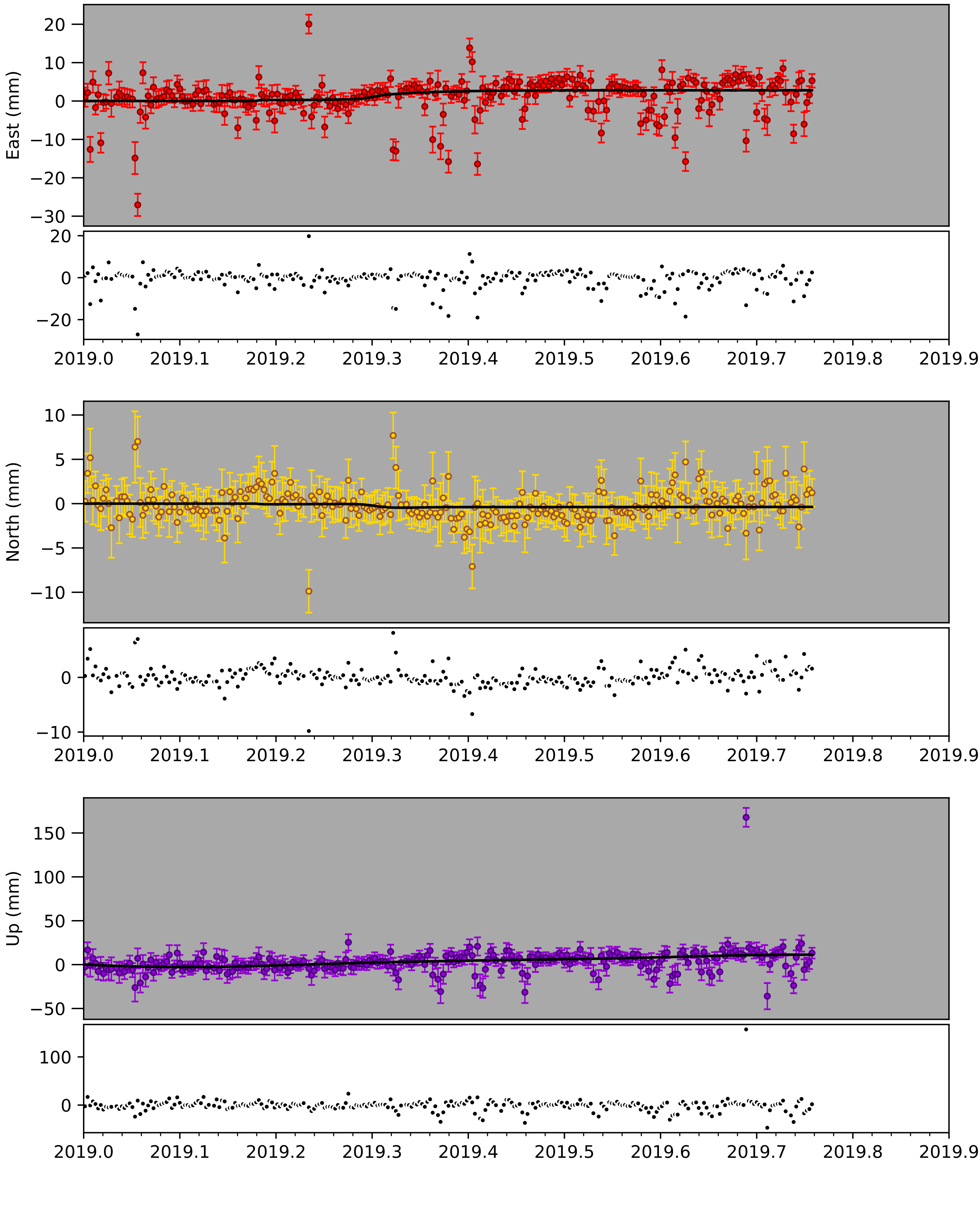

PORA

[176.6352] [-40.2664]

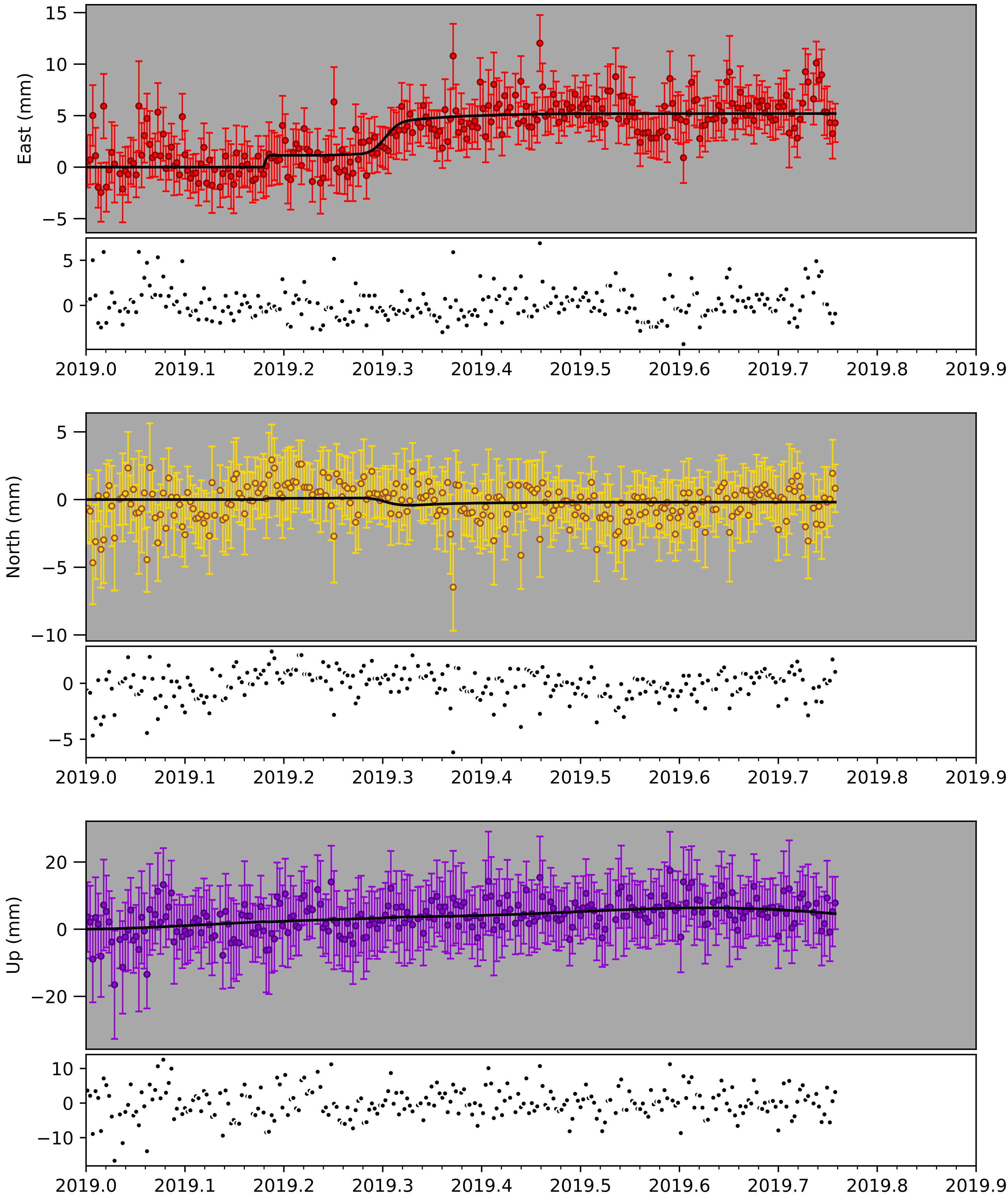

PRTU

[177.6979] [-38.8142]

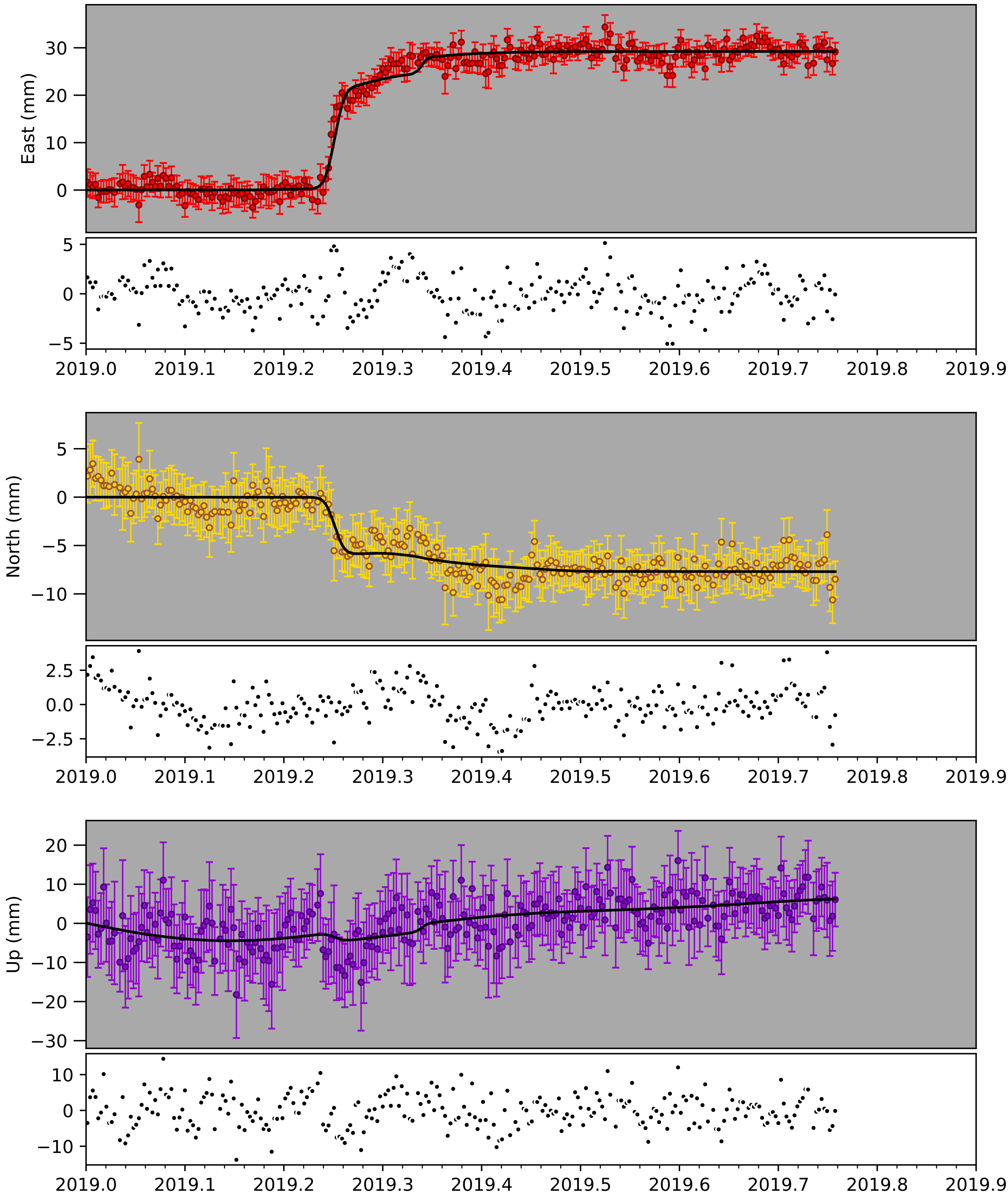

PTOI

[175.9993] [-40.6011]

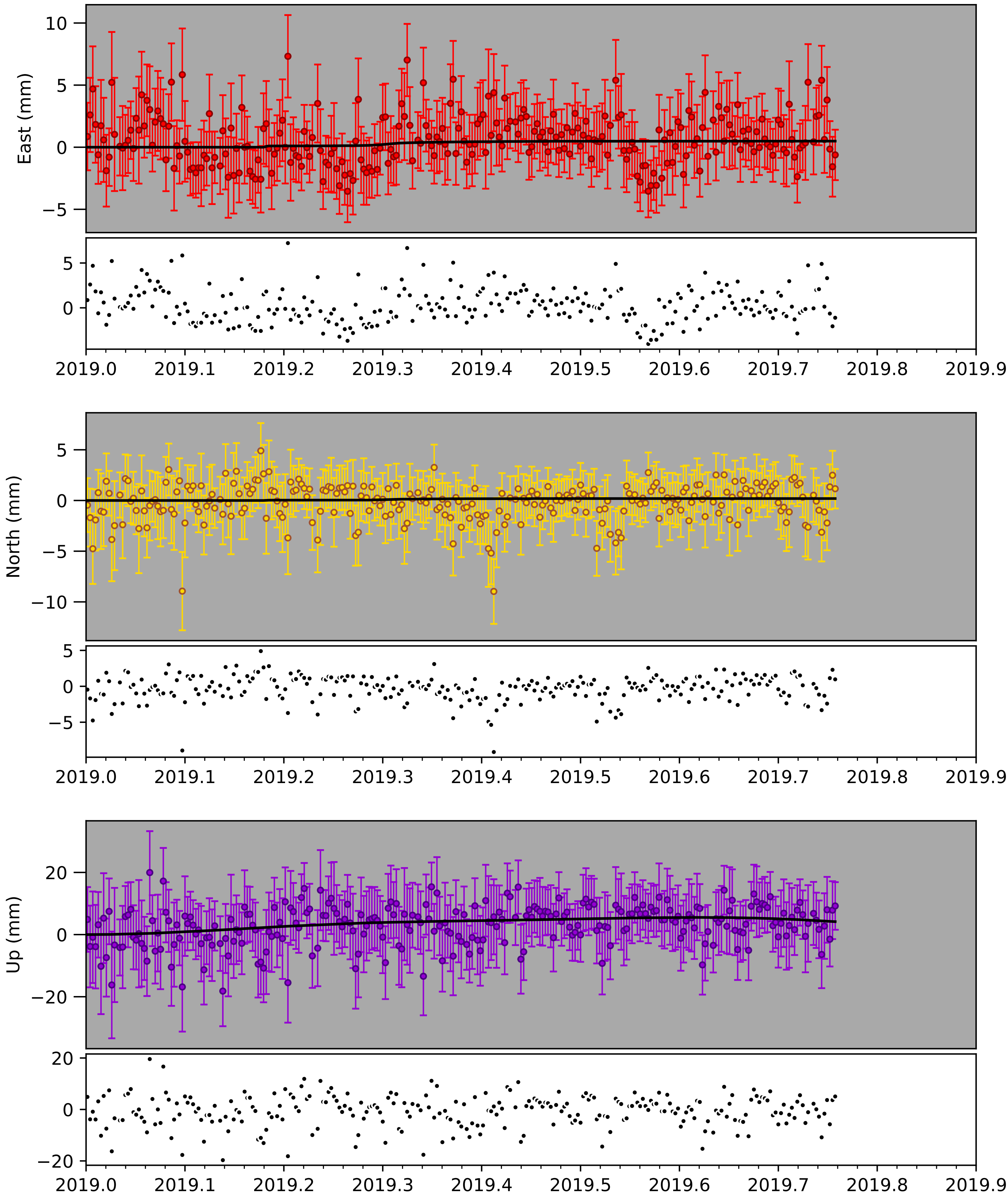

PUKE

[178.2574] [-38.0714]

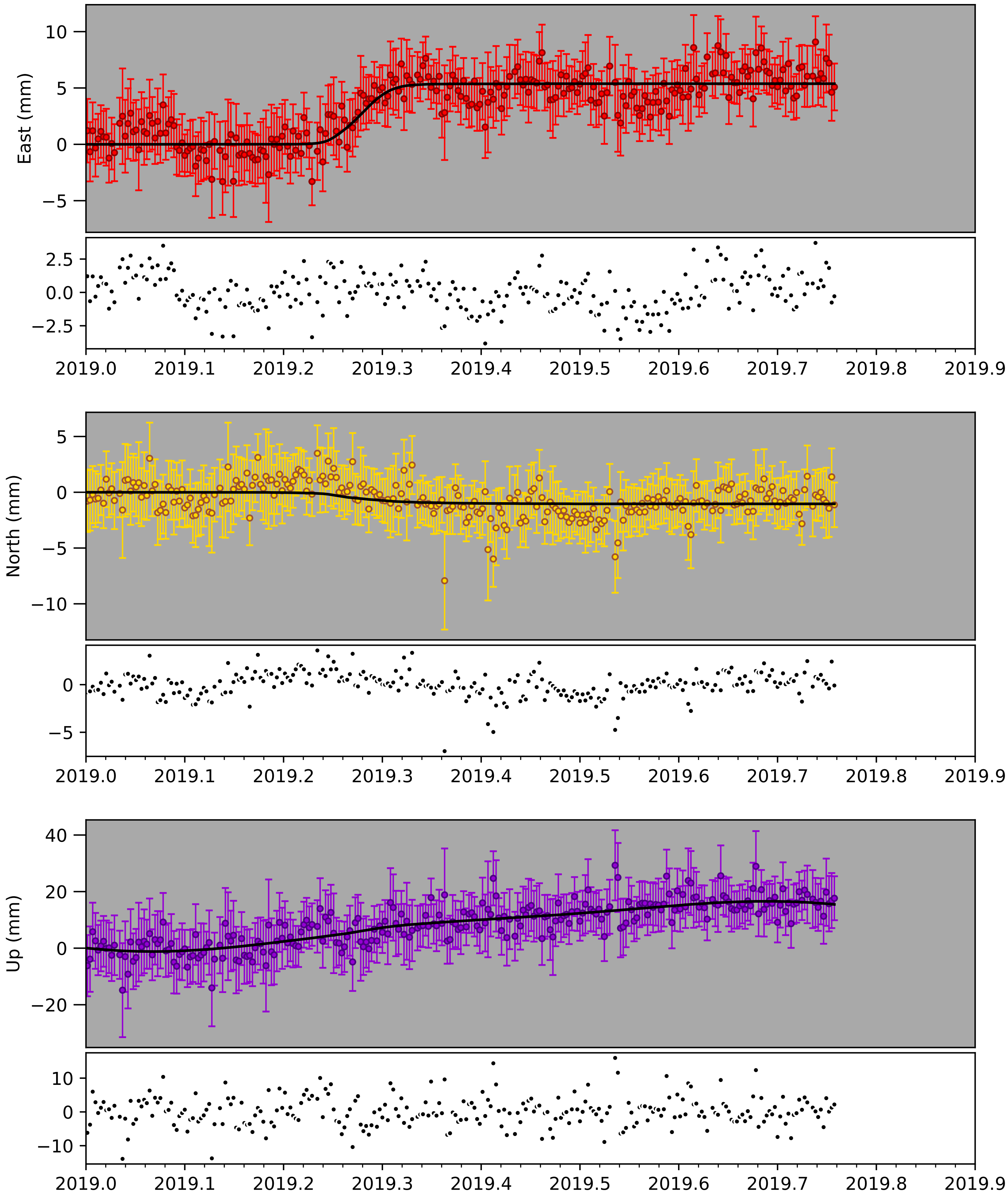

RAHI

[177.0861] [-38.9162]

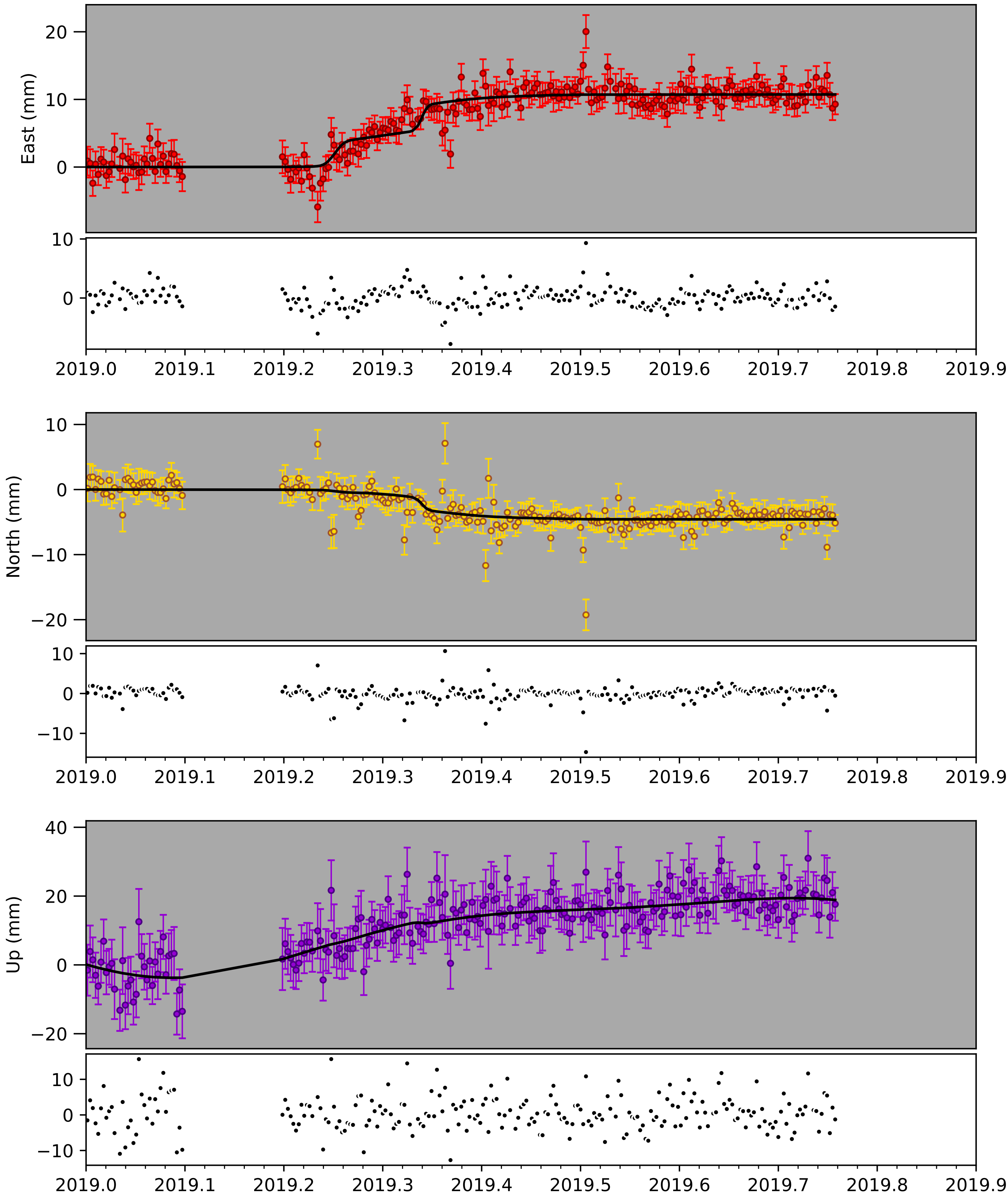

RAKW

[176.6212] [-39.7472]

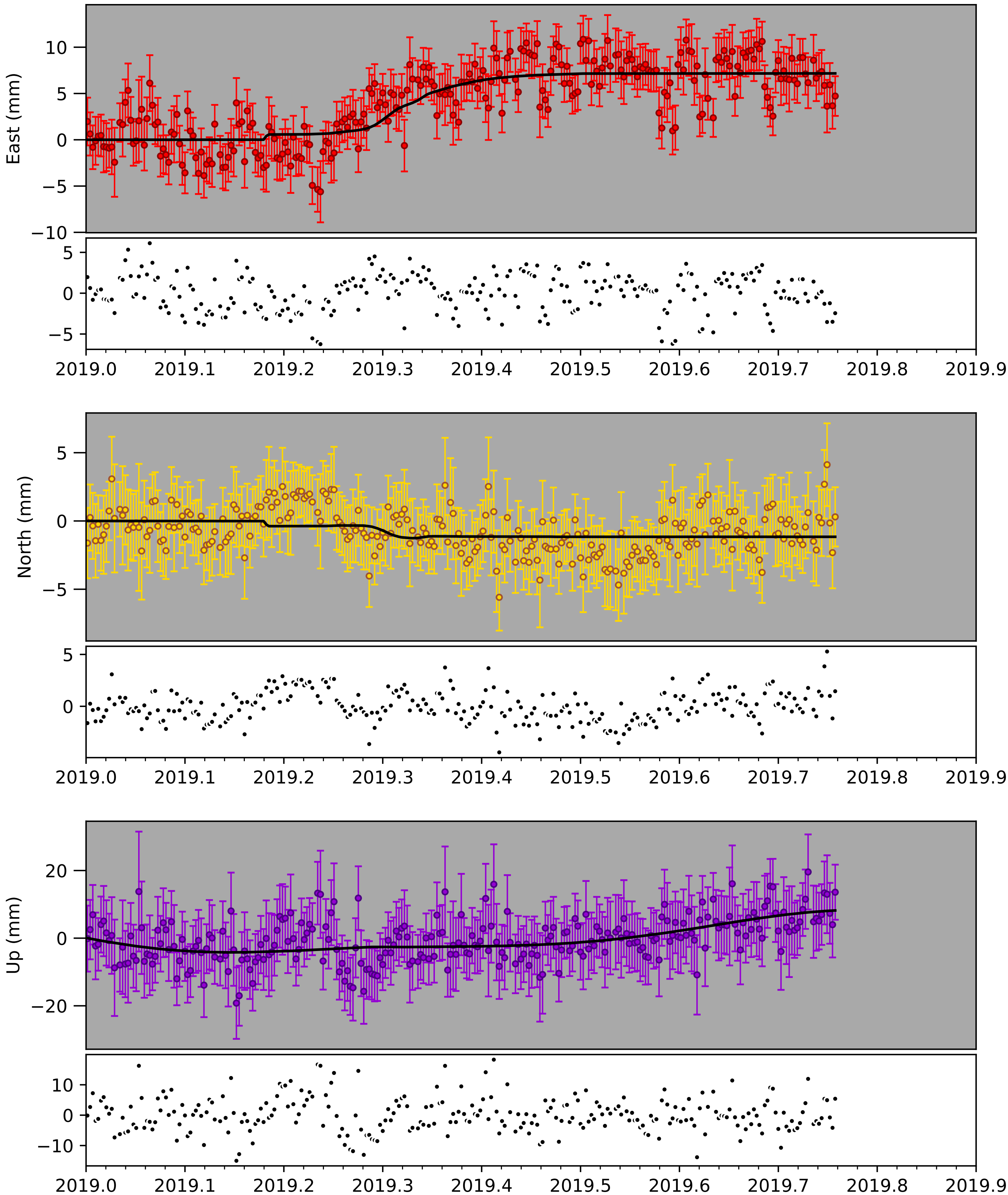

RAUM

[177.6775] [-37.965]

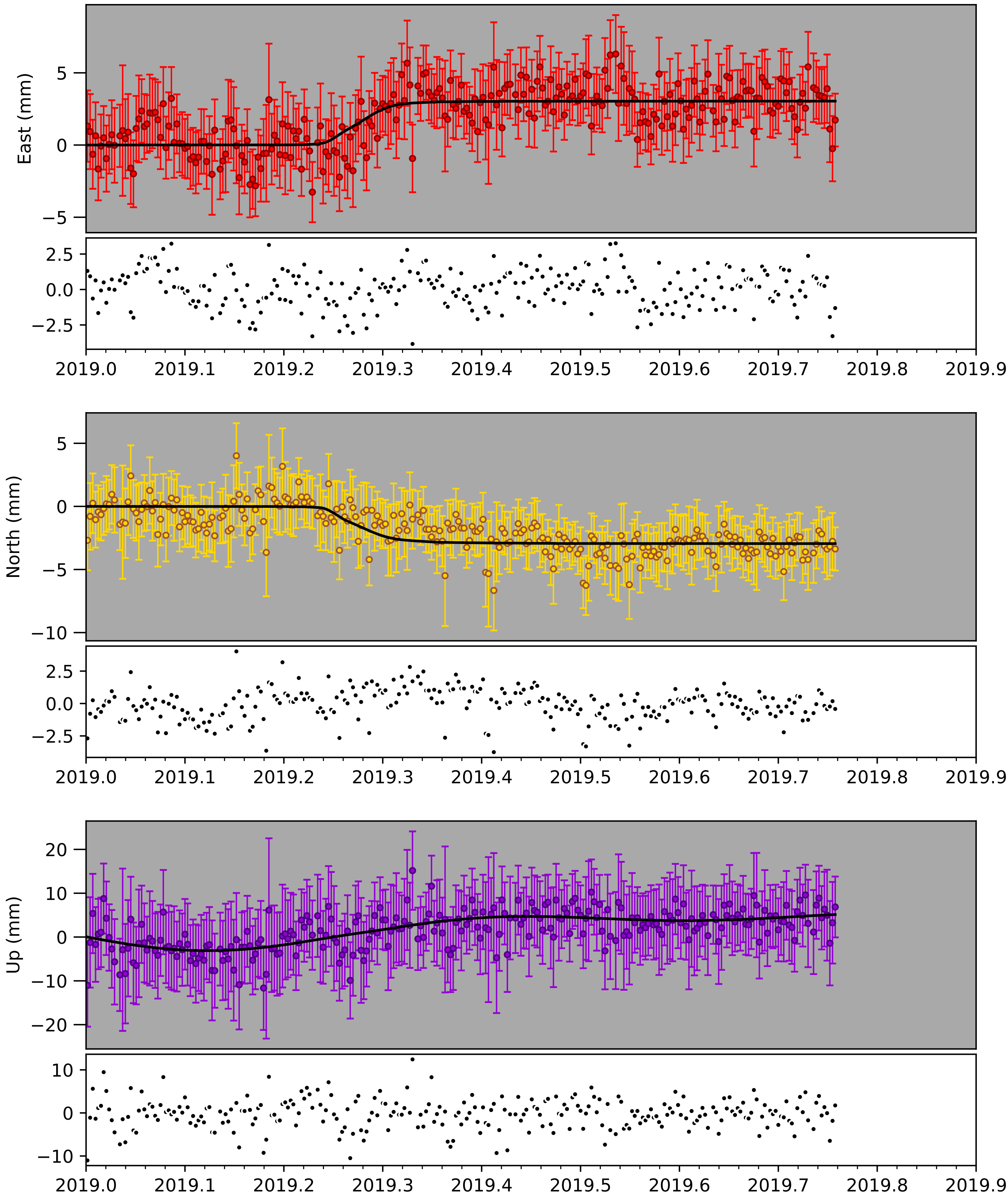

RAWI

[177.4154] [-38.4956]

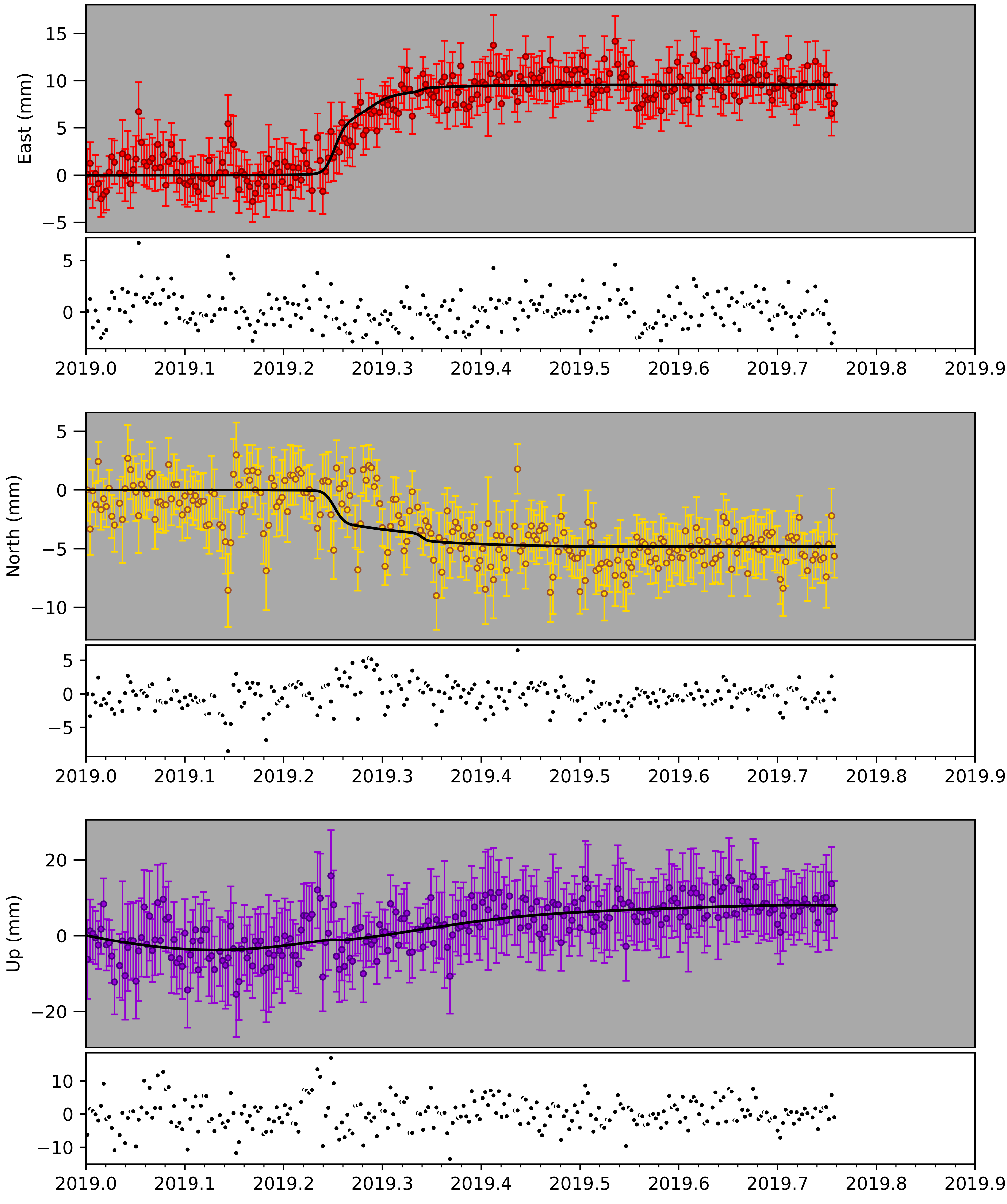

RGAW

[176.8962] [-38.0032]

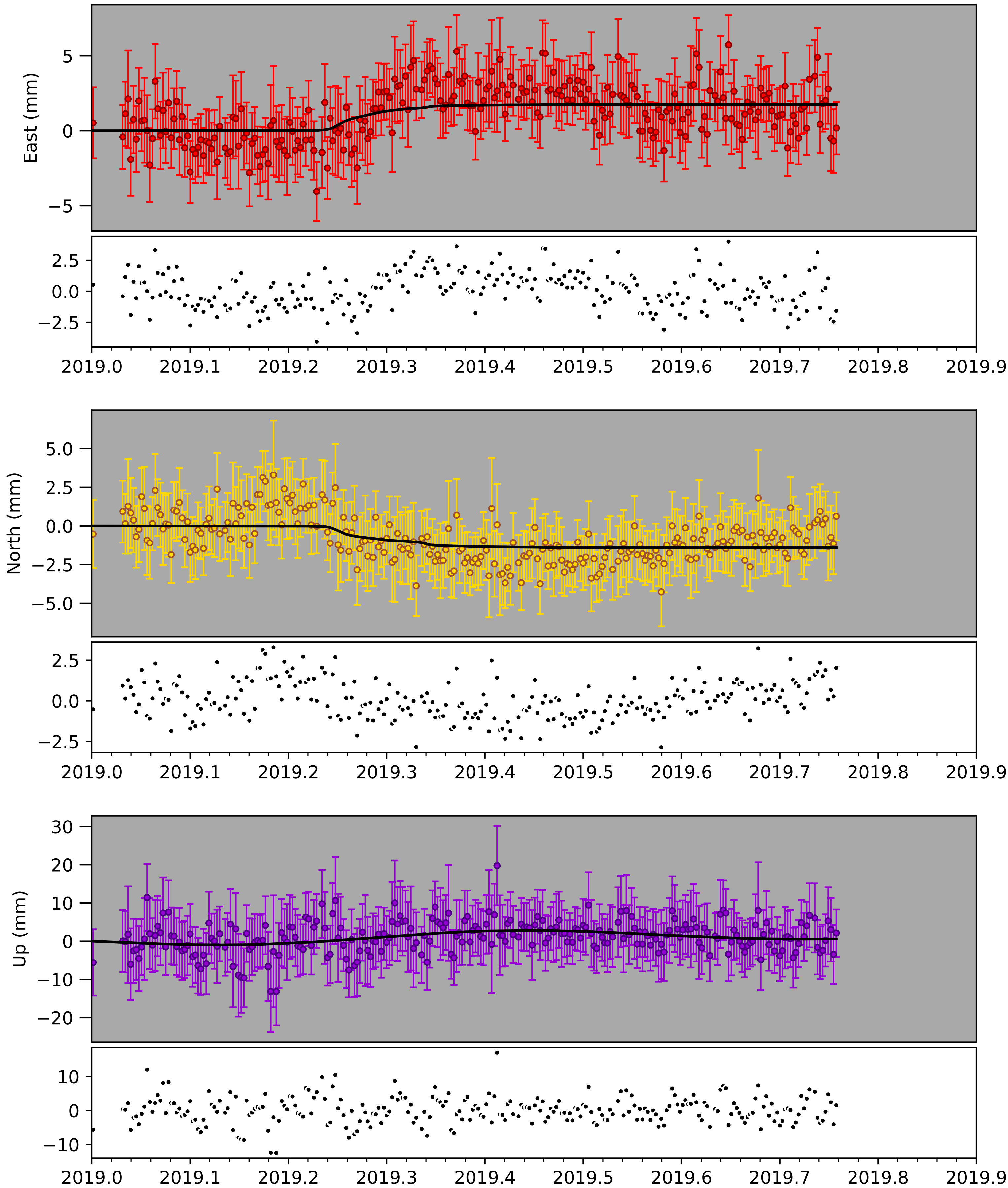

RGRR

[176.5146] [-38.3389]

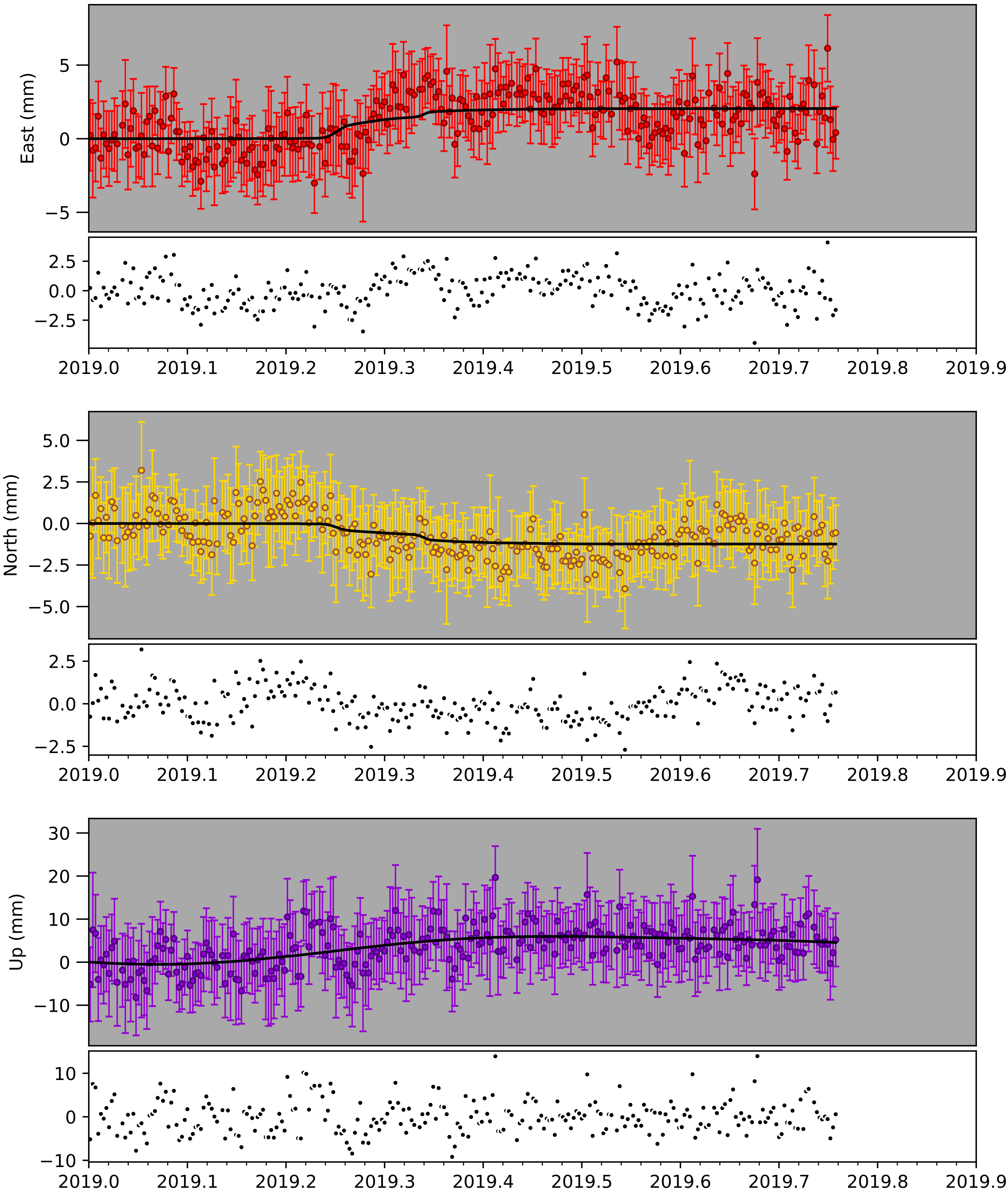

RIPA

[176.4925] [-39.1655]

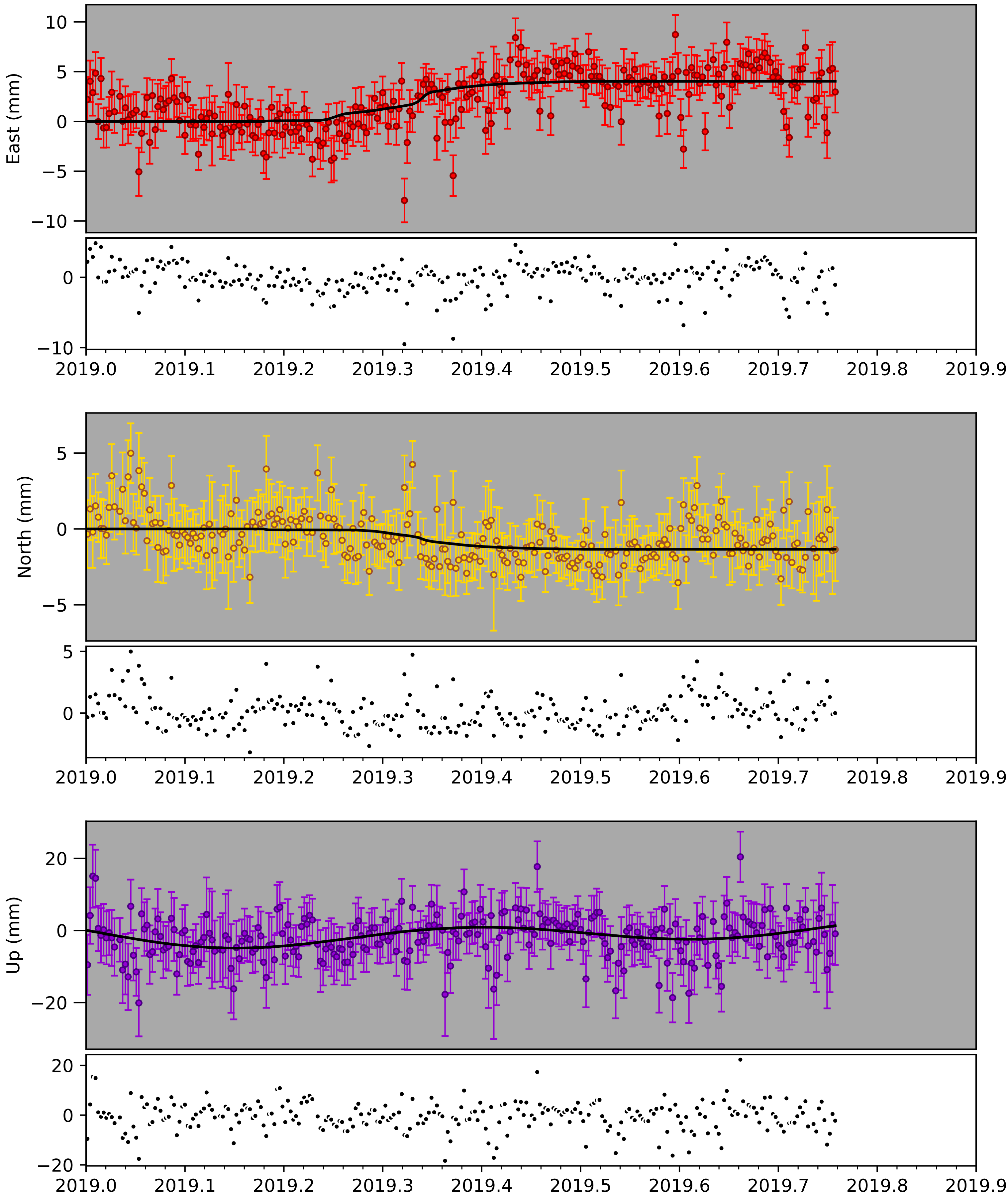

SNST

[177.3475] [-38.7796]

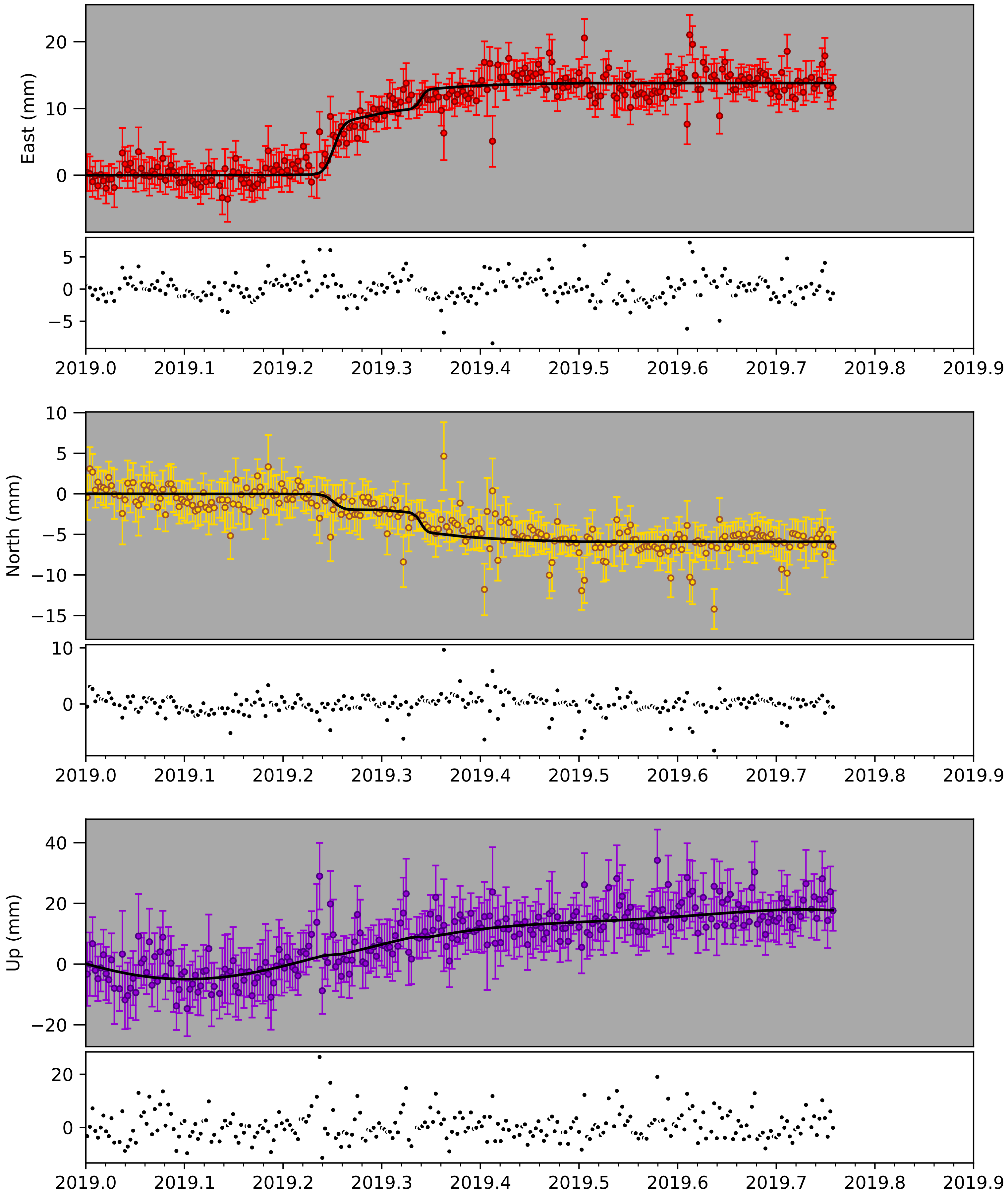

TAKP

[175.9629] [-40.0616]

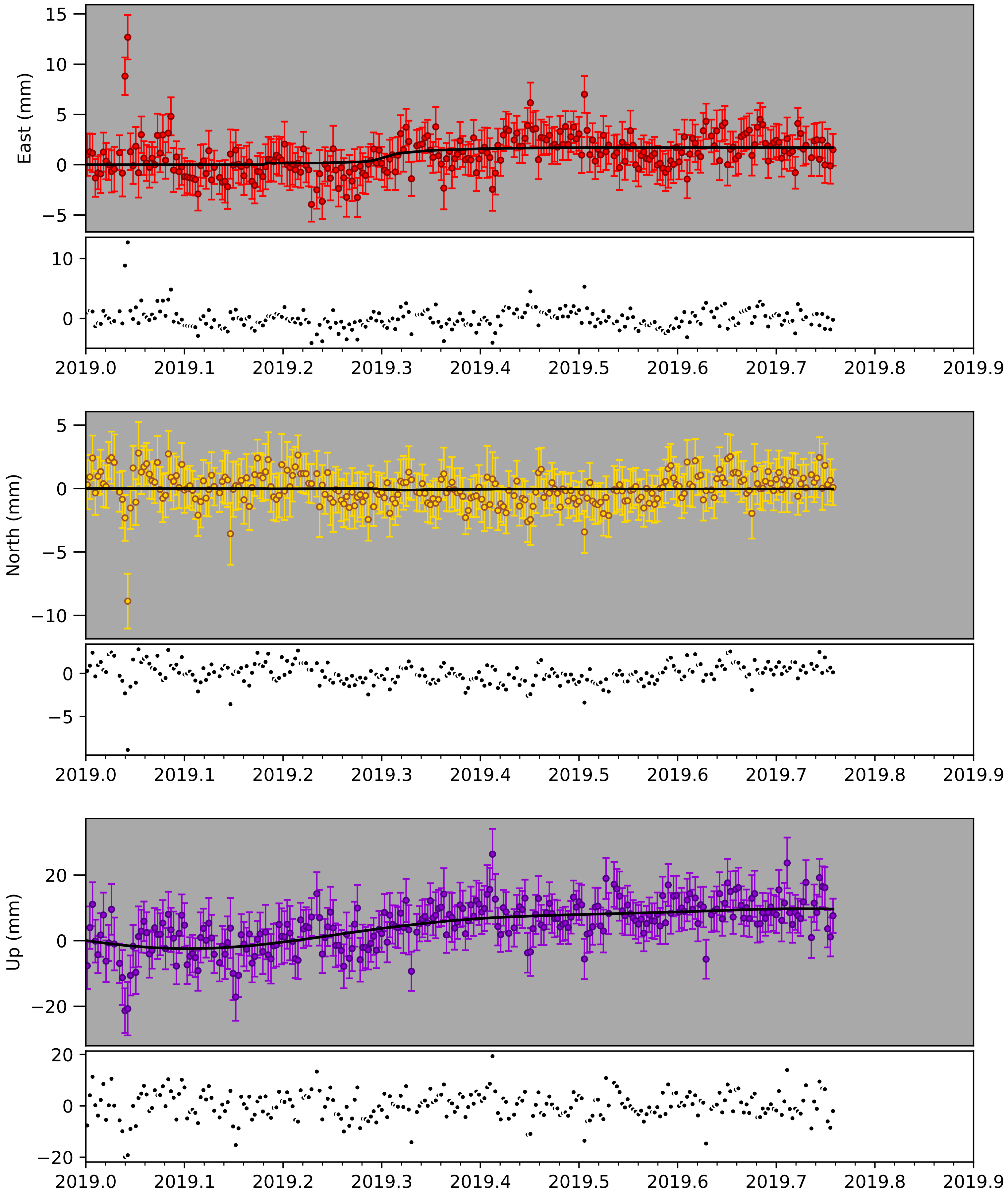

TAUP

[176.081] [-38.7427]

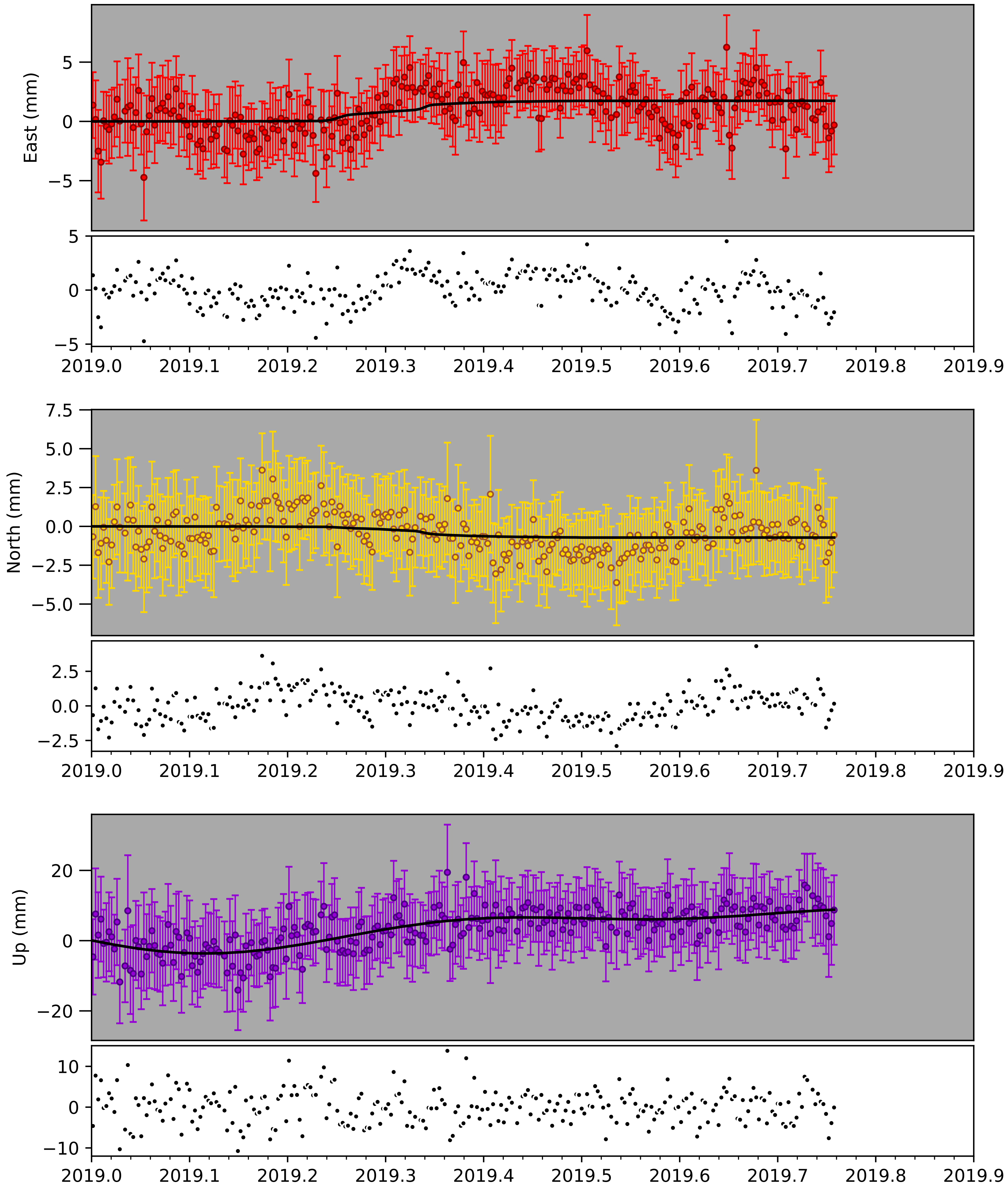

TAUW

[178.0059] [-38.1624]

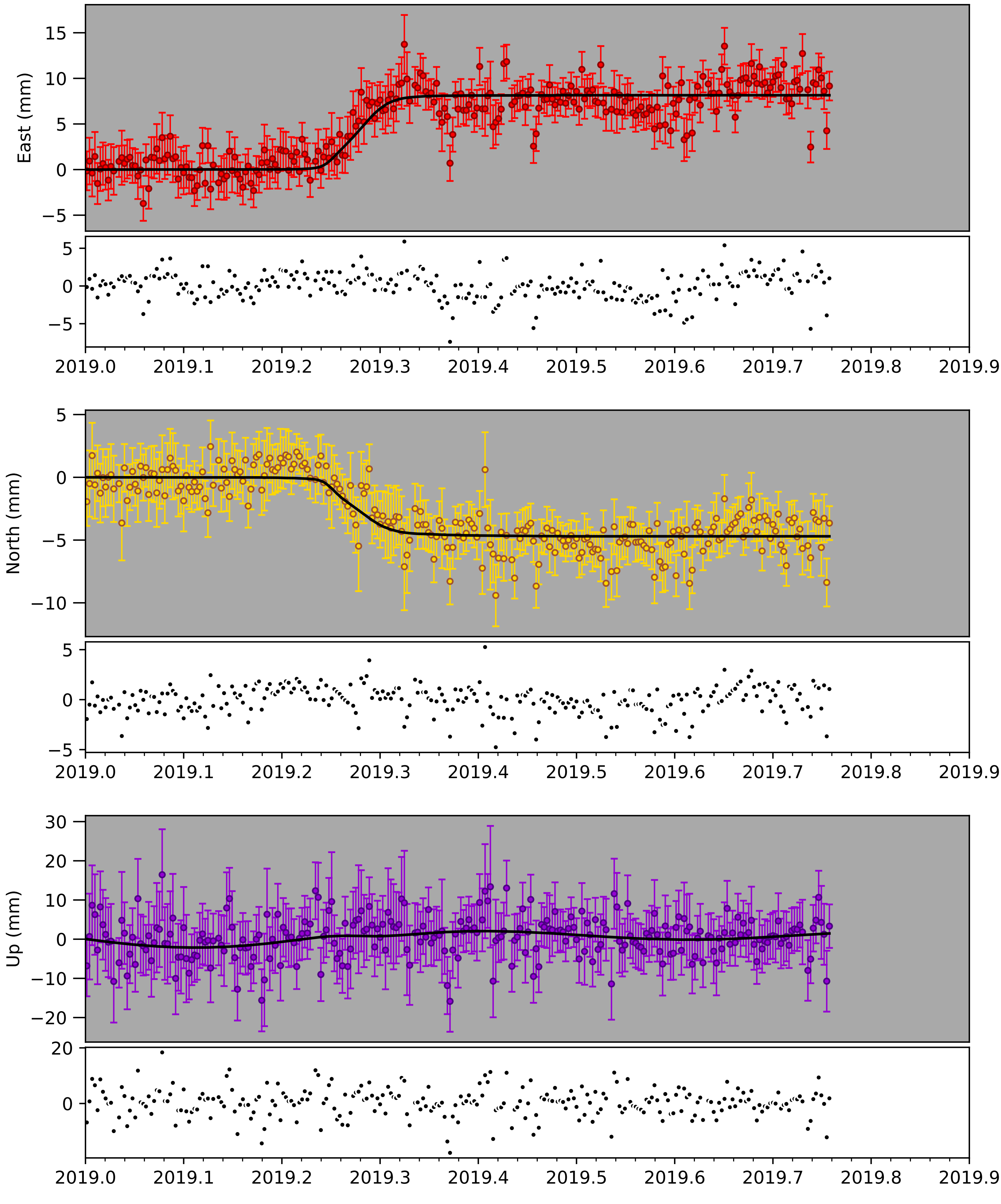

TEMA

[175.8905] [-41.1066]

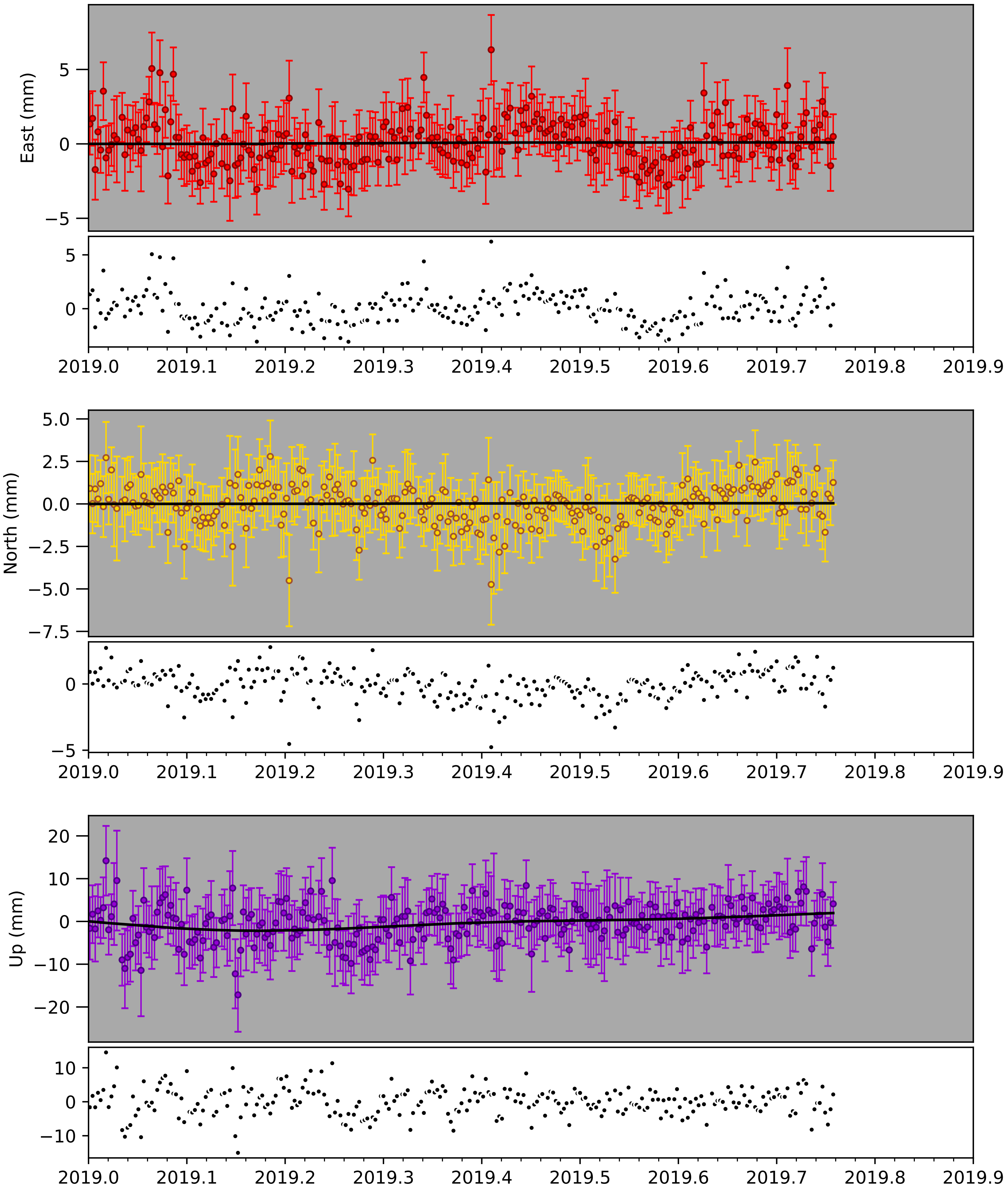

THAP

[175.7856] [-39.6825]

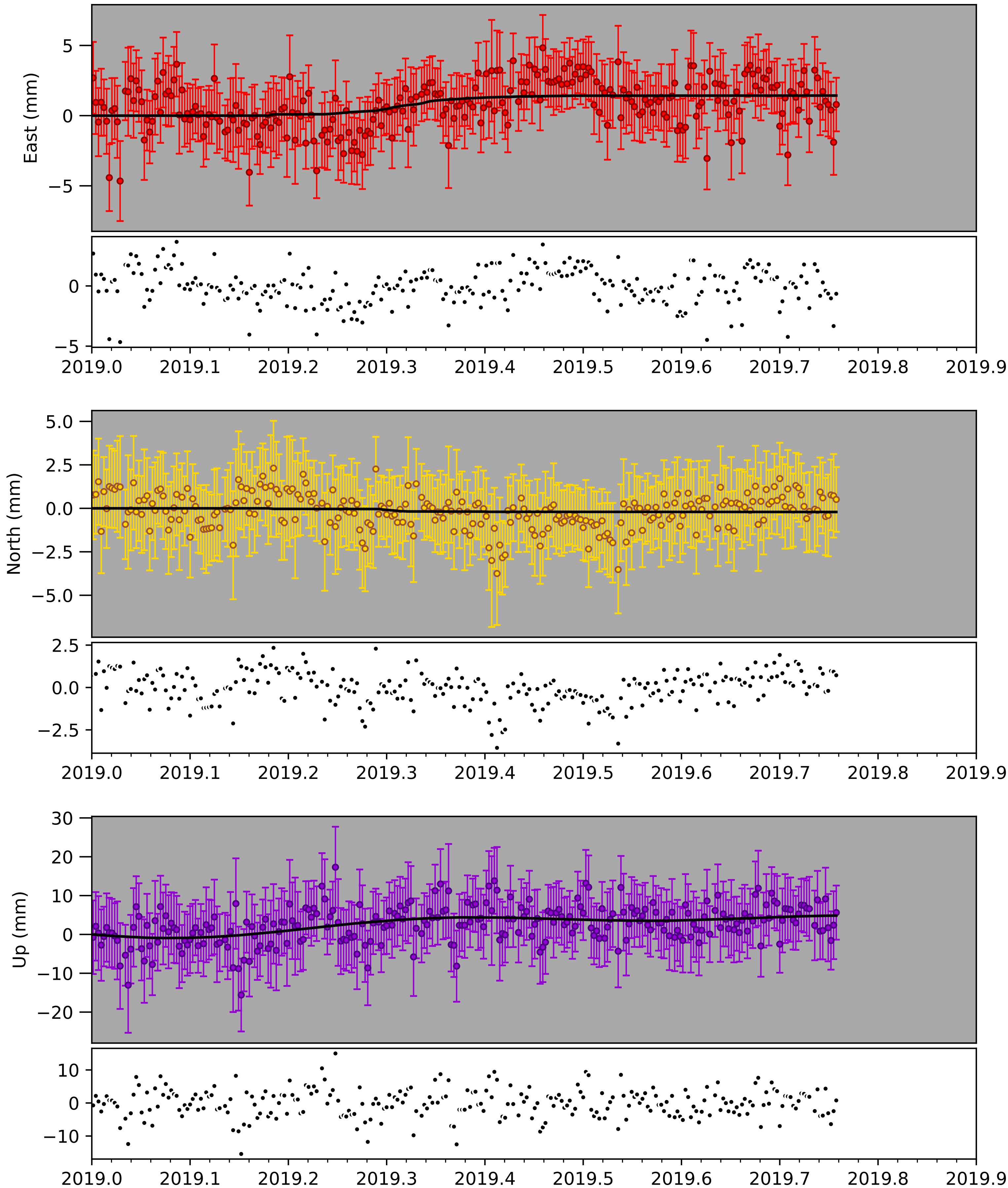

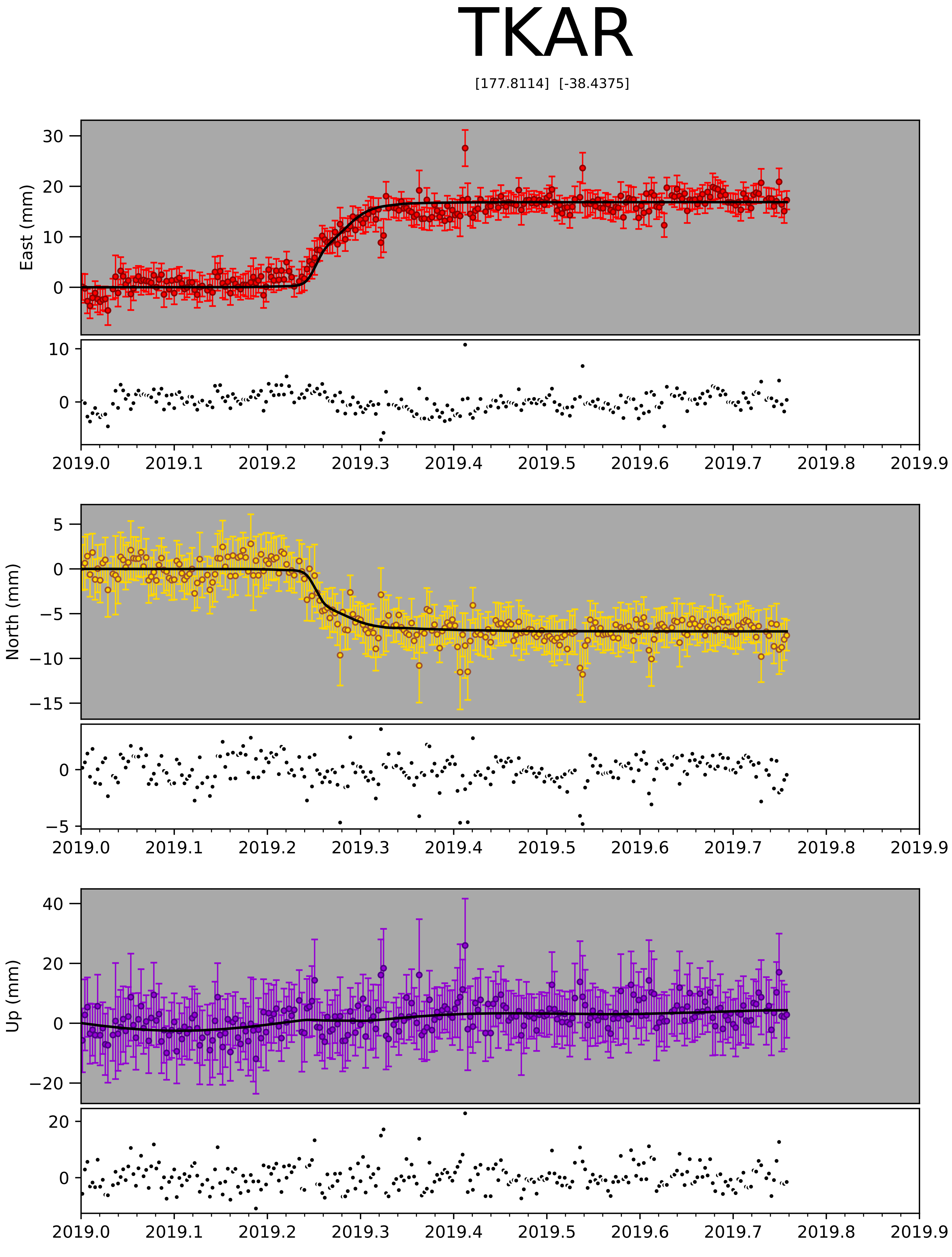

TKAR
[177.8114] [-38.4375]
East (mm)
North (mm)
Up (mm)
2019.0
2019.1
2019.2
2019.3
2019.4
2019.5
2019.6
2019.7
2019.8
2019.9

TURI

[176.3826] [-40.265]

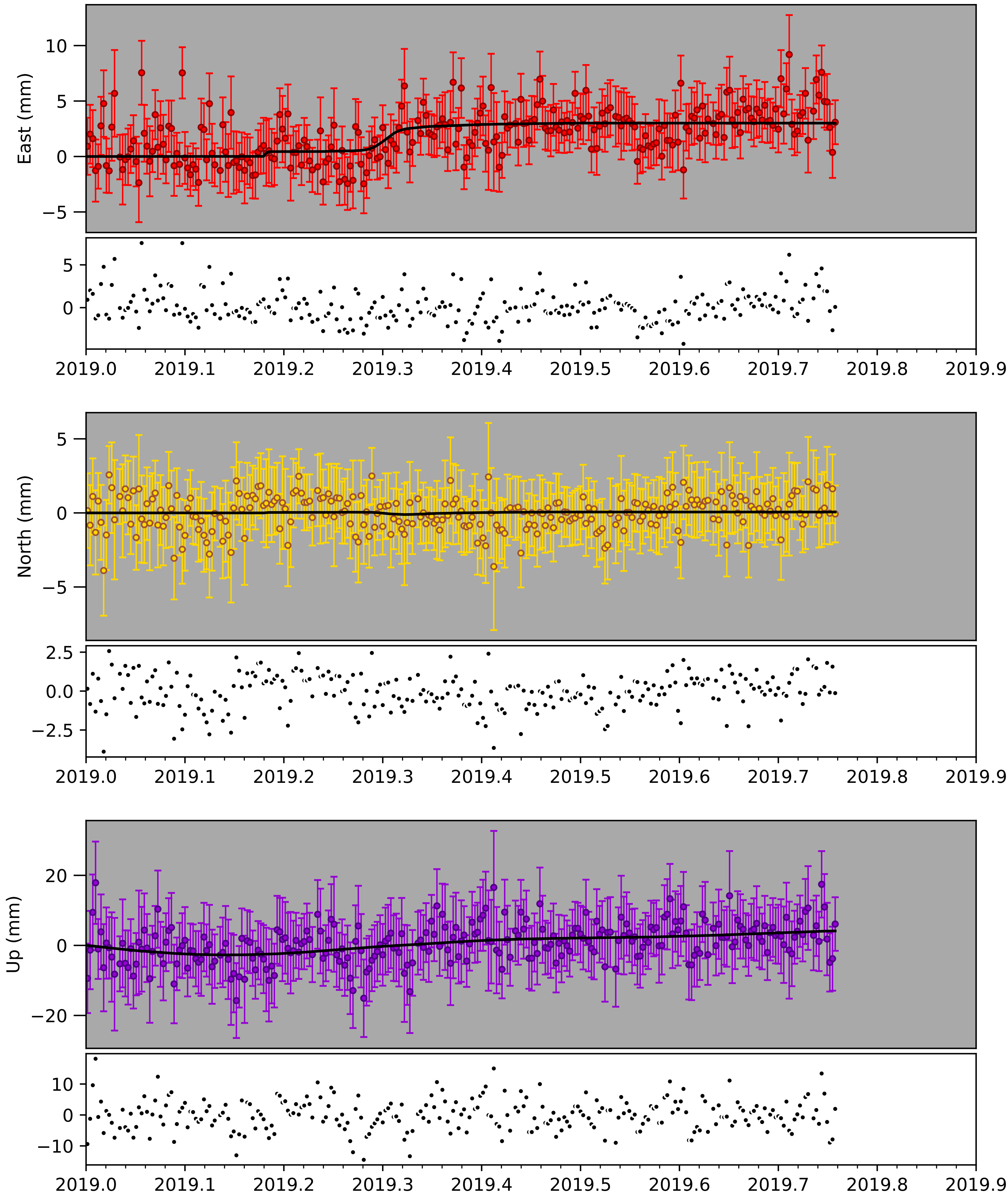

U008

[178.8961] [-38.859]

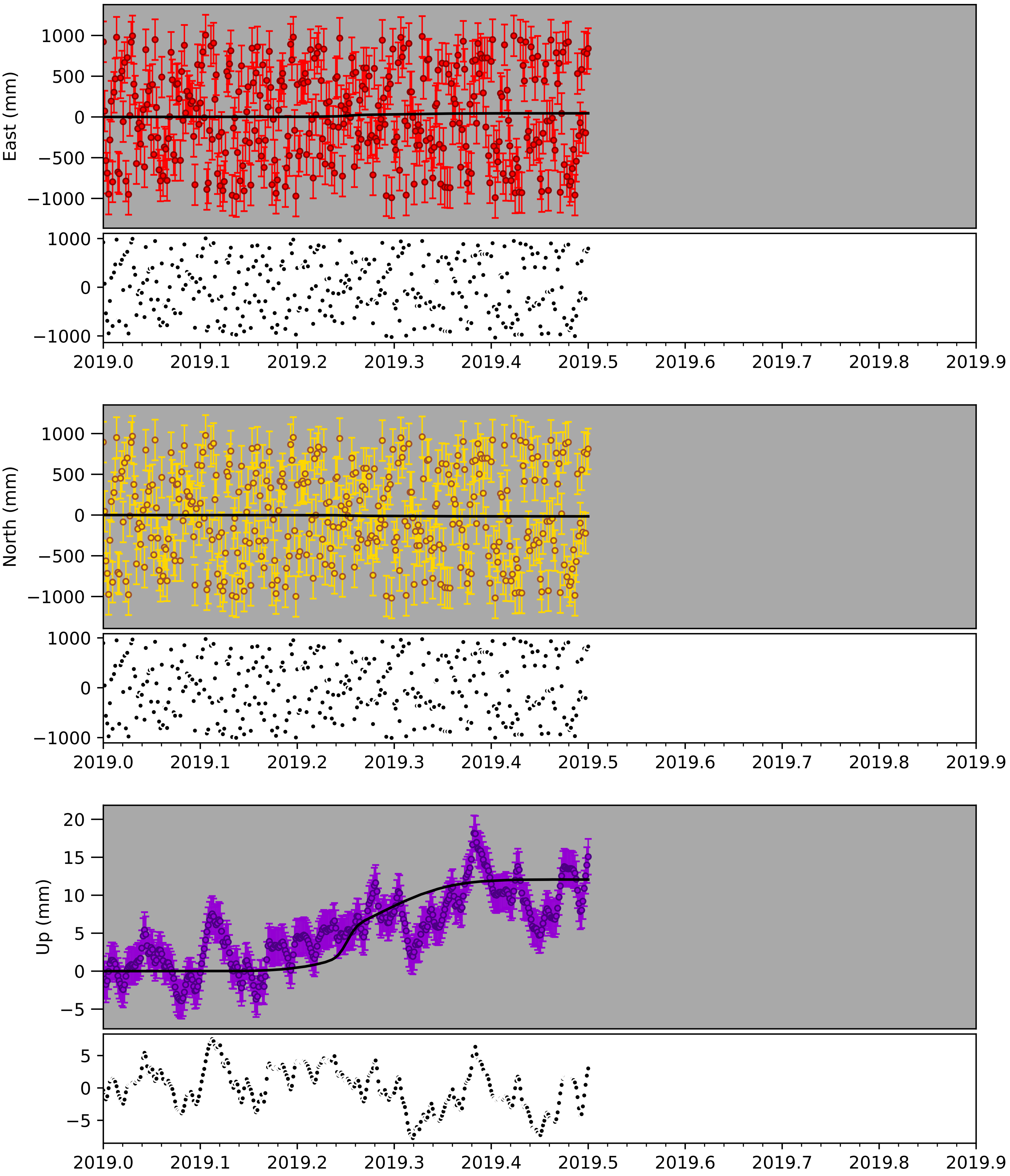

U009

[178.6145] [-38.7273]

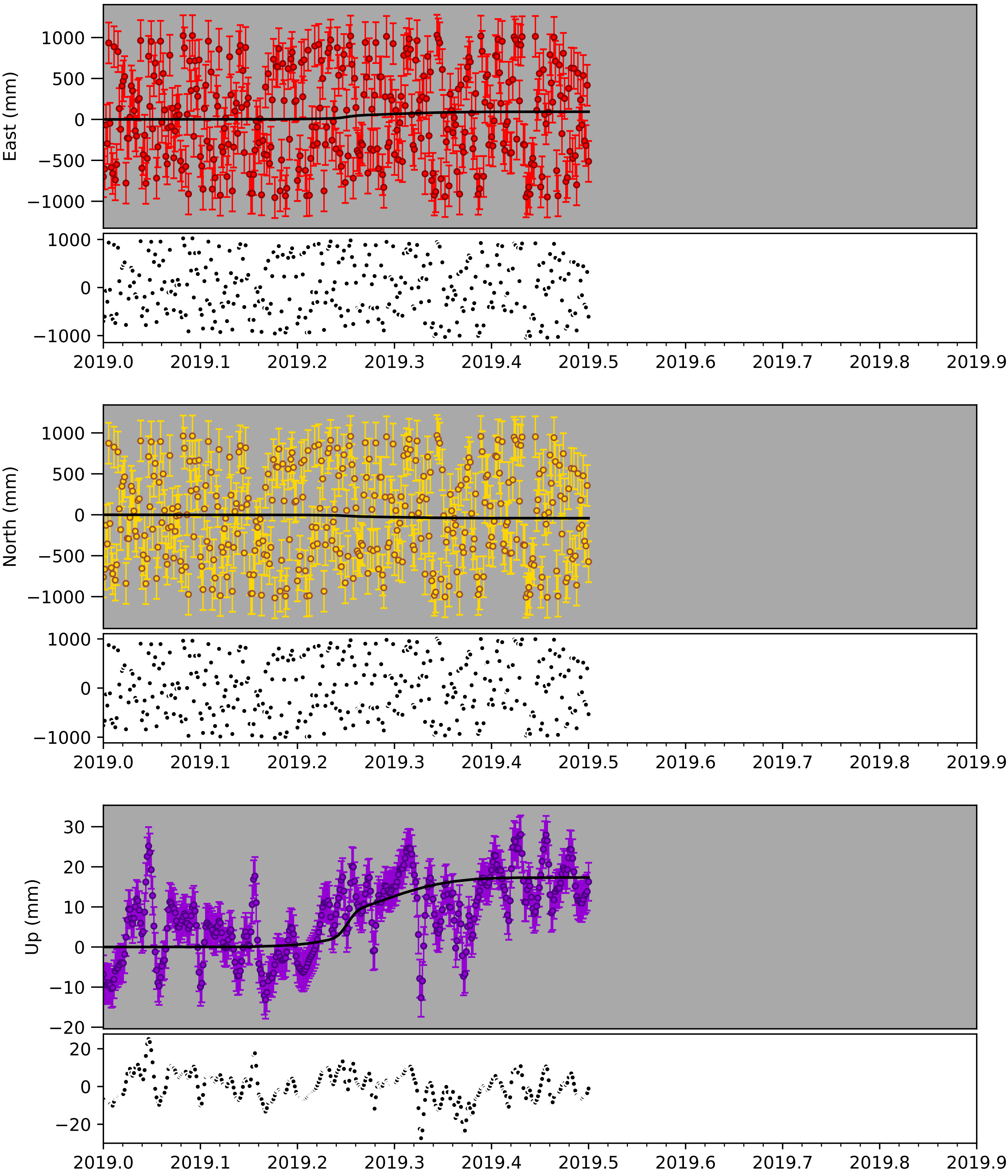

VGMO

[175.7543] [-39.4074]

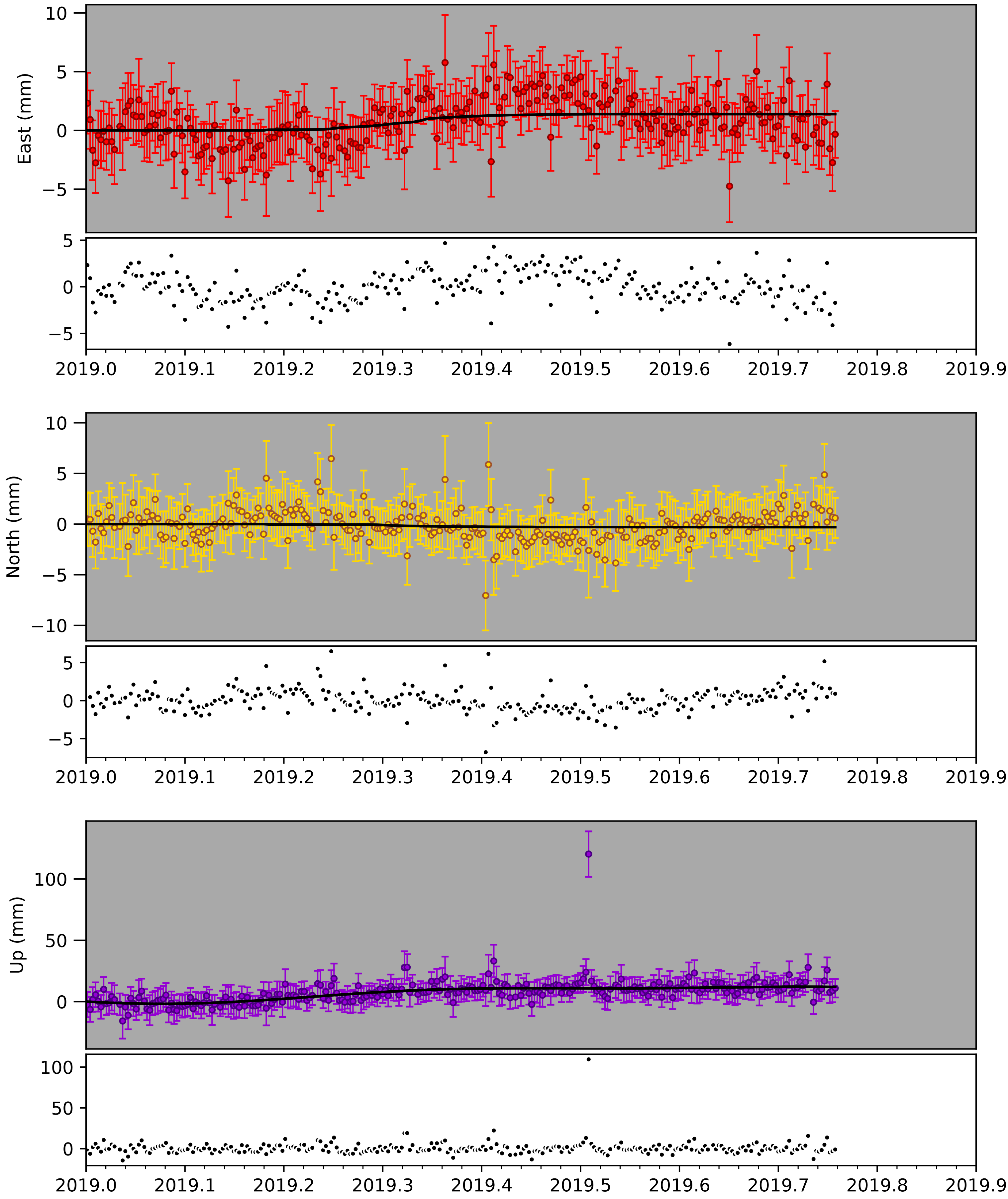

VGMT

[175.4705] [-39.3846]

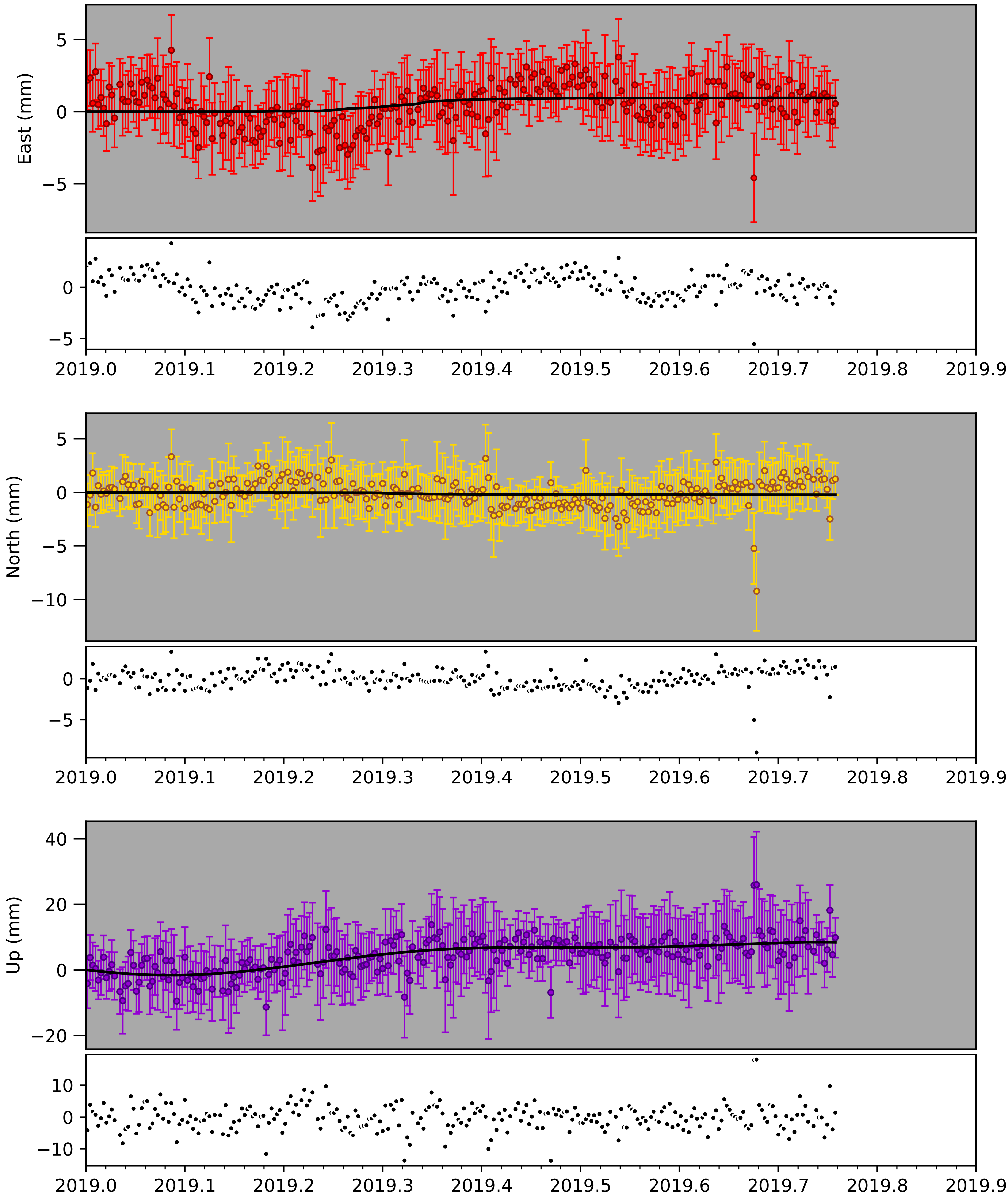

VGOB

[175.5422] [-39.1998]

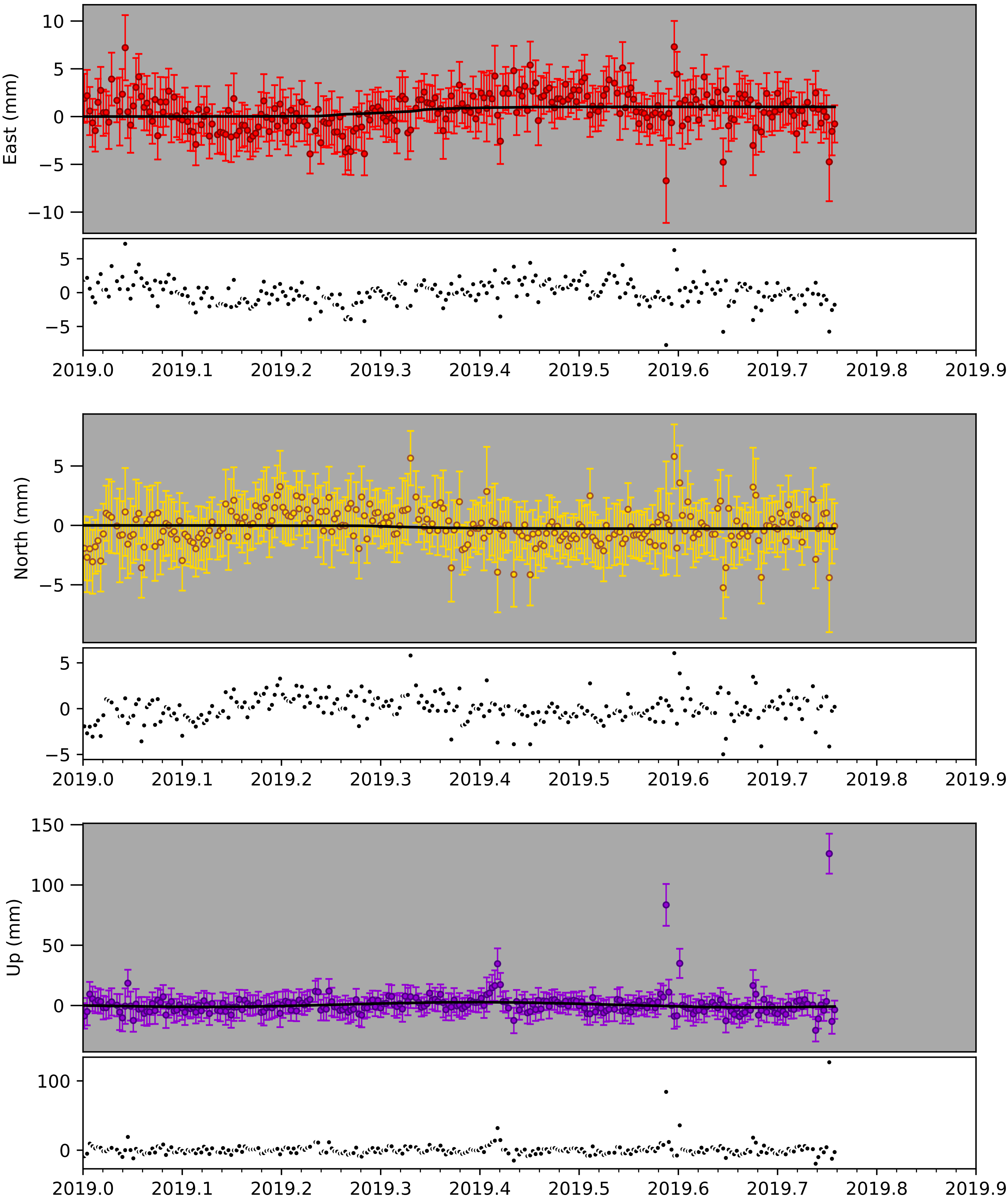

VGWN

[175.5979] [-39.3269]

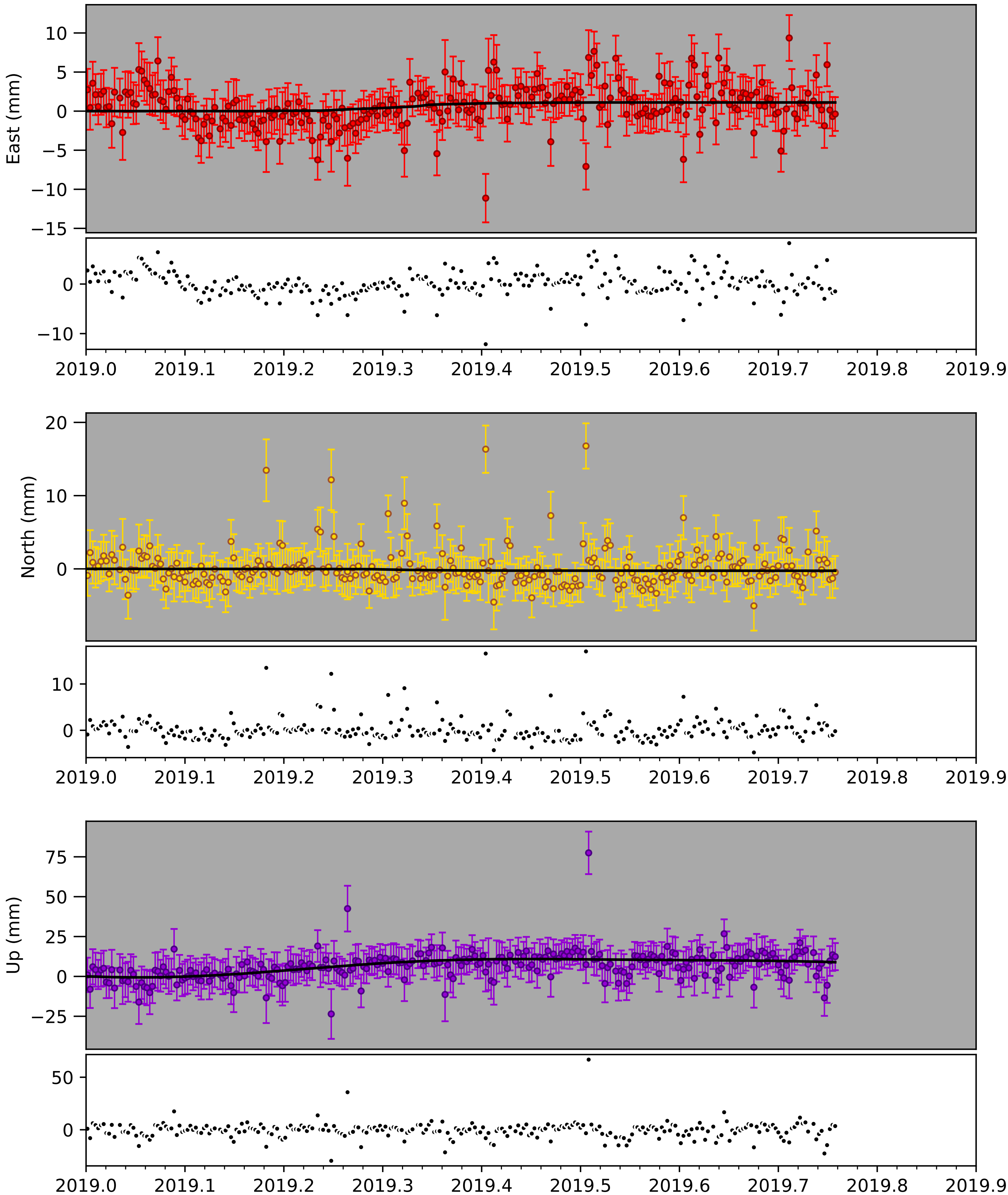

WAHU

[177.2344] [-39.0772]

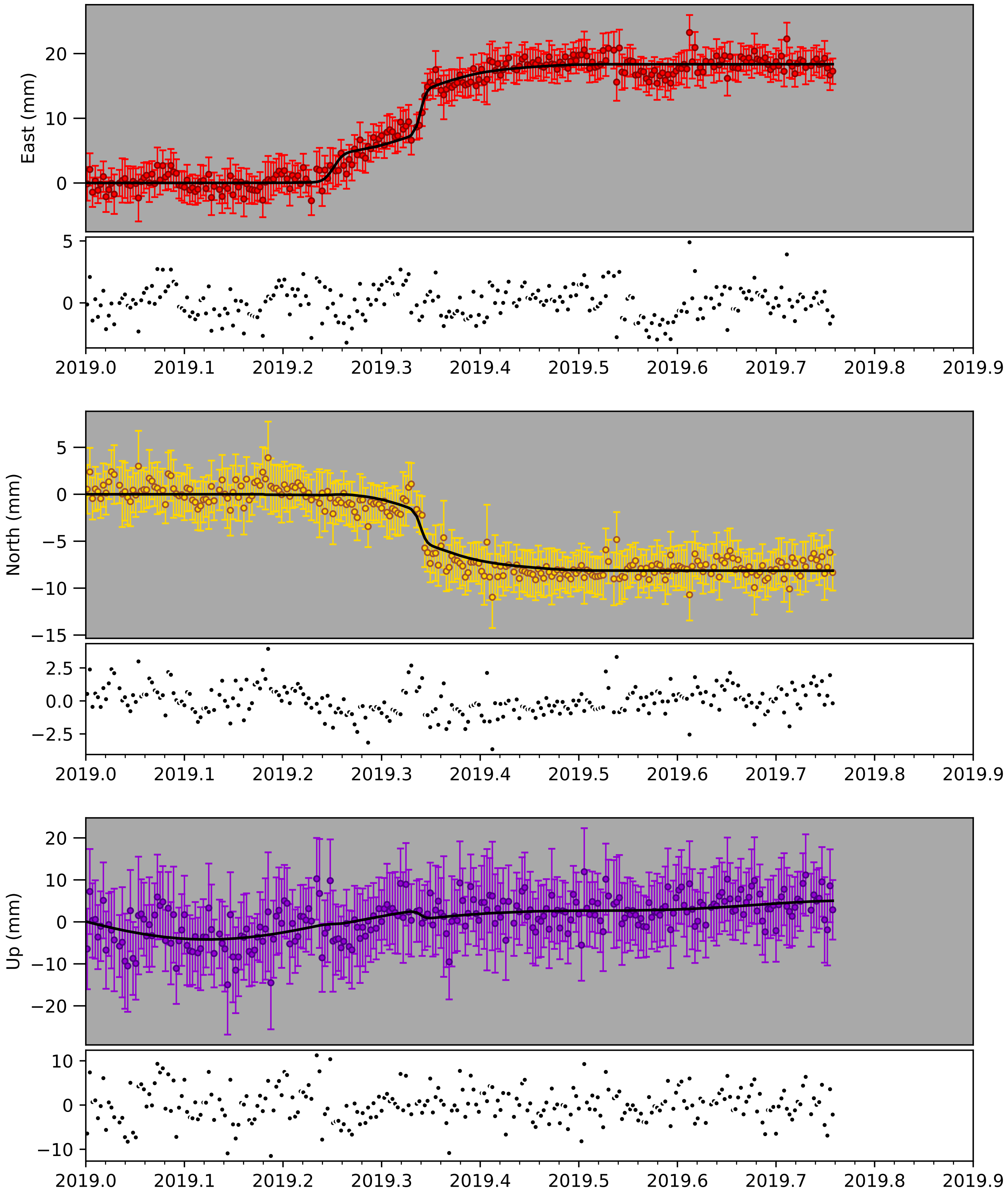

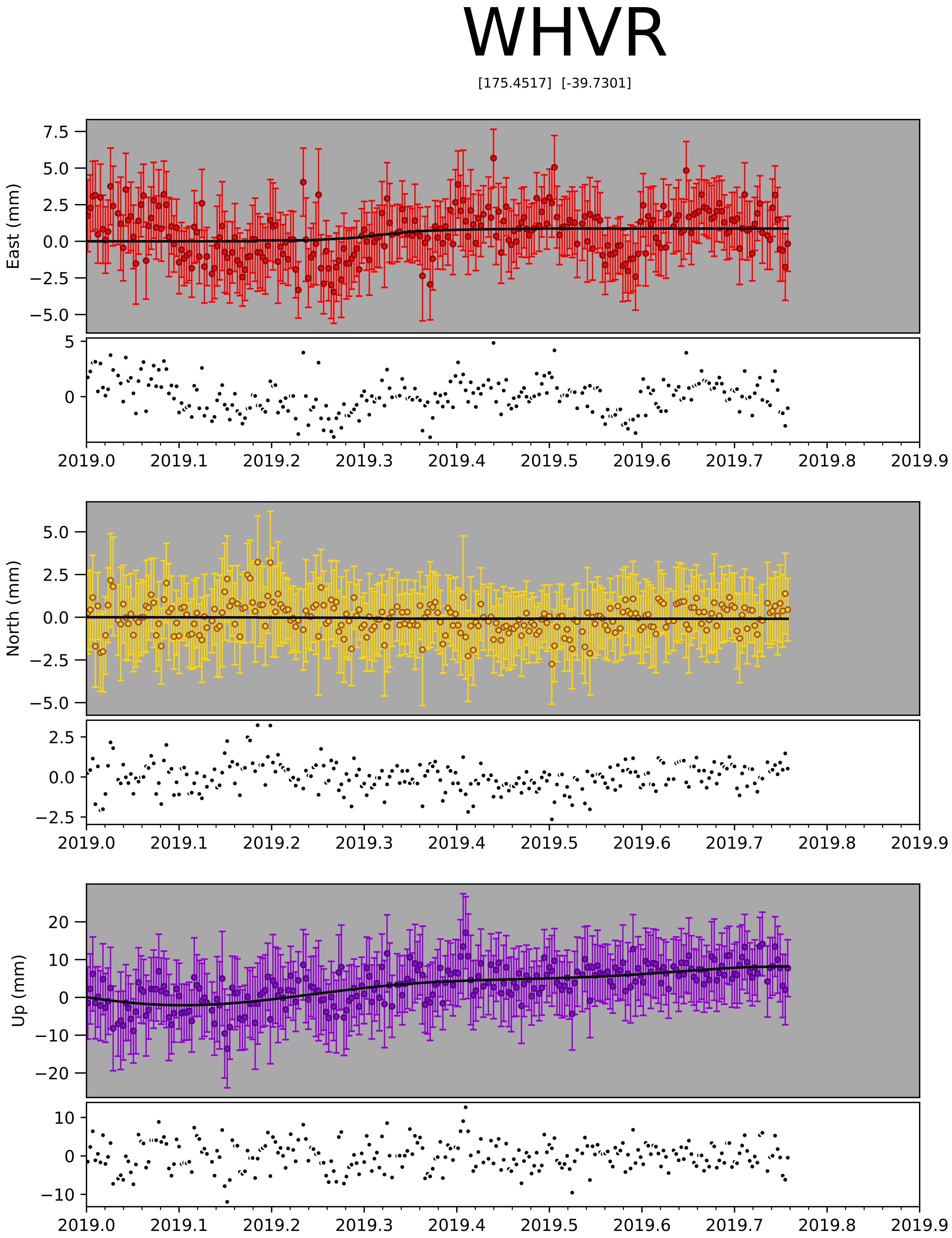
WHVR
[175.4517] [-39.7301]
East (mm)
North (mm)
Up (mm)
2019.0
2019.1
2019.2
2019.3
2019.4
2019.5
2019.6
2019.7
2019.8
2019.9

WMAT

[178.4087] [-37.825]

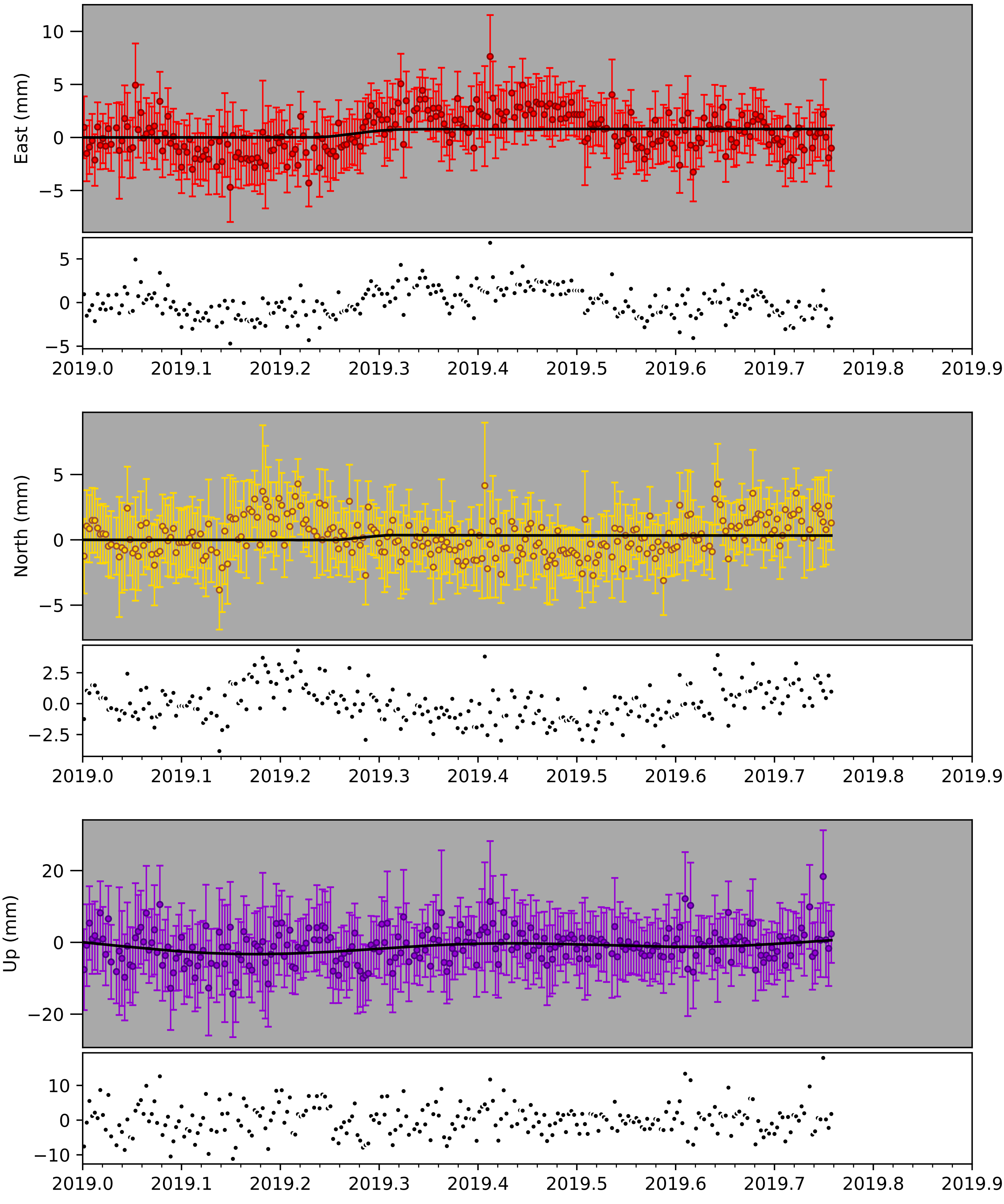

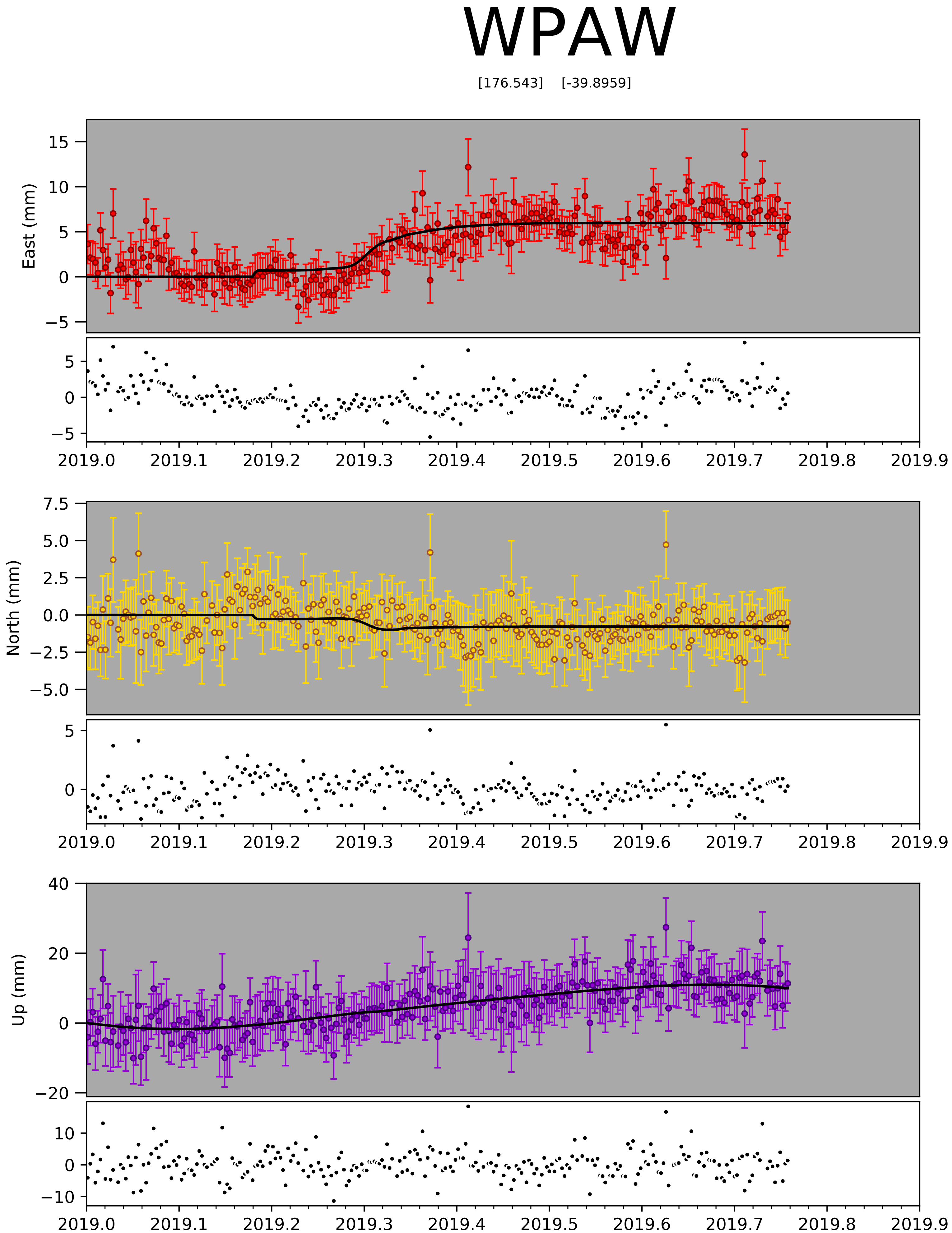

WPAW
[176.543] [-39.8959]
East (mm)
North (mm)
Up (mm)
2019.0
2019.1
2019.2
2019.3
2019.4
2019.5
2019.6
2019.7
2019.8
2019.9

WPUK

[176.4406] [-40.0642]